The PHILOSOPHICAL MAGAZINE

FIRST PUBLISHED IN 1798

. 45 SEVENTH SERIES No. 361 February 1954

A Journal of Theoretical Experimental and Applied Physics

PRICE 15s. 0d.
Annual Subscription £8 0s. 0d. payable in advance

AND PUBLISHED BY TAYLOR & FRANCIS LTD., RED LION COURT, FLEET ST., LONDON, E.C.4.

XV. *Slow Inelastic Collisions between Atomic Systems*

By D. R. Bates
Queen's University, Belfast

and

H. S. W. Massey, F.R.S.
University College, London*

[Received September 18, 1953]

Abstract

The physical mechanisms of the various processes which may occur as a result of encounters between low velocity atoms or ions are discussed, particular attention being paid to the factors which determine whether or not a collision is likely to be near-adiabatic. The following are the processes considered :

excitation, $A+B\rightarrow A+B'$, $A^+ + B\rightarrow A^+ + B'$, $A^+ + B\rightarrow A^{+\prime} + B$;
charge transfer, $A^+ + B\rightarrow A + B^+$, $A^- + B\rightarrow A + B^-$, $A+B\rightarrow A^+ + B^-$, $A^{++} + B\rightarrow A^+ + B^+$;
ionization, $A+B\rightarrow A+B^+ + e$, $A^+ + B\rightarrow A^+ + B^+ + e$, $A^+ + B\rightarrow A^{++} + B + e$;
detachment, $A^- + B\rightarrow A + B + e$, $A^- + B\rightarrow AB + e$.

§ 1. Introduction

Excitation and ionization of atoms or ions by the impact of other atoms or ions may be discussed in a similar way to excitation and ionization by the impact of electrons provided the ratio of the relative velocity of the colliding particles to the relevant orbital velocity is high. When this ratio is low the situation is entirely different for the transitions are then only energetically possible if the encounter is between two massive systems. Such inelastic encounters are of interest in many connections. They are, for example, responsible for the luminosity and other effects resulting from the passage of a meteor through the earth's atmosphere (cf. Herlofson 1948). Again it is important to know whether a significant contribution to ion production in a discharge can arise from slow collisions between the positive ions and the gas atoms (cf. Llewellyn Jones 1953) ; and should negative ions be present to know whether they can suffer appreciable destruction through detachment taking place in slow collisions (cf. Massey 1950). Many technical applications require the production of intense ion beams. One of the limitations on the intensity which may be achieved is the dispersing effect of space-charge. This effect may be neutralized to some effect at least by the electrons liberated in collisions with atoms of the

* Communicated by the Authors.

residual gas. Information on the dependence of the efficiency of such collisions on the relative velocity, and on the nature of the ions and atoms involved, is necessary in order to examine the conditions under which self-neutralization is likely to be adequate.

In a first attempt at classification of the possibilities it has been customary to refer to slow collisions as *near-adiabatic*. This implies that they occur so gradually that the chance of any ultimate transfer of energy is slight. There is experimental evidence that in some cases the associated cross sections are indeed small, and fall off rapidly with decrease of the relative velocity (cf. Massey and Burhop 1952). However, this does not seem to be true in general. Although the results obtained in the laboratory by different investigators are sometimes in conflict they leave little doubt that many slow collisions have not these characteristics (cf. Massey and Burhop 1952). The same conclusion is indicated by the remarkable effectiveness with which ion beams in a good vacuum (10^{-5} mm Hg) can neutralize their own space charge. Further the light and ionization produced by meteors appears to be much more intense and much less dependent on the velocity than would be expected if all slow collisions were near-adiabatic (Öpik 1953, Kaiser 1953).

Progress in the study of slow collisions clearly requires elucidation of the reasons why they are not always near-adiabatic and recognition of the factors which determine whether or not they can be so classified. The present paper represents an exploratory effort in this direction. After noting the predictions of Born's approximation (according to which all slow collisions are near-adiabatic) we consider the effects arising from the crossing of the various potential energy curves (including radiationless transitions into the continuum). Charge transfer, on which reliable experimental data is now becoming available (Hasted 1951, 1952) is amongst the collision processes discussed. No attempt is made at carrying through precise quantal calculations for any specific case.

§ 2. Born's Approximation

Results based on Born's approximation cannot of course be expected to be accurate at low velocities but nevertheless they provide a useful basis for discussion. Consider a system A of effective nuclear charge $Z_A e$ incident on a system B which, for simplicity, will be taken to be comprised of a nucleus of charge $Z_B e$ with an electron in the $1s$ state. By expanding them suitably it may be shown (Bates and Griffing 1953) that in the low energy region the Born approximations to the cross sections for the excitation of B to the $2s$ and $2p$ states reduce to

$$Q(1s-2s) \simeq \{1{\cdot}3\times 10^{-6} Z_A^2 E^4/M^4 \Delta E(1s-2s)^6\}\pi a_0^2, \quad . \; . \; (1)$$

and

$$Q(1s-2p) \simeq \{7{\cdot}4\times 10^{-9} Z_A^2 E^5/M^5 \Delta E(1s-2p)^7\}\pi a_0^2 ; \quad . \; . \; (2)$$

and similarly that the Born approximation to the cross section for ionization reduces to

$$Q(1s-c) \simeq \{1{\cdot}9\times 10^{-7} Z_A^2 E^4/M^4 \Delta E(1s-c)^6\}\pi a_0^2, \quad . \; . \; . \; (3)$$

where a_0 is the radius of the first Bohr orbit (so that πa_0^2 is $8{\cdot}8\times10^{-17}$ cm^2) ; E is the impact energy and ΔE is the energy change, both in ev ; M is the mass of the incident system relative to the mass of the proton. It is apparent from the formulae and from table 1, which gives numerical results for some representative cases, that the cross sections are rapidly increasing functions of E ; that they are rapidly decreasing functions of ΔE and of M ; and that they are greater for excitation than for ionization but are extremely small for both. These features are typical of near-adiabatic collisions, that is, collisions whose effective duration, T, is long compared with the time period, τ, associated with the internal motion (cf. Massey 1949). It is usual to take

$$T=la_0/v, \qquad \tau=\hbar/\Delta E, \quad . \quad . \quad . \quad . \quad . \quad . \quad . \quad . \quad (4)$$

where l is a number of the order of unity measuring the range of the interaction, and v is the velocity of approach. On this basis the near-adiabatic condition

$$T/\tau \gg 1, \quad . \quad . \quad . \quad . \quad . \quad . \quad . \quad . \quad . \quad . \quad (5)$$

becomes

$$6l\Delta E M^{1/2}/E^{1/2} \gg 1, \quad . \quad . \quad . \quad . \quad . \quad . \quad . \quad . \quad (6)$$

energy and mass being in the same units as before. For all cases treated in table 1 T/τ is $2l$ or greater.

Table 1. Data on Representative Near-adiabatic Collisions

Process	Excitation or ionization energy, ΔE (ev)	Incident particle:* mass, $M=30$ square of effective nuclear charge, $(Z_A e)^2=10e^2$			
		Energy E (ev)			
		100	200	400	800
		Cross section (πa_0^2)			
Excitation $1s-2s$	2	$2{\cdot}_6\times10^{-5}$	$4{\cdot}_2\times10^{-4}$	$6{\cdot}_7\times10^{-3}$	$1{\cdot}_1\times10^{-1}$
	3	$2{\cdot}_3\times10^{-6}$	$3{\cdot}_7\times10^{-5}$	$5{\cdot}_9\times10^{-4}$	$9{\cdot}_5\times10^{-3}$
	4	$4{\cdot}_1\times10^{-7}$	$6{\cdot}_5\times10^{-6}$	$1{\cdot}_0\times10^{-4}$	$1{\cdot}_7\times10^{-3}$
$1s-2p$	2	$2{\cdot}_4\times10^{-7}$	$7{\cdot}_6\times10^{-6}$	$2{\cdot}_4\times10^{-4}$	$7{\cdot}_7\times10^{-3}$
	3	$1{\cdot}_4\times10^{-8}$	$4{\cdot}_4\times10^{-7}$	$1{\cdot}_4\times10^{-5}$	$4{\cdot}_5\times10^{-4}$
	4	$1{\cdot}_8\times10^{-9}$	$5{\cdot}_9\times10^{-8}$	$1{\cdot}_9\times10^{-6}$	$6{\cdot}_1\times10^{-5}$
Ionization $1s-c$	6	$5{\cdot}_0\times10^{-9}$	$8{\cdot}_1\times10^{-8}$	$1{\cdot}_3\times10^{-6}$	$2{\cdot}_1\times10^{-5}$
	8	$9{\cdot}_0\times10^{-10}$	$1{\cdot}_4\times10^{-8}$	$2{\cdot}_3\times10^{-7}$	$3{\cdot}_7\times10^{-6}$
	10	$2{\cdot}_3\times10^{-10}$	$3{\cdot}_8\times10^{-9}$	$6{\cdot}_0\times10^{-8}$	$9{\cdot}_6\times10^{-7}$
	12	$7{\cdot}_8\times10^{-11}$	$1{\cdot}_3\times10^{-9}$	$2{\cdot}_0\times10^{-8}$	$3{\cdot}_2\times10^{-7}$

* Here, and in the later tables, results for other cases may easily be obtained by changing M and E by the same factor.

As mentioned in § 1, though many experimentally determined cross section versus energy curves have the characteristics described above others do not even well within what might at first be thought to be the near-adiabatic region. There is no real anomaly. As can be seen most clearly from the perturbed stationary state treatment the criterion derived from the definitions of T and τ given in (4) is much too crude (Bates, Massey and Stewart 1953). Briefly, it is not permissible to regard A and B as separate atoms or ions ; they must instead be regarded as forming a quasi-molecule and account must be taken of the dependence of the various parameters on R, the distance between the nuclei. Because of this it is not possible to express the near-adiabatic condition simply and comprehensively. However, in many cases it is sufficient to modify (6) by replacing $\Delta U(\infty)$ (for which the designation ΔE was used) by $\Delta U(R_M)$ the minimum separation between $U_i(R)$ and $U_f(R)$, the initial and final potential energy curves ; and by replacing l by fl where f is the fraction of the range of interaction over which the separation is near the minimum value. The effect may of course be slight. It will often happen that $U_i(R)$ and $U_f(R)$ come closer together as the systems approach but that $\Delta U(R_M)$ and fl remain large enough for the near-adiabatic condition to be satisfied even at quite high energies. In this event a detailed perturbed stationary state treatment would yield much the same type of result as would the Born approximation, the main difference being that the cross section would become appreciable at rather lower energies. Much more interest is attached to the possibility of collision processes for which $\Delta U(R_M)$ and fl are so small that the near-adiabatic region is virtually non-existent ; and in considering this possibility special attention must obviously be paid to the pseudo-intersection of potential energy curves.

§ 3. Transitions at an Intersection of Potential Energy Curves

Let $U_i^0(R)$ and $U_f^0(R)$ be the zero-order approximations to two potential energy curves, $U_i(R)$ and $U_f(R)$, of the same electronic species. As is well known U_i^0 and U_f^0 may cross at some internuclear separation, $R_x a_0$, but U_i and U_f are prevented from so doing by the mutual interaction (von Neumann and Wigner 1929). However, if the velocity of relative motion, v, is finite there is a certain probability, P, that in passing through R_x the colliding systems transfer from one potential energy curve to the other ; and taking account of the fact that passage through R_x must be made twice, there is therefore a probability

$$\mathscr{P}=2P(1-P) \quad . \quad . \quad . \quad . \quad . \quad . \quad . \quad . \quad . \quad (7)$$

that systems which originally approach along U_i finally recede along U_f, one or both of them being excited. Clearly the cross section for the process is approximately

$$Q=(g\mathscr{P}R_x^2)\pi a_0^2, \quad . \quad . \quad . \quad . \quad . \quad . \quad . \quad . \quad . \quad (8)$$

where g is the ratio of the statistical weight associated with U_i to the sum of the statistical weights associated with all possible initial potential energy curves.

Landau (1932), Zener (1932) and Stueckelberg (1932) (whose treatment of the whole problem is the most complete) have shown that

$$P=\exp(-\delta), \quad \ldots\ldots\ldots \quad (9)$$

where

$$\delta=\left\{\pi|\Delta U|^2\Big/2\hbar v\left|\frac{1}{a_0}\frac{d}{dR}(U_i^0-U_f^0)\right|\right\}_{R=R_x}, \quad \ldots \quad (10)$$

which may be expressed more conveniently as

$$\delta=\left\{9{\cdot}1M^{1/2}|\Delta U|^2\Big/E^{1/2}\left|\frac{d}{dR}(U_i^0-U_f^0)\right|\right\}_{R=R_x}, \quad \ldots \quad (11)$$

the mass of the incident particle being measured relative to that of the proton, the energies in ev and the length in atomic units as usual.

3.1. *Excitation*

In simple excitation

$$A+B\rightarrow A+B', \quad \ldots\ldots\ldots \quad (12)$$

$$\left.\begin{aligned} A^+&+B\rightarrow A^++B',\\ A^+&+B\rightarrow A^{+\prime}+B, \end{aligned}\right\} \quad \ldots\ldots \quad (13)$$

crossing obviously can only occur at small or moderate internuclear separations where the potential energy curves are distorted from their asymptotic form. Consequently the interaction is in general likely to be strong, making $\Delta U(R_x)$ comparable with the distortion. It is important to note that this is not always the case. For instance there may be chance cancellation within the relevant matrix integral; and again violation of the selection rules may cause $\Delta U(R_x)$ to be small but yet not vanishingly so if the quantum numbers are poorly determined. As regards $(d/dR)(U_i^0-U_f^0)_{R=R_x}$, little can be said beyond that in many instances it must be several ev per atomic unit of length. To allow for the uncertainties the probability, $\mathscr{P}$, was computed from formulae (7), (9) and (11) for various choices of the parameters. The values obtained are presented in table 2. It will be observed that over quite a wide range, $\mathscr{P}$ (and hence the cross section), is large and is a slowly varying function of the energy of the incident particle. This suggests that very marked departure from the characteristic near-adiabatic behaviour is not unduly rare when crossing occurs (though it must frequently be prevented by the interaction being too strong). Unfortunately the information available on the potential energy curves of even the better known systems is meagre, and it is not easy to predict in any particular case whether there is, or there is not, crossing. In general, however, the phenomena would seem to be most likely if the colliding systems have a number of low lying levels and least likely if they have only high levels: that is, it would be expected to arise in processes such as

$$\mathrm{O}+\mathrm{Fe}\rightarrow\mathrm{O}+\mathrm{Fe}', \quad \ldots\ldots\ldots \quad (14)$$

rather than in processes such as

$$\mathrm{H}+\mathrm{He}\rightarrow\mathrm{H}+\mathrm{He}'. \quad \ldots\ldots\ldots \quad (15)$$

3.2. *Charge Transfer*

Collisions of the types

$$A^+ + B \rightarrow A + B^+ , \quad . \quad . \quad . \quad . \quad . \quad . \quad . \quad (16)$$

$$A^- + B \rightarrow A + B^- , \quad . \quad . \quad . \quad . \quad . \quad . \quad . \quad (17)$$

Table 2. Data on Representative Curve-crossing Collisions Yielding Excitation

$\lvert \Delta U(R_x) \rvert$ ev	$\left\lvert \frac{d}{dR}(U_i{}^0 - U_f{}^0) \right\rvert_{R=R_x}$ ev per atomic unit of length	Incident particle : mass, $M=30$			
		energy, E (ev)			
		100	200	400	800
		Probability of excitation $\mathscr{P}$			
0·25	1	$3{\cdot}9\times10^{-1}$	$3{\cdot}2\times10^{-1}$	$2{\cdot}5\times10^{-1}$	$1{\cdot}9\times10^{-1}$
	2	$2{\cdot}5\times10^{-1}$	$1{\cdot}9\times10^{-1}$	$1{\cdot}4\times10^{-1}$	$1{\cdot}0\times10^{-1}$
	4	$1{\cdot}4\times10^{-1}$	$1{\cdot}0\times10^{-1}$	$7{\cdot}4\times10^{-2}$	$5{\cdot}3\times10^{-2}$
	8	$7{\cdot}4\times10^{-2}$	$5{\cdot}3\times10^{-2}$	$3{\cdot}6\times10^{-2}$	$2{\cdot}7\times10^{-2}$
0·5	1	$4{\cdot}1\times10^{-1}$	$4{\cdot}9\times10^{-1}$	$5{\cdot}0\times10^{-1}$	$4{\cdot}6\times10^{-1}$
	2	$5{\cdot}0\times10^{-1}$	$4{\cdot}6\times10^{-1}$	$3{\cdot}9\times10^{-1}$	$3{\cdot}2\times10^{-1}$
	4	$3{\cdot}9\times10^{-1}$	$3{\cdot}2\times10^{-1}$	$2{\cdot}5\times10^{-1}$	$1{\cdot}9\times10^{-1}$
	8	$2{\cdot}5\times10^{-1}$	$1{\cdot}9\times10^{-1}$	$1{\cdot}4\times10^{-1}$	$1{\cdot}0\times10^{-1}$
1·0	1	$1{\cdot}3\times10^{-2}$	$5{\cdot}6\times10^{-2}$	$1{\cdot}5\times10^{-1}$	$2{\cdot}8\times10^{-1}$
	2	$1{\cdot}5\times10^{-1}$	$2{\cdot}8\times10^{-1}$	$4{\cdot}1\times10^{-1}$	$4{\cdot}9\times10^{-1}$
	4	$4{\cdot}1\times10^{-1}$	$4{\cdot}9\times10^{-1}$	$5{\cdot}0\times10^{-1}$	$4{\cdot}6\times10^{-1}$
	8	$5{\cdot}0\times10^{-1}$	$4{\cdot}6\times10^{-1}$	$3{\cdot}9\times10^{-1}$	$3{\cdot}2\times10^{-1}$
2·0	1	$4{\cdot}1\times10^{-9}$	$1{\cdot}4\times10^{-6}$	$9{\cdot}1\times10^{-5}$	$1{\cdot}7\times10^{-3}$
	2	$9{\cdot}1\times10^{-5}$	$1{\cdot}7\times10^{-3}$	$1{\cdot}3\times10^{-2}$	$5{\cdot}6\times10^{-2}$
	4	$1{\cdot}3\times10^{-2}$	$5{\cdot}6\times10^{-2}$	$1{\cdot}5\times10^{-1}$	$2{\cdot}8\times10^{-1}$
	8	$1{\cdot}5\times10^{-1}$	$2{\cdot}8\times10^{-1}$	$4{\cdot}1\times10^{-1}$	$4{\cdot}9\times10^{-1}$
4·0	1	$<10^{-10}$	$<10^{-10}$	$<10^{-10}$	$<10^{-10}$
	2	$<10^{-10}$	$<10^{-10}$	$4{\cdot}1\times10^{-9}$	$1{\cdot}4\times10^{-6}$
	4	$4{\cdot}1\times10^{-9}$	$1{\cdot}4\times10^{-6}$	$9{\cdot}1\times10^{-5}$	$1{\cdot}7\times10^{-3}$
	8	$9{\cdot}1\times10^{-5}$	$1{\cdot}7\times10^{-3}$	$1{\cdot}3\times10^{-2}$	$5{\cdot}6\times10^{-2}$

are essentially similar to excitation collisions and hence do not require separate discussion. This is also true of many of the collisions

$$A + B \rightarrow A^+ + B^- , \quad . \quad . \quad . \quad . \quad . \quad . \quad . \quad (18)$$

but in others the Coulomb attraction between the positive and negative ions formed causes crossing to occur so far out that special considerations enter : thus for the *endothermic* processes*

* The electron affinities and ionization potentials used throughout are taken from Massey (1950) and from Moore (1951).

$$K+Br \rightarrow K^+ + Br^- \quad (-0{\cdot}8 \text{ ev}), \quad . \quad . \quad . \quad . \quad . \quad (19)$$

$$Na+Cl \rightarrow Na^+ + Cl^- \quad (-1{\cdot}4 \text{ ev}), \quad . \quad . \quad . \quad . \quad . \quad (20)$$

$$Al+O \rightarrow Al^+ + O^- \quad (-3{\cdot}8 \text{ ev}), \quad . \quad . \quad . \quad . \quad . \quad (21)$$

R_x is about 35, 20 and 7 respectively. Much the same remarks apply to the collisions

$$A^{++}+B \rightarrow A^+ + B^+ \quad . \quad . \quad . \quad . \quad . \quad . \quad . \quad . \quad (22)$$

as here again distant crossing may occur : thus for the *exothermic* processes

$$Si^{++}+N \rightarrow Si^+ + N^+ \quad (+1{\cdot}8 \text{ ev}), \quad . \quad . \quad . \quad . \quad (23)$$

$$A^{++}+He \rightarrow A^+ + He^+ \quad (+3{\cdot}0 \text{ ev}), \quad . \quad . \quad . \quad . \quad (24)$$

R_x is about 15 and 9 respectively.

In cases such as those cited above (and even when R_x is rather less) it is a sufficient approximation to represent the potential energy curves by their asymptotic forms so that (11) may be written

$$\delta = 2{\cdot}5 \times 10^2 M^{1/2} \Delta U(R_x)^2 / E^{1/2} \Delta U(\infty)^2 \quad . \quad . \quad . \quad . \quad (25)$$

which, when substituted in (7) and (9), gives the probability $\mathscr{P}$ in terms of a convenient set of parameters. Some computations were carried out to

Table 3. Data on Representative Curve-crossing Collisions Yielding Charge Transfer and Involving a Coulombic Potential Energy Curve

$\frac{\Delta U(R_x)}{\Delta U(\infty)}$	Incident particle : mass, $M=30$			
	energy, E (ev)			
	100	200	400	800
	Probability of charge transfer $\mathscr{P}$			
0·05	$4{\cdot}1 \times 10^{-1}$	$3{\cdot}4 \times 10^{-1}$	$2{\cdot}6 \times 10^{-1}$	$2{\cdot}0 \times 10^{-1}$
0·10	$3{\cdot}8 \times 10^{-1}$	$4{\cdot}7 \times 10^{-1}$	$5{\cdot}0 \times 10^{-1}$	$4{\cdot}7 \times 10^{-1}$
0·15	$9{\cdot}0 \times 10^{-2}$	$2{\cdot}0 \times 10^{-1}$	$3{\cdot}4 \times 10^{-1}$	$4{\cdot}5 \times 10^{-1}$
0·20	$8{\cdot}6 \times 10^{-3}$	$4{\cdot}2 \times 10^{-2}$	$1{\cdot}2 \times 10^{-1}$	$2{\cdot}5 \times 10^{-1}$
0·25	$4{\cdot}1 \times 10^{-4}$	$4{\cdot}9 \times 10^{-3}$	$2{\cdot}8 \times 10^{-2}$	$1{\cdot}0 \times 10^{-1}$
0·30	$1{\cdot}0 \times 10^{-5}$	$3{\cdot}5 \times 10^{-4}$	$4{\cdot}4 \times 10^{-3}$	$2{\cdot}6 \times 10^{-2}$
0·35	$1{\cdot}2 \times 10^{-7}$	$1{\cdot}5 \times 10^{-5}$	$4{\cdot}8 \times 10^{-4}$	$5{\cdot}5 \times 10^{-3}$
0·40	$1{\cdot}8 \times 10^{-10}$	$4{\cdot}1 \times 10^{-7}$	$3{\cdot}8 \times 10^{-5}$	$9{\cdot}0 \times 10^{-4}$

enable the general position to be assessed easily. From the results of these, presented in table 3, it can be seen that $\mathscr{P}$ is a slowly varying function of the impact energy provided

$$\Delta U(R_x)/\Delta U(\infty) < \sim 0{\cdot}15. \quad . \quad . \quad . \quad . \quad . \quad . \quad (26)^*$$

It may be observed that if $\Delta U(\infty)$ is 3 ev crossing occurs at an internuclear separation of $9{\cdot}1a_0$ and for condition (26) to be satisfied $\Delta U(R_x)$ must be less than about 0·45 ev ; if $\Delta U(\infty)$ is 4 ev the corresponding values are about $6{\cdot}8a_0$ and 0·60 ev ; and if it is 5 ev they are $5{\cdot}4a_0$ and 0·75 ev.

* As usual M is taken as 30 for the sake of definiteness.

The figures just quoted suggest that the condition is quite severe as far as process (18) is concerned, for it appears likely that in many instances $\Delta U(R_x)$ must exceed the relevant limit.* However, it must be borne in mind that a number of potential energy curves are usually associated with a given pair of systems in given states ; and that it is sufficient for the interaction to be less than the appropriate limit at only one crossing point. Some of the possible effects have already been mentioned in connection with excitation collisions. Special attention may be drawn to collisions, such as (21), in which a p (or d) electron is transferred from one system to the other. If $\Delta U(\infty)$ is, say, 4 ev $\Delta U(R_x)$ may well exceed the limit at the crossings associated with the σ orbitals but be less than the limit at the crossings associated with the π orbitals ; for the overlap integral (which gives some measure of the interaction†) is in general very much smaller for the latter than it is for the former.

In the case of processes (22) condition (26) is unlikely to exert so restrictive an influence since the greater compactness of the wave functions tends to make the interaction weaker.

If δ is small compared with unity formulae (7), (8), (9), (11) and (25) may be combined to give

$$Q=\left\{3{\cdot}6\times10^{5}\frac{gM^{1/2}\Delta U(R_x)^2}{E^{1/2}\Delta U(\infty)^4}\right\}\pi a_0^2 \quad . \quad . \quad . \quad . \quad . \quad (27)$$

the notation and units being as before. Some numerical values are given in table 4.

Magee (1940) has made estimates of the interaction energy between each of the various alkali metal-halogen pairs at the (A, B)—(A^+, B^-) crossing points. He finds that when R_x is 20 $\Delta U(R_x)$ is usually at least 2×10^{-2} ev and that when R_x is 30 it is usually at least 1×10^{-3} ev. From these results and the entries in table 4 it would appear a type (18) collision which is endothermic by between perhaps 1 and 3 ev is quite likely to have a large and slowly varying cross section.‡ Because of the increased probability of the interaction being too strong the chance of this is less for one which is endothermic by a much greater amount.

Calculations on the interaction energy at (A^{++}, B)—(A^+, B^+) crossing points have not been performed but in view of the compactness of the

* It is of course certainly satisfied if $\Delta U(\infty)$ is sufficiently small because R_x is then large and hence, as the interaction falls off exponentially, $\Delta U(R_x)$ is minute.

† Indeed Magee (1940) proposes that if the transition is allowed, and R_x is not too extreme, $\Delta U(R_x)$ may usually be taken to be of order $(10S/R_x)$ ev where S is the overlap integral between the initial and final wave functions of the active electron. Tables of overlap integrals have been published by Mulliken, Rieke, Orloff and Orloff (1949).

‡ The two limits given here should not be treated as other than illustrative. It is of course impossible to formulate any precise general rule since $\Delta U(R_x)$ depends not only on R_x but also on other factors such as the orbitals involved, and the energies associated with each (which control the amplitudes of the wave functions in the region of most interest).

relevant wave functions there is no doubt that at the corresponding internuclear separations $\Delta U(R_x)$ is much lower than the values obtained by Magee. Consequently a type (22) collision process will almost certainly have a small cross section if it is only slightly exothermic. One which is exothermic by rather more than perhaps about 2 ev* is quite likely to have a large and slowly varying cross section ; but it is less probable that one which is very exothermic has such a cross section.

Table 4. Further Data on Representative Curve-crossing Collisions Yielding Charge Transfer and Involving a Coulombic Potential Energy Curve

($\delta \ll 1$)

	Incident particle : mass $M=30$ energy $E=100$ ev	
Energy change, $\Delta U(\infty)$ (ev)	Internuclear separation at crossing, R_x (a_0)	Cross section per unit statistical weighting ratio, Q/g (πa_0^2)
1·0	27·2	$2{\cdot}0\times10^5$ $\Delta U(R_x)^2$
1·5	18·1	$3{\cdot}9\times10^4$ $\Delta U(R_x)^2$
2·0	13·6	$1{\cdot}2\times10^4$ $\Delta U(R_x)^2$
2·5	10·9	$5{\cdot}0\times10^3$ $\Delta U(R_x)^2$
3·0	9·1	$2{\cdot}4\times10^3$ $\Delta U(R_x)^2$
3·5	7·8	$1{\cdot}3\times10^3$ $\Delta U(R_x)^2$
4·0	6·8	$7{\cdot}7\times10^2$ $\Delta U(R_x)^2$
		(with $\Delta U(R_x)$ in ev)

It is perhaps worth drawing specific attention to the fact that a few collision processes of type (18) are exothermic, and many of type (22) are endothermic. Most of these should exhibit near-adiabatic characteristics since curve-crossing must be very rare. The former group does not include any important cases but the latter group includes

$$Ca^{++}+O \rightarrow Ca^{+}+O^{+} \quad (-1{\cdot}7 \text{ ev}), \quad . \ . \ . \ . \ . \quad (28)$$

and several others which are of geophysical or astrophysical interest.

§ 4. Transitions into the Continuum

4.1. *Ionization*

Ionizing collisions

$$A+B \rightarrow A+B^{+}+e \quad . \ . \ . \ . \ . \ . \ . \ . \quad (29)$$

can take place as a result of curve-crossing but they must be treated rather differently from excitation or charge transfer owing to the fact that the final state is in the continuum.

Suppose that at an internuclear separation of $R_x a_0$ there is an intersection of one of the potential energy curves along which A and B may come

* Once again a definite limit cannot be given.

together and one of the potential energy curves of the complex comprised of A, B^+ and an ejected electron of zero energy. At smaller internuclear separations radiationless transitions may occur, that is, the quasi-molecule, $(A+B)$, may suffer auto-ionization. If t is the lifetime towards this process (measured in sec) the cross section associated with (29) is approximately

$$Q=\{gR_x^2[1-\exp(-R_x a_0/vt)]\}\pi a_0^2 \quad . \quad . \quad . \quad . \quad . \quad . \quad . \quad (30)$$

$$=\{gR_x^2[1-\exp(-3{\cdot}8\times 10^{-15}M^{1/2}R_x/E^{1/2}t)]\}\pi a_0^2 \quad . \quad . \quad (31)$$

(provided of course E is sufficiently high to permit the necessary close approach). In many instances the exponential coefficient in (31) is small so that the formula simplifies to

$$Q=\{3{\cdot}8\times 10^{-15}gM^{1/2}R_x^3/E^{1/2}t\}\pi a_0^2. \quad . \quad . \quad . \quad . \quad (32)$$

It is clear from the above that cross sections for ionization (or simultaneous ionization and excitation) may be slowly varying functions of the impact energy ; and moreover, since in favourable cases t may be as short as 10^{-15} sec (Shenstone 1931, 1948, Wu 1944, Bransden and Dalgarno 1953) they may be quite large. As in the case of simple excitation reliable predictions on the prevalence of curve-crossing are difficult to make. It may, however, be noted that because of the character and position of the final potential energy curves the phenomena must be rare in collisions of the types

$$A^+ + B \rightarrow A^+ + B^+ + e, \quad . \quad . \quad . \quad . \quad . \quad . \quad . \quad (33)$$

$$A^+ + B \rightarrow A^{++} + B + e, \quad . \quad . \quad . \quad . \quad . \quad . \quad . \quad (34)$$

so that a departure from near-adiabatic behaviour would not be expected in either. In certain cases the sequence of process (16) followed by (29) might of course make a slowly moving positive ion an indirect but quite effective liberator of electrons.

4.2. *Detachment*

Finally we will briefly consider detachment

$$A^- + B \rightarrow A + B + e. \quad . \quad . \quad . \quad . \quad . \quad . \quad . \quad . \quad (35)$$

This may of course occur in the manner just described. In many instances the crossing point may be reached even in collisions of thermal energies.*† For example the theoretical work of Eyring, Hirschfelder and Taylor (1936) on the structure of H_2^- shows that H atoms and H^- ions approach along an attractive potential energy curve which intersects the H_2 ground state potential energy curve at an internuclear separation of about $3{\cdot}4a_0$. Again, though proper calculations have not been carried out it seems likely (Bates and Massey 1943) that several of potential energy curves along with O atoms and O^- ions approach are also attractive and intersect the lower O_2 potential energy curves at comparable internuclear

* At such energies the reaction path is $A^- + B \rightarrow AB + e$.

† This is naturally also possible in de-excitation collisions and in exothermic charge transfer collisions.

separations. Such thermal processes (which are referred to as *associative detachment*) may be important in the upper atmosphere and in discharges. Because of lack of knowledge of t it is not possible to give a reliable estimate of the cross section in any particular case; but it is apparent from formula (30) (modified to allow for the fact that the variation of the kinetic energy of relative motion with the internuclear separation cannot here be neglected) that cross-sections of order $10^{-4}\pi a_0^2$ are possible even if this time is as long as 10^{-10} sec.

Another detachment mechanism remains to be described. The system formed on bringing two nuclei together may have no bound state for an excess electron. If the affinity becomes zero at an internuclear separation of $R_x a_0$ the excess electron is free to leave the system at closer separations, and it is apparent therefore that the detachment cross section is of order $(gR_x^2)\pi a_0^2$. The phenomenon is essentially the same as the ionization of atomic hydrogen by negative mesons which has recently been discussed by Wightman (1950). It should be noted, however, that the united limits which may be reached adiabatically may all be doubly excited; and doubly excited states of a negative ion may be bounded even though the normal state is unbounded. Because of this, detachment through lack of affinity will not occur in many cases where it might at first be expected. However in such cases, there must of necessity be curve-crossing so that detachment may proceed through radiationless transitions as described above.

Acknowledgments

We wish to thank Dr. E. J. Öpik of Armagh Observatory and Dr. T. R. Kaiser of Manchester University for helpful discussions on the evidence about slow collisions provided by the study of meteors. It was largely these discussions which stimulated us to attempt the present survey.

References

Bates, D. R., and Griffing, G., 1953, *Proc. Phys. Soc.* A, **66,** 961.
Bates, D. R., and Massey, H. S. W., 1943, *Phil. Trans. Roy. Soc.* A, **239,** 269.
Bates, D. R., Massey, H. S. W., and Stewart, A. L., 1953, *Proc. Roy. Soc.* A, **216,** 437.
Bransden, B. H., and Dalgarno, A., 1953, *Proc. Phys. Soc.* A, **66,** 904 and 911.
Eyring, H., Hirschfelder, J. O., and Taylor, H. S., 1936, *J. Chem. Phys.*, **4,** 479.
Hasted, J. B., 1951, *Proc. Roy. Soc.* A, **205,** 421; 1952, *Ibid.*, **212,** 235.
Herlofson, N., 1948, *Reports on Progress in Physics*, **11** (London: Physical Society), p. 444.
Kaiser, T. R., 1953, *Advances in Physics*, **2,** 495.
Landau, L., 1932, *Z. Phys. Sowjet*, **2,** 46.
Llewellyn Jones, F., 1953, *Reports on Progress in Physics*, **16** (London: Physical Society), p. 216.
Magee, J. L., 1940, *J. Chem. Phys.*, **8,** 687.

Massey, H. S. W., 1949, *Reports on Progress in Physics*, **12** (London : Physical Society), p. 248 ; 1950, *Negative Ions* (2nd edn.) (Cambridge : University Press).

Massey, H. S. W., and Burhop, E. H. S., 1952, *Electronic and Ionic Impact Phenomena* (Oxford : Clarendon Press).

Moore, C., 1951, *Atomic Energy Levels* (Washington : Bureau of Standards).

Mulliken, R. S., Rieke, C. A., Orloff, D., and Orloff, H., 1949, *J. Chem. Phys.*, **17**, 1248.

Öpik, E. J., 1953 (in course of preparation).

Shenstone, A. G., 1931, *Phys. Rev.*, **38**, 873 ; 1948, *Phil. Trans. Roy. Soc.* A, **241**, 297.

Stueckelberg, E. C. G., 1932, *Helv. phys. Acta*, **5**, 370.

von Neumann, J., and Wigner, E., 1929, *Physik. Z.*, **30**, 467.

Wightman, A. S., 1950, *Phys. Rev.*, **77**, 516.

Wu, Ta-You, 1944, *Phys. Rev.*, **66**, 291.

Zener, C., 1932, *Proc. Roy. Soc.* A, **137**, 696.

XVI. *An Attempt to Find Anisotropy in the Superconductive Properties of Gallium*

By A. J. Croft and Mrs. J. L. Olsen-Baer
Clarendon Laboratory, Oxford University
and
R. W. Powell
National Physical Laboratory*

[Received November 24, 1953]

Abstract

Gallium has a marked anisotropy in its electrical resistivity; these experiments, which cover the temperature range 0·2°K to 1°K, show that any dependence of superconductive transition point on crystallographic direction is less than *c.* 0·002°K.

§ 1

Gallium is a superconductor with a transition point just above 1°K (De Haas and Voogd 1929, Shoenberg 1940, Goodman and Mendoza 1951). Since it possesses the largest known anisotropy in electrical resistance, which has been shown to persist down to the superconducting transition point (Powell 1951, Olsen-Baer and Powell 1951), the question arises whether the superconductive properties are affected by this anisotropy. (It is true that de Haas and Voogd (1931) could find no anisotropy in the superconductive properties of single crystals of tin, but the anisotropy in the resistivity is very much less marked than in gallium.)

Two possible effects must be considered:

(*a*) An anisotropic single crystal might at a certain temperature be superconducting in one direction and not in another.

(*b*) The temperature at which the superconductive phase-change takes place in an external magnetic field might depend on the angle between the field and the crystal axes.

Although it seems rather improbable that the first effect occurs, this is not so in the case of the second. It is true that both effects might be very small but in the absence of a complete theory of superconductivity we decided to look for them.

Two different cryostats were used in both of which the specimen is immersed in a bath of liquid helium and is therefore in as strain-free a state as possible. One apparatus consisted simply of a bath of liquid helium which could be pumped down to just below 1°K; the other was a demagnetization apparatus in which a bath of liquid helium could be cooled to 0·2°K (Croft *et al.* 1953).

* Communicated by Professor F. E. Simon, C.B.E., F.R.S.

§ 2. Measurements above 1°K

Three gallium single-crystals grown along the directions of greatest, least and intermediate resistivity were prepared as already described (Olsen-Baer and Powell 1951) and were mounted in the liquid helium bath. Currents of up to 100 ma were used and the potentials measured with a galvanometer amplifier circuit as described in the paper just mentioned. The temperature was determined by measuring the vapour pressure and allowing for the Knudsen effect.

It was found that in zero field and in a field of 10 gauss the transitions occurred at temperatures which were the same to the limit of accuracy of the experiment: that is, a few thousandths of a degree.

§ 3. Measurements below 1°K

Some different specimens of similarly high purity were used in these experiments. Preliminary experiments showed that the transition points of the different crystals in various fields at temperatures down to 0·2°K were very nearly the same and that they agreed fairly well with the data published by Goodman and Mendoza (1951).

Two crystals with their long axes in the high and low resistivity directions were then mounted close together in the apparatus so that an accurate comparison could be made in a magnetic field which was at different angles to the crystal axes. Each specimen had an independent current supply and the potentials were joined in series opposition; in this way, if as the bath warmed up from 0·2°K one specimen became normally conducting before the other, a deflection in the galvanometer would be seen first in one direction and then in the other. By timing the interval between the swings, one could deduce the temperature interval from the rate of warming up. After demagnetization, a field of 55 gauss was applied by means of a solenoid and the galvanometer watched while the temperature passed through the transition point in this field, i.e. *c.* 0·24°K. (The transitions were very sharp; this is a guarantee of the homogeneity of the field.) The field was then reduced and the same procedure repeated several times. Temperature measurements were taken magnetically at intervals. The time taken to warm up from 0·2°K to 1°K was about 20 minutes.

At all temperatures between 0·2°K and 1°K in several experiments consistent small differences were found of about 0·005°K. To see whether these were due to inhomogeneity of field, temperature or the specimen, one of the crystals was cut in half, the two halves mounted exactly as before and the experiment repeated. We then found differences of about 0·003°K. Any real difference in transition temperature must therefore have been less than, say, 0·002°K.

§ 4. Conclusion

From these two sets of experiments, we conclude that any difference between the transition points of gallium single crystals measured along the different crystal axes is less than a few thousandths of a degree.

This work, which was carried out at the Clarendon Laboratory, also formed part of the general research programme of the National Physical Laboratory and is published with the approval of the Director.

References

Croft, Faulkner, Hatton and Seymour, 1953, *Phil. Mag.*, **44,** 289.
de Haas and Voogd, 1929, *Comm. Phys. Lab. Leiden*, 199d ; 1931, *Ibid.*, 214c.
Goodman and Mendoza, 1951, *Phil. Mag.*, **42,** 594.
Olsen-Baer and Powell, 1951, *Proc. Roy. Soc.* A, **209,** 542.
Powell, 1951, *Proc. Roy. Soc.* A, **209,** 525.
Shoenberg, 1940, *Proc. Camb. Phil. Soc.*, **36,** 85.

XVII. *Pile Modulation and Statistical Fluctuations in Piles*

By O. R. Frisch* and D. J. Littler
Atomic Energy Research Establishment, Harwell, England†

[Received January 21, 1953, revised November 12, 1953]

Abstract

A theory is given of the statistical fluctuation of the number of neutrons in a pile. An experimental verification of this theory is described, and the results of the theory are used to evaluate the accuracy of the measurement of neutron absorption cross sections with a pile oscillator.

§ 1. Introduction

For some years, a ' pile oscillator ' has been used on the Graphite Low Energy Experimental Pile (G.L.E.E.P.) at Harwell for measuring thermal neutron absorption cross sections. A sample of the element to be measured is moved periodically in and out of the pile and produces a modulation in the number of neutrons in the pile. The depth of modulation produced by the sample is compared with that produced by a boron sample of known cross sectional area, and hence the total cross sectional area of the unknown sample may be determined. In this way the thermal neutron absorption cross sections of about forty of the elements have been measured (Colmer and Littler 1950).

The ultimate accuracy of the method depends on the fluctuations in the number of neutrons in the pile. This paper gives a theory of these fluctuations, describes an experimental verification of the theory and shows how the fluctuations affect the accuracy of the absorption cross section measurements.

§ 2. Description of the G.L.E.E.P. Oscillator

A small graphite boat holds the sample to be measured and is oscillated between the outside and the centre of the pile. Transfer between these two positions is as rapid as possible (the twenty feet between the two positions are covered in one second), so as to minimize the effects on pile multiplication of neutrons scattered by the sample ; this effect vanishes when the sample is at the centre of the pile. At each of the two extreme positions the boat is stationary for an adjustable time, usually much longer than the transit time. Under these conditions

* Now at University of Cambridge.
† Communicated by the Authors.

the motion of the sample produces an almost perfect square wave modulation in the reproduction constant of the pile. The boat, which can carry loads up to about three kilogramms, is driven by a conventional type of servo mechanism, the only novel feature being that the position of the boat at the centre of the pile is always reproduced to within $\pm\frac{1}{8}$ inches. The servo mechanism is triggered twice during each period of oscillation by a master control unit which accurately governs the total period of the oscillator.

§ 3. Theory of Pile Modulation

Since there are delayed neutrons in the pile, the square wave modulation in the pile reproduction constant produces a complex periodic modulation of the number of neutrons in the pile, superimposed upon the steady level N_0 obtained when the reproduction constant has its mean value K_0. Suppose that the change in the reproduction constant produced by a sample going from the outside to the centre of the pile is Δ. Let N_1 be the amplitude of the first harmonic component in the modulation of the number of neutrons in the pile, then,

$$N_1/N_0=(2\Delta/\pi)A(\omega). \quad . \quad . \quad . \quad . \quad . \quad . \quad (3.1)$$

$A(\omega)$ is a function which is usually called the pile amplification factor. If Δ is small, it may be shown that $A(\omega)$ is given by (Gilbert and Fergusson 1948)

$$1/A^2(\omega)=[\omega\tau+c\omega\Sigma\mu_j\lambda_j/(\lambda_j{}^2+\omega^2)]^2+[c\omega^2\Sigma\mu_j/(\lambda_j{}^2+\omega^2)+1-K_0]^2 \quad . \quad (3.2)$$

where $\omega/2\pi$ is the frequency of oscillation of the sample,

τ is the mean life time of a neutron in the pile (time being between being born as a fission neutron and being captured as a thermal neutron),

K_0 is the reproduction constant of the pile when there is no modulation,

cK_0 is the total number of delayed neutrons produced per thermal neutron captured in the pile,

μ_j is the fraction of c corresponding to the production of delayed neutrons with a decay constant λ_j, and the summations extend over all the delayed neutron periods.

K_0 is not quite equal to unity since some neutrons are produced in the pile by other means than neutron induced fission (e.g. by spontaneous fissions, alpha-neutron reactions, cosmic rays). However, in practice, provided that the pile is run at more than a few watts power we may put $K_0=1$ in (3.2).

Experimentally, Gilbert and Fergusson have determined the values of $A(\omega)$ for periods ranging between 1 and 500 seconds by making measurements on the Zero Energy Experimental Pile (Z.E.E.P.) at Chalk River, Canada. Their experiment consisted in rotating a cadmium shutter at a fixed position in the pile in such a way as to produce a pure sinusoidal change in the pile reproduction constant, and then measuring the modulation produced in the number of neutrons in the pile. If

allowance is made for the different values of τ in the two piles (G.L.E.E.P. is a graphite-moderated pile and Z.E.E.P. a heavy water moderated pile), their values may be used to give the values of $A(\omega)$ for G.L.E.E.P. ; for modulation periods longer than 20 seconds, the values of $A(\omega)$ for the two types of pile differ by less than 3%.

Although the expression (3.2) is obtained from the pile kinetic equations by assuming that Δ is small, the Harwell Computing Group have shown by numerical integration that (3.2) gives the value of $A(\omega)$ to within $\frac{1}{2}$% for values of Δ up to 3×10^{-3}, and for all values of modulation period up to 100 seconds.

For values of Δ up to 3×10^{-3} therefore and for a fixed period of oscillation, we see from (3.1) and (3.2) that N_1/N_0 is proportional to Δ and therefore to the cross sectional area of the sample being measured.

§ 4. Measuring Arrangement

Experimentally, therefore, we measure the ratio N_1/N_0 and take this to be proportional to the cross sectional area of the sample, the constant of proportionality being determined by a calibration with boron as mentioned in § 1. The determination of the ratio N_1/N_0 may be understood by referring to fig. 1. The neutrons in the pile are detected by a boron trifluoride ionization chamber in series with a 10^8 ohm resistor.

Fig. 1

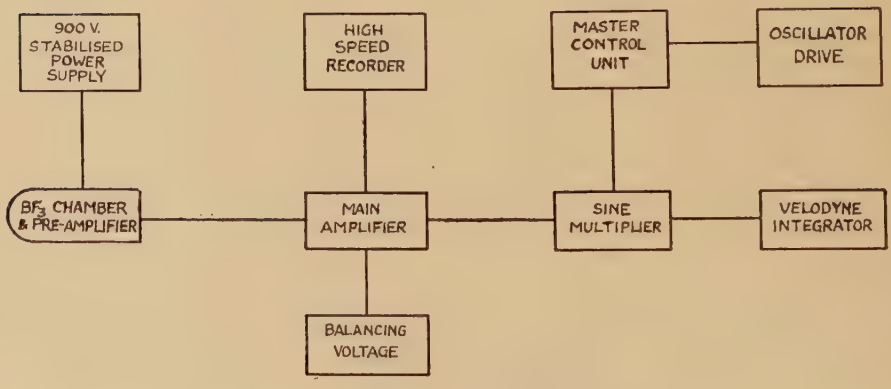

Schematic diagram of electrical equipment.

To the earthy end of this resistor a potentiometer is connected, which ' backs off ' the voltage produced by the current component corresponding to N_0. A pre-amplifier followed by a main amplifier then amplifies only the difference in voltage between the balancing potentiometer and that produced across the 10^8 ohm resistor. The voltage produced at the amplifier output is then of the same form as the modulation of the number of neutrons in the pile. A high speed recorder is connected to the amplifier output so that the pile modulation may be observed.

To obtain the desired Fourier component there is connected across the output of the amplifier a potentiometer with a sliding contact which moves with sinusoidal motion. This sliding contact is driven by the master control unit and has the same period as the sample oscillator. Because of the delayed neutrons in the pile, the first harmonic component in the pile modulation lags in phase behind the first harmonic component in the change in reproduction constant produced by the motion of the sample. By suitably advancing the phase of the motion of the sample with respect to that of the sliding contact on the potentiometer, it can be arranged that the first harmonic component in the voltage produced at the amplifier output is multiplied by a sine term in phase with it.

After the sine multiplication the output voltage of the amplifier is fed into a velodyne integrator* and integrated over one modulation cycle. The sine multiplication followed by the integration thus performs an electro-mechanical Fourier analysis on the pile modulation. The answer recorded by the integrator is therefore proportional to N_1 multiplied by half the modulation period. If we denote the recorded integrator result by $I(\omega)$, we will have from (3.1)

$$I(\omega)/V=(2\alpha\Delta/\omega)A(\omega), \qquad . \quad . \quad . \quad . \quad . \quad (4.1)$$

where V is the value of the balancing voltage and α is a constant which converts the amplitude of sinusoidal voltages applied to the pre-amplifier input into answers recorded on the integrator. α may be measured by applying a known sinusoidal voltage to the amplifier input ; in fact this is frequently done during the course of modulation experiments, in order to ensure that the electronic equipment maintains a constant calibration.

Thus for a constant modulation period the values of $I(\omega)/V$ are proportional to the total cross sectional area of the sample being measured, provided that Δ does not exceed 3×10^{-3}.

Statistical fluctuations in the number of neutrons in the pile will produce fluctuations in the recorded values of $I(\omega)/V$. Since we perform a Fourier analysis on the pile modulation in order to obtain the amplitude of its first harmonic component, it follows that the fluctuations in $I(\omega)/V$ will only be due to the Fourier component of the pile fluctuations which has the same periodicity as the motion of the sample being measured. In other words, the method we use automatically eliminates a considerable proportion of the pile fluctuations.

There still remains, however, the question of whether there is an optimum modulation period which can be used. That is to say, is there a modulation period such that the signal given by (4.1) divided by the 'noise' due to the pile fluctuations has a maximum value ? In order to answer this question we must know the Fourier spectrum of the pile fluctuations, and this is deduced in the next section.

* Basically this is a system in which an electric motor rotates at an angular speed which is strictly proportional to the output voltage from the amplifier ; the angle through which the motor turns is therefore proportional to the integral of the output voltage. The system has been extensively described in engineering literature (e.g. *J. Instn. Elect. Engrs.*, 1947, **94,** Part IIA, 112).

§ 5. Fourier Spectrum of Statistical Fluctuations in a Pile

Since a pile is a chain reacting system, we must use that branch of probability theory which deals with stochastic processes. A comprehensive account of the earlier work in this field is given by Bartlett, Kendall and Moyal (1949).

For the sake of completeness we will state several theorems concerning stochastic processes ; the proofs of some of these theorems will be found in the papers by Bartlett *et al.*

We may define a probability generating function (conveniently abbreviated to p.g.f.) by

$$A=a_0+a_1x+a_2x^2+ \ldots . a_nx^n \quad \ldots . \quad (5.1)$$

where the coefficient of x^n is the probability of obtaining an answer n in an experiment, and thus $\Sigma a_n=1$. If we denote $(\partial A/\partial x)_{x=1}$ by A_x and $(\partial^2 A/\partial x^2)_{x=1}$ by A_{xx}, then the mean value M and the variance v in the experiment are given by

$$\left.\begin{aligned} M\equiv\bar{n}&=A_x,\\ v\equiv\overline{(n-\bar{n})^2}&=A_{xx}-A_x{}^2+A_x. \end{aligned}\right\} \quad \ldots \quad (5.2)$$

If we consider two experiments A and B, and the p.g.f. for the sum of their outcomes is C, then

$$\left.\begin{aligned} C&=AB,\\ C_x&=A_x+B_x,\\ v_c&=v_A+v_B. \end{aligned}\right\} \quad \ldots \ldots \quad (5.3)$$

(It is assumed that the outcome of one experiment has no influence on the other.)

As an extension of (5.3) we see that if we perform the same experiment K times (p.g.f. is A each time), then the p.g.f. is A^K.

We shall now consider what we may call a ' chain experiment ' in which the outcome of a first experiment decides how many times a second experiment is to be made. This type of combination will occur whenever we divide a chain reaction process into two stages. The first stage ends, for instance, with the production of n neutrons, and the probability distribution of the values of n is described by a p.g.f. $P=\Sigma p_n x^n$. In the second stage, every one of these neutrons will produce an independent reaction of its own, resulting in the occurrence of l fissions, $Q=\Sigma q_l x^l$ being the appropriate p.g.f. To obtain the p.g.f. for the complete process, we remember that the p.g.f. for the added results of n identical experiments Q is Q^n. Now if the first experiment always had the result n, there would always be n neutrons at the beginning of the second stage, and the answer to our problem would be Q^n. Actually, the first experiment allows a number of alternatives, each with its probability p_n. Now the probability of any event is equal to the sum of the probabilities of all the alternatives which lead to it. Hence our required p.g.f. is

$$R=p_0Q^0+p_1Q^1+p_0Q^2+ \ldots .$$

This however, can be written more briefly as $R=P(Q)$, i.e. letting P operate on Q.

We may then show that

$$\left.\begin{aligned} R_x &= P_x Q_x, \\ v_R &= P_x v_Q + Q_x{}^2 v_p. \end{aligned}\right\} \quad . \quad . \quad . \quad . \quad . \quad . \quad (5.4)$$

In dealing with fluctuations in a reactor, the difficulty arises that what actually happens at any time depends on the number of neutrons present at that time, while what we are interested in is the number of fissions which have happened up to that time, or what we might call the fission score. As long as we merely want to know average values we can assume that the fission score grows at a rate proportional to the neutron number, but not when we are interested in the fluctuations. Instead we shall introduce a new type of p.g.f., a function of two variables x and y: $F(x, y, t)=\Sigma\Sigma f_{nl}(t)x^n y^l$, where $f_{nl}(t)$ is the probability of finding, at the time t, a number n of neutrons in the reactor, and a fission score of l.

It is easily verified that the mean values and the fluctuations can again be found by forming the appropriate derivatives

$$F_x \equiv (\partial F/\partial x)_{x=y=1} = \bar{n}, \qquad F_y \equiv (\partial F/\partial y)_{x=y=1} = \bar{l},$$

$$F_x \equiv (\partial^2 F/\partial x^2)_{x=y=1} = \overline{n(n-1)}, \quad F_{yy} \equiv (\partial^2 F/\partial y^2)_{x=y=1} = \overline{l(l-1)},$$

$$F_{xy} \equiv (\partial^2 F/\partial x \partial y)_{x=y=1} = \overline{nl}.$$

The quantity $\overline{nl}$ is of no interest in itself but will appear as a link in the calculation.

Consider a small time interval dt after a time t, and what happens to one neutron in that interval.*

If τ is the mean neutron lifetime, the probability of the neutron number being zero at the end of dt is

$$(dt/\tau)(1-K/\nu)$$

where K is the reproduction constant of the pile, ν is the mean number of neutrons per fissions, and the term in brackets is the probability of unproductive neutron capture.

The chance that the neutron score is still one is $1-dt/\tau$ and the chance of fission taking place is $(dt/\tau)\,.\,K/\nu$. Thus the p.g.f. for the chain experiment with one neutron in the time dt is (ϕ if the p.g.f. for the number of neutrons per fission)

$$(dt/\tau)(1-K/\nu)+(1-dt/\tau)x+(dt/\tau)(K/\nu)\phi(y) \quad . \quad . \quad . \quad (5.5)$$

since if fission does take place we have a fission score of unity. In order to study the fluctuations of the Fourier component we consider a detector which has a chance γ to detect a fission, and will contribute an

* We will neglect the presence of delayed neutrons in order to simplify the treatment of the problem. Their presence can be allowed for (unpublished calculations by O. R. Frisch) and does not alter the significance of the present results.

amount $\cos \omega t$ to the result for every fission detected. The p.g.f. for this detector will then be $1-\gamma+\gamma y^{\cos \omega t}$ and we may rewrite (5.5) as

$$x+(dt/\tau)[1-K/\nu-x+(K/\nu)\phi(1-\gamma+\gamma y^{\cos \omega t})]=x+g\,dt. \quad . \quad . \quad (5.6)$$

Now actually we start at time t with n neutrons ; that is we can consider the pile plus measuring equipment as a chain experiment, where the exponent of x (the neutron number) decides how often the experiment described by the p.g.f. (5.6) is to be done in dt. Hence, we obtain the p.g.f. for the system at $t+dt$, that is $F(t+dt, x, y)$, by letting $F(t, x, y)$ operate on $x+g\,dt$; that is, we replace the x in $F(t, x, y)$ by $x+g\,dt$ (cf. the paragraph preceding eqns. (5.4)).

Hence, $F(t+dt, x, y)=F(t, x+g\,dt, y)$.

Also we must have an independent source emitting neutrons at a rate S (if dt is small enough for only one of these neutrons to be emitted during this time, the p.g.f. for this independent source will be $1-S\,dt+S\,dt\,x$), then, by (5.3),

$$F(t+dt, x, y)=F(t, x+g\,dt, y)(1-S\,dt+S\,dt, x).$$

Using Taylor's theorem, and discarding higher powers of dt, we get

$$\partial F/\partial t=g\,\partial F/\partial x+S(x-1)F. \quad . \quad . \quad . \quad . \quad . \quad . \quad (5.7)$$

Differentiating this equation partially with respect to x gives

$$(\partial^2 F/\partial x\,dt)=(\partial g/dx)(\partial F/\partial x)+g(\partial^2 F/\partial x^2)+S(x-1)(\partial F/\partial x)+SF$$

and since $\phi=1$, $g=0$, $F=1$ when $x=y=1$

$$\dot{F}_x=g_x F_x+S.$$

Also from (5.6),

$$\tau g_x=(K/\nu)\phi_x-1=K-1$$

hence

$$\dot{F}_x=F_x(K-1)/\tau+S.$$

If the pile is running steadily $\dot{F}_x=0$, and

$$F_x=S\tau/(1-K). \quad . \quad . \quad . \quad . \quad . \quad . \quad . \quad . \quad (5.8)$$

By differentiating (5.7) partially with respect to y, twice with respect to y, twice with respect to x, once each with respect to x and y, we may obtain

$$\dot{F}_y=g_y F_x, \quad . \quad . \quad . \quad . \quad . \quad . \quad . \quad . \quad . \quad . \quad . \quad . \quad (5.9)$$

$$\dot{F}_{yy}=g_{yy}F_x+2g_y F_{xy}, \quad . \quad . \quad . \quad . \quad . \quad . \quad . \quad . \quad . \quad (5.10)$$

$$\dot{F}_{xx}=(g_{xx}+2S)F_x+2g_x F_{xx}, \quad . \quad . \quad . \quad . \quad . \quad . \quad . \quad (5.11)$$

$$\dot{F}_{xy}=g_{xy}F_x+g_x F_{xy}+g_y F_{xx}+SF_y. \quad . \quad . \quad . \quad . \quad (5.12)$$

In which F_x is a constant given by (5.8) and

$$\left.\begin{aligned} g_{xx}&=K\phi_{xx}/\nu\tau, & g_{xy}&=(K\gamma/\tau)\cos \omega t, \\ g_y&=(K\gamma/\nu\tau)\cos \omega t, & g_{yy}&=(K\gamma/\nu\tau)(\cos^2 \omega t-\cos \omega t). \end{aligned}\right\} \quad (5.13)$$

Integrating (5.9) we have, since $F_y=0$ when $t=0$,

$$F_y=(K\gamma/\omega\nu\tau)(\sin \omega t)F_x. \quad . \quad . \quad . \quad . \quad . \quad . \quad (5.14)$$

If the pile is running steadily, $\dot{F}_{xx}$ as well as $\dot{F}_x$ must be zero.

Therefore from (5.11) we have

$$F_{xx}=-F_x(g_{xx}+2S)/2g_x. \quad . \quad . \quad . \quad . \quad . \quad (5.15)$$

Since at $t=0$, F_y and v_y are both zero, it follows that F_{yy} and $\dot{F}_{yy}$ are both zero at $t=0$. Also for $t=0$, $g_{yy}=0$, and therefore from (5.10), $F_{xy}=0$ at $t=0$.

Thus solving (5.12), using this boundary condition and eqns. (5.14) and (5.15), we have

$$F_{xy}=F_x(\omega^2+\lambda^2)^{-1/2}[A\sin(\omega t-\alpha)-B\sin(\omega t+\beta)-\rho\gamma/2\tau^2(\omega^2-\lambda^2)^{1/2}] \quad (5.16)$$

where $A=[\gamma/2(1-K)][(\rho/\tau)+(2SK/\nu)]$, $B=SK\gamma/\omega\nu\tau$,

$\tan\alpha=g_x/\omega$, $\tan\beta=\omega/g_x$,

$\lambda=(1-K)/\tau$, $\rho=(K/\nu)^2\phi_{xx}+2K(1-K)$.

We can now solve eqn. (5.10) for F_{yy}, using the boundary condition that $F_{yy}=0$ at $t=0$. In the sclution we insert the conditions that $t=2\pi m/\omega$ (i.e. an integral multiple of the modulation period) and that $t\gg 1/\lambda$. We then obtain finally

$$F_{yy}=\frac{F_xK\gamma t}{2\nu\tau}\left\{1+\frac{\rho\gamma}{(1-K)^2(1+\omega^2/\lambda^2)}\right\}$$

since $\omega/\pi m\lambda\ll 1$.

Again since $F_y=0$ for $t=2\pi m/\omega$, $v_y=F_{yy}$, so that,

$$v_y=\frac{\gamma tN_F}{2}\left\{1+\frac{\rho\gamma}{(1-K)^2(1+\omega^2/\lambda^2)}\right\} \quad . \quad . \quad . \quad . \quad (5.17)$$

where $N_F=F_xK/\nu\tau$, the mean fission rate in the pile.

Referring to eqn. (3.2), we see that for the case we are considering, namely a model in which there are no delayed neutrons, $C=0$, and

$$A^2(\omega)=1/(1-K)^2(1+\omega^2/\lambda^2).$$

Thus the variance in the fission score is given by

$$v_y=\pi m\gamma N_F\{1+\rho\gamma A^2(\omega)\}/\omega. \quad . \quad . \quad . \quad . \quad . \quad . \quad (5.18)$$

We have seen that the value of ρ is given by $\rho=\phi_{xx}(K/\nu)^2+2K(1-K)$, and as we have already mentioned, K is very nearly equal to unity for all pile powers above a few watts, so that writing v_ν for the variance in the number of neutrons per fission,

$$\rho=(v_\nu+\nu^2-\nu)/\nu^2. \quad . \quad . \quad . \quad . \quad . \quad . \quad (5.19)$$

Equations (5.18) and (5.19) therefore give the form of the Fourier spectrum of fluctuations in the pile. We have taken a model with no delayed neutrons, but will assume that (5.18) still expresses the form of the pile fluctuations correctly, provided that $A(\omega)$ is now of the form given by (3.2).

If we are only concerned with one modulation cycle of period T and we write $v_y=\sigma_y^2(\omega)$ ($\sigma_y(\omega)$ is the standard deviation in the fission score), then

$$\sigma_y^2(\omega)=T\gamma N_F\{1+\rho\gamma A^2(\omega)\}/2.$$

Now if we are recording these fluctuations on the velodyne integrator, the integrator answers will be proportional to $\sigma_\eta(\omega)$ with the same proportionality factor that the balancing voltage will bear to γN_F—since this latter quantity is the mean fission rate recorded by the ionization chamber. Thus, calling $\sigma(\omega)$ the standard deviation recorded on the integrator, we have

$$\sigma(\omega)/V=\alpha\{T(1+\rho\gamma A^2(\omega))/2\gamma N_F\}^{1/2} \quad . \quad . \quad . \quad . \quad (5.20)$$

where α is a constant of the measuring equipment as explained in § 4.

When the pile fluctuations came to be measured, it was found that the results were complicated by current noise fluctuations from the 10^8 ohm resistor. Current noise is observed only when current is flowing through the resistor and is said to be due to variation in contact resistance between the carbon composition granules which form the resistor (Bisby, Brown and Brownrigg 1952).

We conclude this section by showing how eqn. (5.18) is modified by current noise fluctuations.

Suppose a pulse distribution with p.g.f. A be presented to a chamber which has a chance γ to detect a pulse. The p.g.f. for the chamber will be $1-\gamma+\gamma x$, and from eqn. (5.4) we see that the mean value Z_x and the variance $v_Z=\sigma_Z^2$ recorded by the chamber are given by (in the first instance we neglect the current noise)

$$\begin{aligned} Z_x&=\gamma A_x, \\ v_Z&=Z_x\{1+\gamma(v_A-A_x)/A_x\}, \\ \sigma_Z/Z_x&=\{1+\gamma(v_A-A_x)/A_x\}^{1/2}/Z_x^{1/2}. \quad . \quad . \quad . \quad . \quad (5.21) \end{aligned}$$

Let us denote the p.g.f. for the current noise by I, the mean value of the current per pulse by M_I, and the variance in the current by v_I. Then if C denotes the p.g.f. for the experiment when current noise is considered, we have from (5.4)

$$\begin{aligned} C_x&=M_IZ_x=\gamma A_xM_I, \\ v_c&=\gamma A_xv_I+M_I^2Z_x\{1+\gamma(v_A-A_x)/A_x\}, \\ \sigma_c/C_x&=\{1+v_I/M_I^2+\gamma(v_A-A_x)/A_x\}^{1/2}/Z_x^{1/2}. \quad . \quad . \quad . \quad . \quad . \quad (5.22) \end{aligned}$$

We see from (5.21) and (5.22) that the effect of current noise is to insert the quantity $(1+v_I/M_I^2)$ instead of unity in to the expression for the 'noise to signal ratio' for the experiment.

We may therefore take current noise fluctuations into account in eqn. (5.20) by writing

$$\sigma(\omega)/V=\alpha\{T(1+B(\omega)+\rho\gamma A^2(\omega))/2\gamma N_F\}^{1/2} \quad . \quad . \quad . \quad (5.23)$$

where the term $B(\omega)$ represents the effect of the current noise fluctuations, and is a function of ω since the current noise has a Fourier spectrum.

For a given modulation period and a constant current through the resistor, $B(\omega)$ will be constant; it would, of course, be zero if the resistor were free from current noise.

§ 6. Verification of the Formula for the Pile Fluctuations

Before making measurements on the pile, it was thought necessary to test the electronic equipment on a fluctuation measurement that had been previously studied. To do this, the boron trifluoride ionization chamber was replaced by a high-pressure argon chamber close to a 200 millicurie radium source.

Measurements were made on the integrator using a three-second integration period, and the integrator answers were found to follow a Gaussian distribution.

In this case, it can be shown that

$$\sigma(\omega)/V=\alpha\{T(1+v/m^2)/2\gamma r\}^{1/2}$$

where γ is the chance the argon chamber has to detect a gamma ray, m and v are the mean and variance of the pulses produced in the chamber, and r is the rate of emission of gammas by the source.

Due to the difficulty in estimating γ and v/m^2 exactly, it is not easy to check the width of the Gaussian against the foregoing formula, but the measured value of $\sigma(\omega)$ was certainly of the correct order of magnitude. We were therefore confident that the electronic equipment measured fluctuations correctly. Also, with the boron chamber re-connected but still out of the pile (no current from the chamber) it was found that the integrator recorded zero results. This showed that the pile measurements would not be complicated by any form of electronic noise other than current noise.

Returning now to the measurements on the pile, it is, of course, not necessary to actually modulate the pile in order to measure $\sigma(\omega)$; a measurement with the pile running steadily at any given power level will yield the same values as a modulation experiment. Since it is much easier to make all the fluctuations measurements with the pile running at steady power, this was what was done.

Our measurements were made with a boron neutron detector and not with a fission detector as assumed in the last section. To calculate γ (eqn. (5.23)), therefore, we observe that it will be the ratio of the rate of detection of neutrons by the chamber, to the fission rate in the pile. Also the rate of detection of neutrons by the chamber is proportional to the chamber current and therefore to the balancing voltage, so that we may write $\gamma=CV/N_F$.

It is easy to see that C is the reciprocal of the chamber resistor (10^8 ohms) multiplied by the mean charge produced per boron disintegration in the chamber. This latter quantity is only known with an accuracy of $\pm 30\%$ for our type of chamber, so that γ can only be calculated approximately. We have, therefore, avoided inserting numerical values for γ, except to obtain an order of magnitude.

We may now rewrite (5.23) as

$$\sigma^2(\omega)/VT=\alpha^2\{1+B(\omega)+\rho\gamma A^2(\omega)\}/2C. \quad . \ . \ . \quad (6.1)$$

Since we are trying to make an estimate of the standard deviation in the pile fluctuations, it is useful to know how many observations it is necessary to take in order to obtain an accurate measure of $\sigma(\omega)$. If the individual answers on a set of measurements taken on the pile follow a Gaussian distribution, then the standard deviation in $\sigma(\omega)$ is given by $\sigma(\omega)/\sqrt{(2n)}$ (Whittaker and Robinson 1937), where n is the number of observations.

To make sure that the individual answers recorded on the integrator do give a Gaussian distribution, one set of measurements was taken with a fixed chamber position and a three-second integration period. About 2000 readings of $\sigma^2(\omega)/VT$ were obtained, and these are plotted in fig. 2 ; it will be seen that the distribution is Gaussian.

Fig. 2

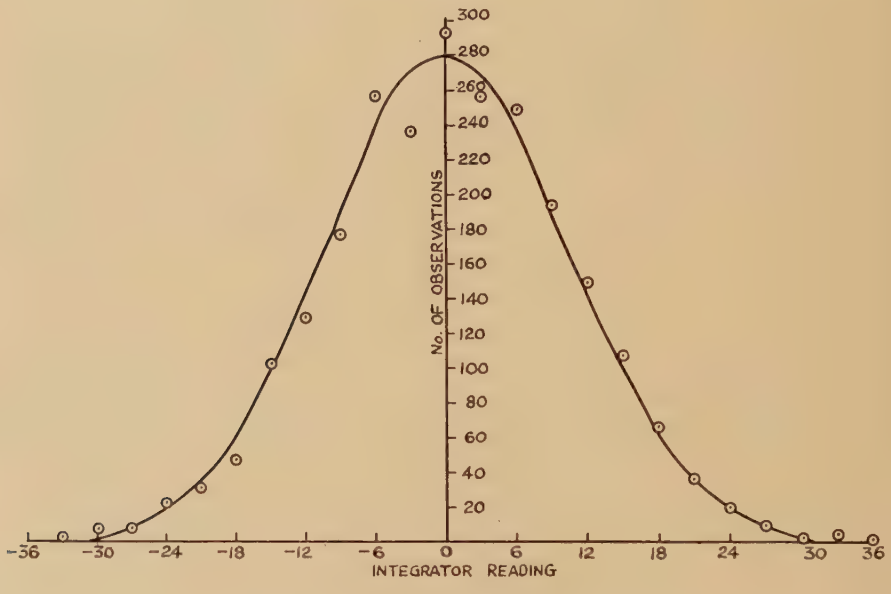

Gaussian distribution from pile fluctuations.

Thereafter, only enough observations were taken for an estimate of $\sigma(\omega)$ to be made with about 10% accuracy, the accuracy being computed from the formula-standard deviation is $\sigma(\omega)/\sqrt{(2n)}$.

It was also found that in many sets of measurements, the mean integrator answer obtained was not zero ; this would be expected for a small number of observations. However, there was no significant difference whether $\sigma(\omega)$ was computed from the measured mean value or from a mean value of zero.

The first experiments were made with the boron trifluoride chamber situated near the centre of the pile ($\gamma \sim 10^{-4}$). It will be seen from eqn. (6.1) that for a constant modulation period ($A(\omega)$ and $B(\omega)$ constant)

and a fixed chamber position (constant γ), the values of $\sigma^2(\omega)/VT$ will be independent of pile power. This was checked by a series of runs made at various pile powers with a constant integration period of 3 seconds, and found correct within the accuracy of the measurements.

Next, the integration period was varied between 1 second and 100 seconds. This range of periods is the range we are interested in using with the pile oscillator; periods of less than 1 second cannot be used because of the time taken to move the sample in and out of the pile, and periods of greater than 100 seconds are unsuitable because it is found in practice that atmospheric pressure variations upset the measurements by changing the amount of nitrogen in the pores of the graphite and hence changing the reproduction constant of the pile.

Fig. 3

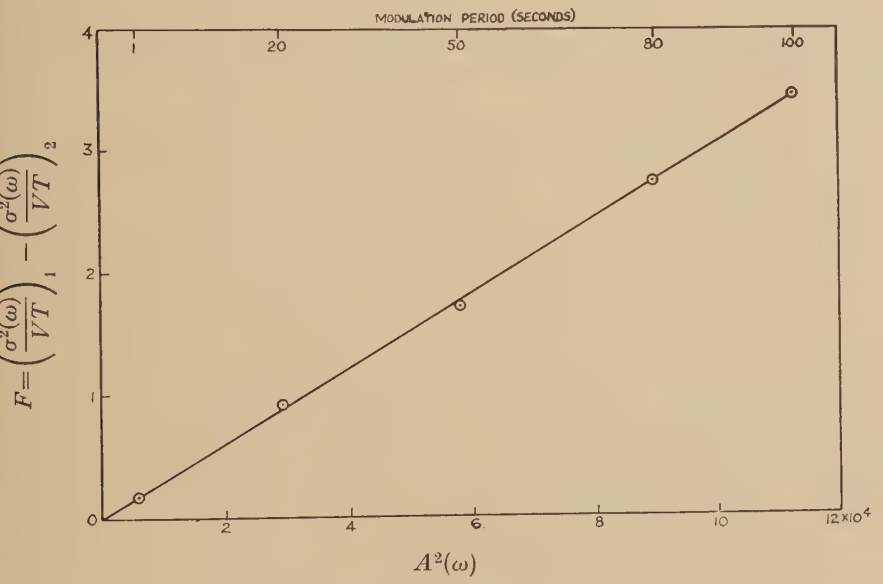

Pile fluctuations as a function of $A^2(\omega)$.

In order to eliminate the term $B(\omega)$ in eqn. (6.1), the measurements were repeated with a different chamber position such that $\gamma \sim 10^{-6}$, the pile power being raised so that the chamber current, and therefore $B(\omega)$, was the same as before. The term $\rho\gamma A^2(\omega)$ in eqn. (6.1) is now negligible, and so we have

$$\{\sigma^2(\omega)/VT\}_2=\alpha^2\{1+B(\omega)\}/2C. \quad . \quad . \quad . \quad . \quad . \quad (6.2)$$

Subtracting the individual sets of measurements in the two experiments we have

$$F=\{\sigma^2(\omega)/VT\}_1-\{\sigma^2(\omega)/VT\}_2=\alpha^2\rho V A^2(\omega)/2N_F. \quad . \quad (6.3)$$

The values of the fluctuation difference F are plotted in fig. 3 against the values of $A^2(\omega)$ determined by Gilbert and Fergusson. It will be seen that F varies linearly with $A^2(\omega)$ as predicted by (6.3).

From the slope of the line in fig. 3, and the known values of α and N_F/V, we may determine ρ. It was found that

$$\rho = 1{\cdot}21 \pm 0{\cdot}15$$

the error in ρ being assessed somewhat arbitrarily since the errors in the experimentally determined values of $A(\omega)$ are not accurately known.

This fits the assumption that the distribution in the number of neutrons per ^{235}U fission is Poisson, when $v_p = \nu$, and therefore from (5.19) $\rho = 1$.

It therefore appears that the formula (5.23) correctly predicts the pile fluctuation spectrum and that $\rho = 1$.

§ 7. Sensitivity of the G.L.E.E.P. Oscillator

We are now in a position to answer the question posed at the end of § 4 as to what is the optimum modulation period to use with the oscillator. First, we notice that we should use a chamber resistor which does not exhibit any current noise, so that the term $B(\omega)$ in (5.23) will be zero. This has now been done on the G.L.E.E.P. oscillator; the carbon composition resistor which was originally used has now been replaced by a 10^8 ohm wire-wound resistor, from which there is no observable current noise.

Putting $B(\omega) = 0$ and $\rho = 1$, we see from (4.1) and (5.23) that the signal/noise ratio for a single modulation experiment of period T is

$$\frac{I(\omega)}{\sigma(\omega)} = \frac{\Delta}{\pi}\left\{\frac{2\gamma N_F T A^2(\omega)}{1+\gamma A^2(\omega)}\right\}^{1/2}.$$

If we perform m modulation experiments each of period T, the signal/noise ratio for the mean of the m experiments, $S(\omega)$, will be improved by a factor $\sqrt{m}$. So that writing $T_0 = mT$ for the total time taken for these m experiments, we have for the signal noise ratio of the mean,

$$S(\omega) = \frac{\Delta}{\pi}\left\{\frac{2\gamma N_F T_0 A^2(\omega)}{1+\gamma A^2(\omega)}\right\}^{1/2}. \quad \ldots\ldots \quad (7.1)$$

For a fixed pile power (N_F constant) a fixed modulation period ($A(\omega)$ constant) and a fixed time T_0, $S(\omega)$ will increase as γ is increased and will tend to the limiting value

$$S = \Delta(2N_F T_0)^{1/2}/\pi. \quad \ldots\ldots \quad (7.2)$$

It will be seen that this expression is independent of modulation period and depends only on the total time taken for the set of experiments. We have the result, therefore, that provided that γ is large enough, the signal/noise ratio is independent of the modulation period chosen.

On the G.L.E.E.P. oscillator itself, we have made γ as large as possible by placing the detecting chamber as near to the centre of the pile as possible. We have also replaced the boron trifluoride chamber by a boron coated chamber, since using this latter chamber we are able to

use high pile powers whilst still keeping the chamber saturated. The highest pile power we can use with the boron coated chamber in its position near the centre of the pile is 3 kw, at which power $N_F \sim 10^{14}$ fissions/sec.

In its position near the centre of the pile the value of γ for the boron coated chamber $\sim 6 \times 10^{-6}$. With this value of γ we have the values (table 1) for the factor by which the theoretical maximum value for the signal/noise ratio (7.2) must be multiplied in order to obtain the actual signal/noise ratio for a given modulation period.

Table 1

Modulation period (seconds)	1	10	20	40	60	80	100	∞
$\left\{\frac{\gamma A^2(\omega)}{1+\gamma A^2(\omega)}\right\}^{1/2}$	0·24	0·33	0·40	0·48	0·54	0·60	0·62	1

We have chosen to use a 40-second period with the G.L.E.E.P. oscillator since this gives us about 0·5 of the theoretical maximum signal/noise ratio, and at this period our measurements are not disturbed very much by atmospheric pressure fluctuations, which at 100 seconds modulation period would have been much more troublesome.

A normal run on the G.L.E.E.P. oscillator consists of twenty measurements each of 40 seconds period ($T_0 = 800$ seconds) done at a pile power of 3 kw. We would therefore expect the signal/noise ratio for the mean of the twenty measurements to be

$$S = 0{\cdot}48 \Delta (2 \times 10^{14} \times 800)^{1/2}/\pi$$
$$= 6 \times 10^7 \Delta. \quad . \quad . \quad . \quad . \quad . \quad . \quad . \quad . \quad (7.3)$$

It is of interest to know what is the standard error in measuring an absorption cross section in such a run. From the boron calibration of the oscillator it is known that 1 cm² of cross sectional area gives a value of $\Delta \sim 1{\cdot}4 \times 10^{-5}$. (Since, as mentioned in § 3, we can use values of Δ up to 3×10^{-3}, this means that we can, in principle, measure cross sectional areas up to 200 cm².) From (7.3) we have, therefore, $S = 8{\cdot}5 \times 10^2 \Sigma$, where Σ is the cross sectional area being measured (expressed in cm²). The standard error in determining a cross section is the value of Σ given by this expression when $S = 1$; the value found is 0·12 mm².

It is found in practice that the standard error of twenty measurements is of the order of $\pm 0{\cdot}16$ mm². This is remarkably close to the value of $\pm 0{\cdot}12$ mm² which would be expected if the pile fluctuations were the only cause of variations in the integrator answers.

Acknowledgments

The theory of the pile fluctuations given in this paper was worked out by O. R. Frisch. The pile measurements were made by D. J. Littler who would like to thank Mr. W. G. L. Brownrigg for his assistance in making these measurements.

Both authors would like to thank the Director of the Atomic Energy Research Establishment for permission to publish this paper.

References

Bartlett, M. S., Kendall, D. G., and Moyal, J. E., 1949, *J. Roy. Statist. Soc.* B, **11** [2], p. 230.

Bisby, H., Brown, L. H., and Brownrigg, W. G. L., 1952, *Electron. Engng.*, **24,** No. 294, p. 385.

Colmer, F. C. W., and Littler, D. J., 1950, *Proc. Phys. Soc.* A, **63,** 1175.

Gilbert, C. W., and Fergusson, G. J., 1948, *Chalk River Report* No. CRP.377.

Whittaker, E. T., and Robinson, G., 1937, *The Calculus of Observations* (London : Blackie), p. 201.

XVIII. *Electronic Conduction in Grey Tin*

By J. T. Kendall*
Electrical Engineering Department,
Imperial College of Science and Technology, London, S.W.7†

[Received in final form November 5, 1953]

Summary

The conductivity and Hall constant of grey tin alloys containing antimony and gallium were measured over a temperature range of 77°K to 286°K. From the results the number of charge carriers and their mobility were calculated as functions of temperature. Large variations of conductivity and Hall constant in a magnetic field were noted. A comparison is drawn with the similar semiconductors silicon and germanium.

In the intrinsic range the conductivity is given by

$$\sigma = 1{\cdot}6 \times 10^4 \exp[-0{\cdot}064/2KT].$$

The energy gap between the filled and unfilled bands, 0·064 ev, does not vary significantly with temperature. The number of charge carriers is therefore given by

$$n_e n_h = 2{\cdot}4 \times 10^{31}\ T^3 \exp[-0{\cdot}064/KT]$$

combined with the expression for electrical neutrality

$$n_e - n_h = n_s$$

where n_s is the number of charge carriers due to the impurity atoms.

In the p-type alloys the Hall constant reverses sign, and from the temperature of this reversal the ratio of the lattice scattering mobilities for electrons and holes can be calculated as

$$C = \mu_e/\mu_h = 1{\cdot}3.$$

In the lattice scattering range the mobilities are given by

$$\left.\begin{aligned} \mu_e &= 11{\cdot}6 \times 10^6\ T^{-3/2}, \\ \mu_h &= 8{\cdot}9 \times 10^6\ T^{-3/2}. \end{aligned}\right\}$$

§ 1. Introduction

Electronic conduction in grey tin has been studied by Busch, Wieland and Zoller (1951), Blum and Goryunova (1950), and Kendall (1950). It has been shown to be a semiconductor similar to silicon and germanium with a separation between the filled and unfilled bands of approximately

---

* Now at The Plessey Company Ltd., Caswell, Towcester.
† Communicated by the Author.

0·1 ev. In the present investigation measurements of electrical conductivity and Hall constant have been made over a temperature range from 77°K to 286°K on grey tin specimens containing known amounts of antimony and gallium. One alloy containing lead was also investigated. The data are analysed to determine the variation of the concentration of current carriers and their mobility with impurity concentration and temperature. The results are interpreted in terms of existing theories of conduction in semiconductors.

The results presented here differ considerably from the above earlier results, particularly in the lower value obtained for the intrinsic activation energy (0·064 ev) and in the much more coherent picture obtained of the variation of the number of charge carriers and their mobility with temperature.

§ 2. Preparation of Specimens

'Spectroscopically pure' tin was obtained from Johnson-Matthey Ltd. Chemical analysis by the suppliers gave the following results :—

Lead	0·0012%	Antimony	0·001%
Iron	0·00027%	Copper	0·0002%
Arsenic	0·0002%	Bismuth	0·0001%
Sulphur	0·0003%	Tin	99·997%

The alloys shown in table 1 were made by melting the constituents *in vacuo*, and were then converted to the grey modification by seeding with a minute quantity of pure grey tin and storing at −50°C *in vacuo* until conversion was complete, as determined by an x-ray powder photograph. During the conversion the metal crumbles to a fine powder.

Table 1. Compositions of Tin Alloys

1 Sample	2 Impurity	3 Atomic % added	4 Atoms/cc added	5 Carriers/c.c. at low temp.	6 Sign of carriers	7 Carriers due to added impurity	8 Carriers/ atoms
(1)	—	0	0	$3{\cdot}25\times10^{17}$	—	0	—
(2)	Sb	0·0143	$4{\cdot}18\times10^{18}$	$2{\cdot}52\times10^{18}$	—	$2{\cdot}20\times10^{18}$	0·53
(3)	Sb	0·0279	8·17	4·08	—	3·76	0·46
(4)	Sb	0·0740	$2{\cdot}16\times10^{19}$	8·47	—	8·15	0·38
(5)	Sb	0·310	9·07	$2{\cdot}16\times10^{19}$	—	$2{\cdot}13\times10^{19}$	0·24
(6)	Ga	0·0060	$1{\cdot}76\times10^{18}$	$7{\cdot}0\times10^{17}$	+	$1{\cdot}02\times10^{18}$	0·58
(7)	Ga	0·0119	3·48	$1{\cdot}24\times10^{18}$	+	1·56	0·45
(8)	Ga	0·0806	$2{\cdot}36\times10^{19}$	8·15	+	8·48	0·36
(9)	Ga	0·322	9·42	$2{\cdot}70\times10^{19}$	+	$2{\cdot}73\times10^{19}$	0·29
(10)	Ga	0·063	$1{\cdot}84\times10^{19}$				
	Sb	0·056	$1{\cdot}63\times10^{19}$				
	Difference		$2{\cdot}1\times10^{18}$	$4{\cdot}40\times10^{17}$	+	$7{\cdot}65\times10^{17}$	0·36
(11)	Pb	0·025	$7{\cdot}32\times10^{18}$	$8{\cdot}00\times10^{17}$	—	$4{\cdot}75\times10^{17}$	0·065

Unsuccessful attempts were made to prepare crystals by electrolytic deposition at a temperature below the transition point (13·2°C), evaporation *in vacuo* on a cold surface of grey tin, crystallization from concentrated hydrochloric acid, and crystallization from mercury.

It was found possible to press grey tin powder into cylindrical specimens (0·25″ diameter and slightly over 0·5″ long) by carrying it out at a temperature of approximately −125°C. A pressure of 10 tons/sq. in. was used and the mould was cooled with liquid nitrogen. The specific gravity of the specimens was 5·75, and no lines of tetragonal white tin were observed in an X-ray powder photograph. Usually some reversion to white tin occurred on the side-surfaces of the specimens. This was easily removed either by dissolving the surface in dilute hydrochloric acid or by storing the specimen at −50°C overnight.

If grey tin powder at ordinary temperature is subjected to pressure it reverts back to white tin. A study of the dependence of the transition temperature on pressure has been made by Komar (1936) and he finds that it changes according to $\partial T/\partial P = -5\times10^{-2}$ °C/Atmosphere. A pressure of 10 tons/sq. in. will thus lower the transition temperature to −62°C. Using a mould cooled with liquid nitrogen a thermocouple measurement of the temperature of the inside of the mould filled with grey tin powder was −125°C under working conditions.

§ 3. Experimental Procedure

3.1. *Conductivity*

The electrical conductivity was measured by a potential-probe method. The voltage drop along the length of the specimen was measured independently of the current carrying circuit by the introduction of probe electrodes. The specimen holder is shown in fig. 1, and it is seen that the polystyrene tube enclosing the specimen is perforated by two holes through which thin platinum-iridium wires (0·06 mm diameter) are pushed into contact with the grey tin. These holes were placed 0·50″ apart and arranged to be near the end surfaces of the grey tin cylinder.

The specimen holder was immersed in a vacuum flask filled with methyl cyclohexane for temperatures down to about −80°C and with liquid propane for lower temperatures. This liquid medium was kept stirred with a small motor-stirrer and was cooled by additions of liquid nitrogen. For the very lowest temperature the specimen holder was immersed directly in liquid nitrogen.

The temperature was measured by means of an Fe/NiCr thermocouple recessed into the polystyrene cylinder as shown in fig. 1. The thermocouple was calibrated at several fixed temperatures. After addition of liquid nitrogen to the bath an interval of about 5 minutes was required for the attainment of temperature equilibrium. In practice about 10 minutes was allowed. It was found convenient to carry out measurements at a series of fixed temperatures corresponding to $10^3/T = 13, 12, 11, 10, 9, 8, 7, 6{\cdot}5, 6, 5{\cdot}5, 5, 4{\cdot}5, 4, 3{\cdot}5$.

The electrical measuring circuit was conventional, a d.c. potentiometer being used for measuring all voltages. In practice the use of the probe electrodes did not appear to be really necessary as the voltage drop across the current-carrying contacts was always very small compared with the voltage drop along the length of the specimen.

3.2. *Hall Effect*

Platinum–iridium probe electrodes were placed on opposite sides of the grey tin specimen as shown in fig. 1. The specimen holder and its container were placed between the poles of an electromagnet, the Hall probes being transverse to the direction of the field. The current through the sample and the direction of the magnetic field were both reversed

Fig. 1

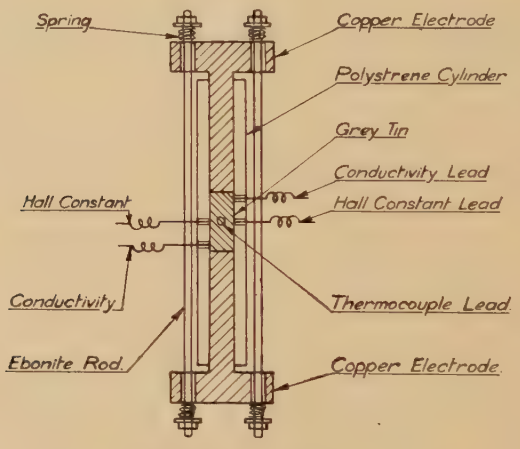

Specimen holder.

independently and the four Hall voltages thus obtained generally differed slightly (presumably due to thermo-electric effects). The mean value was taken. The magnetic field strength was determined by measuring the current through the windings after calibrating by means of a small search coil and ballistic galvanometer.

The Hall constant R, in cm^3/Coulomb, was calculated from the relation

$$R=10^8Vt/HI \quad . \quad . \quad . \quad . \quad . \quad . \quad . \quad . \quad (1)$$

where V is the measured Hall voltage in volts, t is the thickness of the sample in cm, H the magnetic field strength in gauss, and I the current in amperes.

The use of a cylindrical specimen for Hall measurements is unusual, but it is not thought necessary to introduce any geometric factor into the above formula. Isenberg (1948) has shown that for a rectangular specimen with a ratio of length to width of 2 (as used here) the Hall constant is reduced to 0·93 of its normal value. However, for a

cylindrical specimen this reduction will be smaller, and we have therefore taken the geometric factor to be unity in the present case.

3.3. *Variation of R and σ with Magnetic Field Strength*

A considerable variation of R and σ with H was noticed with the purer alloys especially at low temperatures. This effect was used to estimate mobilities of charge carriers. The current through the specimen was maintained constant, and values of the potential difference along the length of the specimen and of the Hall e.m.f. were measured as functions of field strength.

§ 4. Experimental Results

4.1. *Conductivity (at zero magnetic field)*

The results are given in fig. 2. For the straight-line portion of curve (1) (pure grey tin) the conductivity is given by

$$\sigma=\sigma_0 \exp\left[-\epsilon/2KT\right] \quad . \quad . \quad . \quad . \quad . \quad . \quad . \quad (2)$$

where $\sigma_0=1{\cdot}6\times10^4$ ohm^{-1} cm^{-1} and $\epsilon=0{\cdot}064$ ev.

Fig. 2

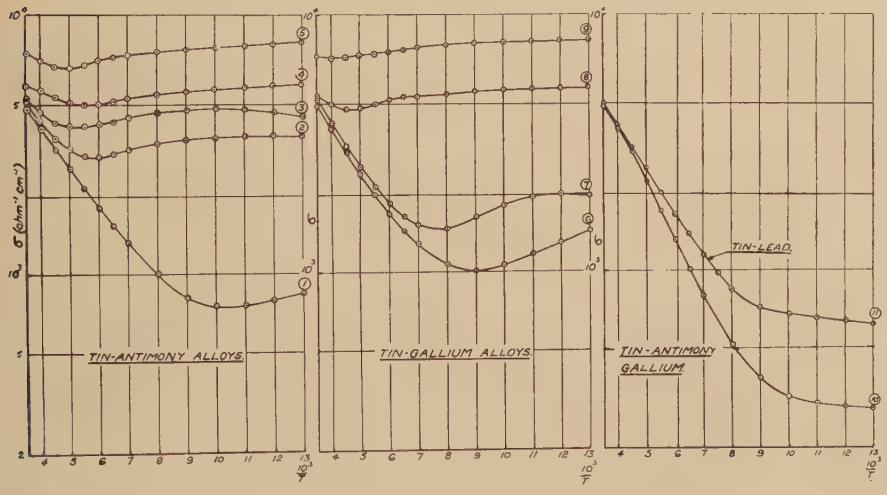

Variation of conductivity with temperature.

This value of ϵ is also obtained from the other curves, except the alloy containing approximately equal amounts of gallium and antimony. Slightly different values of σ_0 are obtained for the different alloys, the smallest value being for the purest material.

4.2. *Hall Constant (at zero magnetic field)*

The results are given in fig. 3. It will be seen that as the temperature is decreased R increases exponentially until a saturation value is reached corresponding to the number of impurity charge-carriers.

In the case of alloys (6)–(10) positive values of R were obtained,

indicating hole-conduction, except at high temperatures in the case of alloys (6), (7) and (10). In these curves a reversal of sign took place and from the curves a temperature can be found for which $R=0$.

4.3. *Variation of R and σ with H*

The results for alloys (1) and (6) are given in figs. 4 and 5. The effect was also measured for the other alloys. In the case of alloy (1) the variation of R is plotted against H^2 for low fields in figs. 6 and 7. This procedure is necessary in order to extrapolate to $H=0$, thus finding the Hall constant at zero field. The same procedure was followed for all the alloys.

Fig. 3

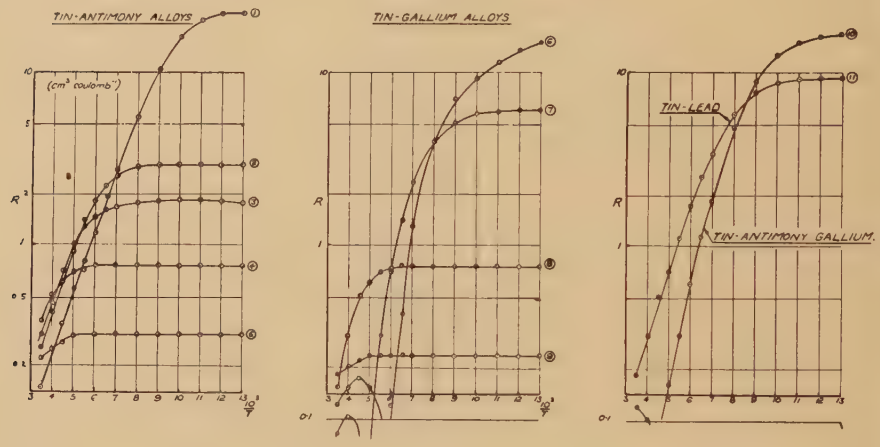

Variation of Hall constant with temperature.

§ 5. Interpretation of Conductivity and Hall Constant Measurements

(*a*) It will be noted that ϵ does not vary with temperature (within the limits of experimental error).

We may therefore use the relation derived from statistical mechanics (Fowler):

$$n_e n_h = 2{\cdot}4 \times 10^{31} \times T^3 \times \exp\,[-\epsilon/KT]. \quad . \quad . \quad (3)$$

This relationship will hold whatever the purity of the sample.

In the case of Si a multiplying factor of 32·5 is needed on the right-hand side of this equation, and in the case of Ge a multiplying factor of 3·5.

If this is taken to be due to a linear variation of ϵ with T,

i.e. $$\epsilon_T = \epsilon_0 - \beta_T. \quad . \quad . \quad . \quad . \quad . \quad . \quad . \quad . \quad (4)$$

Then we have

$$\exp\,[-\epsilon_T/KT] = \exp\,[\beta/K] \times \exp\,[-\epsilon_0/KT]. \quad . \quad . \quad . \quad (5)$$

The multiplying factor is thus $\exp\,[\beta/K]$.

Since in the case of grey tin β must be very small we may take the multiplying factor to be unity.

Fig. 4

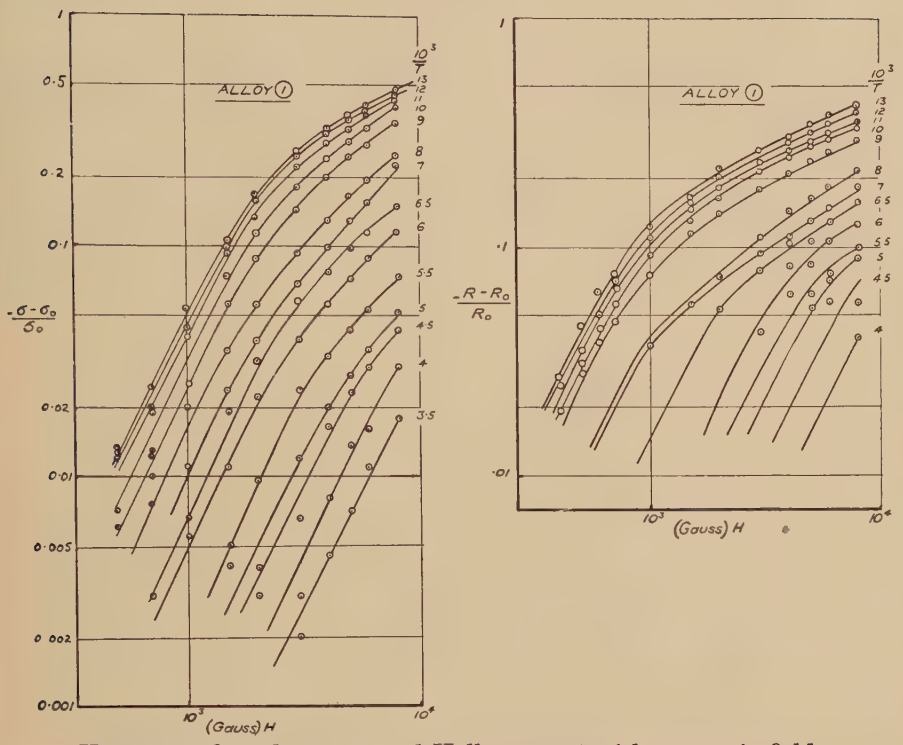

Variation of conductivity and Hall constant with magnetic field.

Fig. 5

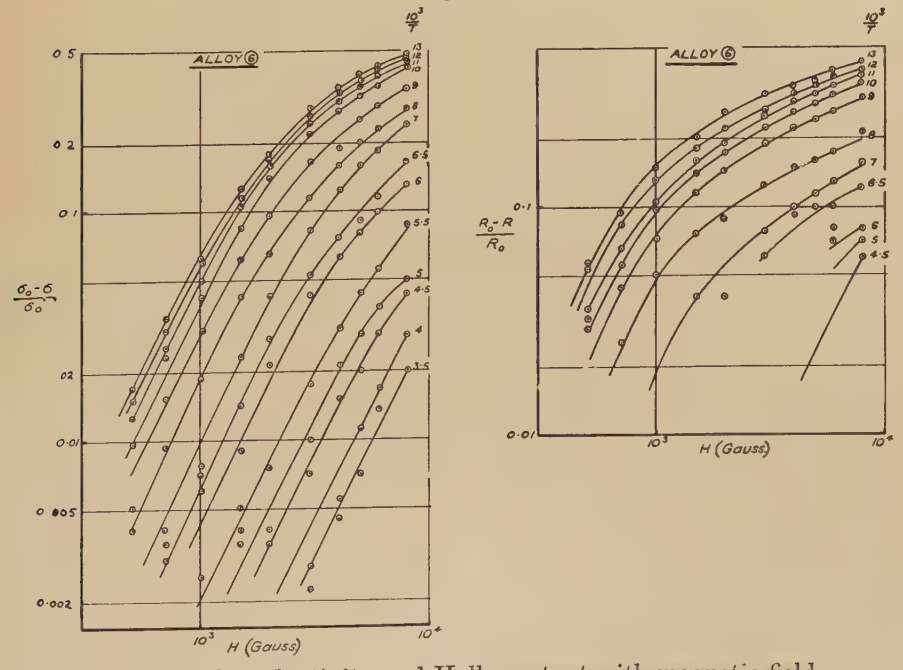

Variation of conductivity and Hall constant with magnetic field.

(*b*) From fig. 3 (Hall constant for tin–gallium alloys) the maximum values of R are :

Alloy (6)$\sim$10·6, Alloy (7) 6·0.

Assuming these alloys are non-degenerate at low temperatures and that $n_e \ll n_h$ then we may calculate the number of charge carriers due to impurities as

$$n_s = -7{\cdot}4 \times 10^{18}/R = (6)\ 7{\cdot}0 \times 10^{17},\ (7)\ 1{\cdot}24 \times 10^{18}.$$

Also from fig. 3, $R=0$ when $10^3/T = (6)$ 5·65, (7) 4·90.

Fig. 6

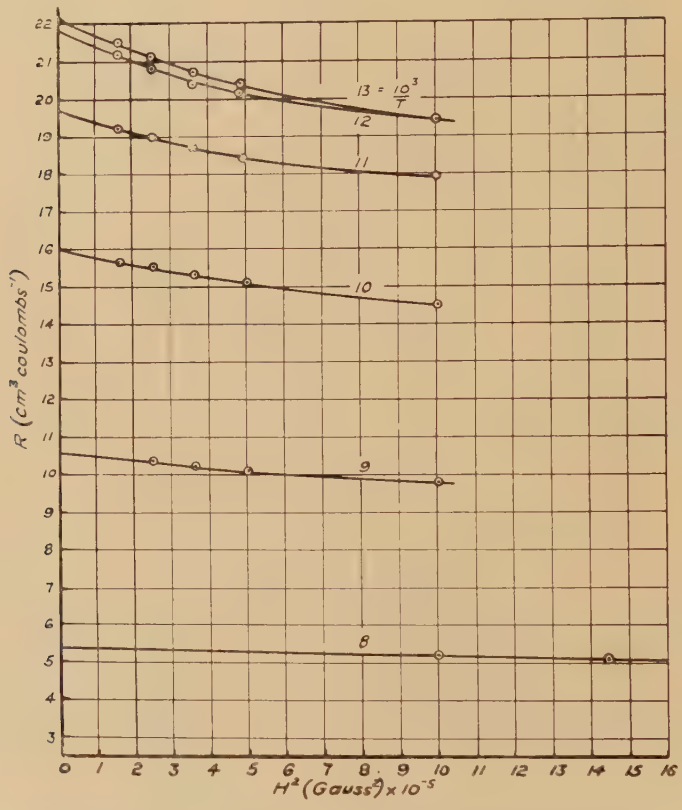

Variation of Hall constant with magnetic field, alloy (1).

Using eqn. (3) we may calculate $n_e n_h$ at the temperature at which $R=0$,

$$n_e n_h = (6)\ 2{\cdot}08 \times 10^{36},\ (7)\ 5{\cdot}55 \times 10^{36}.$$

Also, at all temperatures

$$n_s = n_h - n_e. \qquad \ldots\ldots\ldots \quad (6)$$

From eqn. (3) for $n_e n_h$ and (6) for $n_h - n_e$ we may now calculate n_e and n_h separately at all temperatures.

For temperatures at which $R=0$ we obtain :

$$\left.\begin{aligned}(6)\ n_e&=1{\cdot}05\times10^{18},\quad n_h=1{\cdot}75\times10^{18},\\(7)\ n_e&=1{\cdot}82\times10^{18},\quad n_h=3{\cdot}05\times10^{18}.\end{aligned}\right\}$$

Now at $R=0$, the Hall constant is given by

$$R=-7{\cdot}4\times10^{18}(n_eC^2-n_h)/(n_eC+n_h)^2=0 \quad . \quad . \quad . \quad . \quad (7)$$

where $C=\mu_e/\mu_h$.
Therefore, at these temperatures, $C=\sqrt{(n_h/n_e)}=$(6) 1·29, (7) 1·30. We will take $C=1{\cdot}3$.

Fig. 7

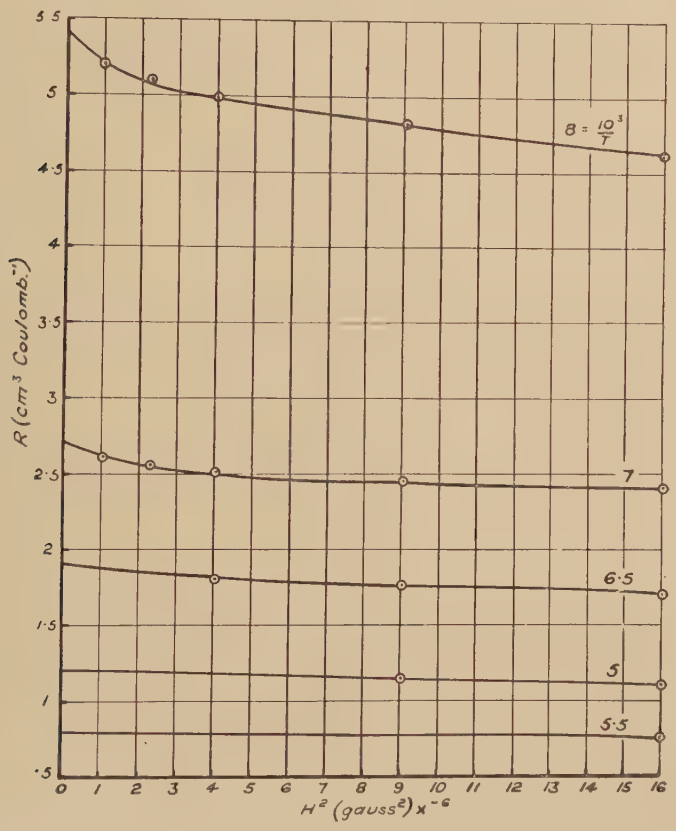

Variation of Hall constant with magnetic field, alloy (1).

(*c*) The critical temperature (T_c) for the transition from non-degenerate to degenerate conditions is that for which the energy of an electron or hole corresponding to the energy at the surface of the Fermi distribution is equal to KT_c.
We thus have

$$T_c=(h^2/8\ \mathrm{km})(3/\pi)^{2/3}n^{2/3}=4{\cdot}2\times10^{-11}n^{2/3}. \quad . \quad . \quad . \quad (8)$$

(*d*) Using eqn. (6) and the relationship

$$R=-7{\cdot}4\times10^{18}(n_eC^2-n_h)/(n_eC+n_h)^2 \quad . \quad . \quad . \quad . \quad (9)$$

we may now calculate n_e and n_h separately at all temperatures for the non-degenerate samples.

For the degenerate samples we may substitute the numerical factor 6·25 in place of 7·4 in eqn. (9). For samples which are on the border-line between degenerate and non-degenerate we may use a weighted mean of the two numerical factors.

In the lattice scattering range we take $C=1{\cdot}3$. In the impurity scattering range we take $C=1$. In the transitional range a weighted mean (obtained graphically) must be used. In practice this variation of C makes only a slight difference in the cases of some of the alloys over a range where $n_e \approx n_h$ corresponds with the transitional region.

Fig. 8

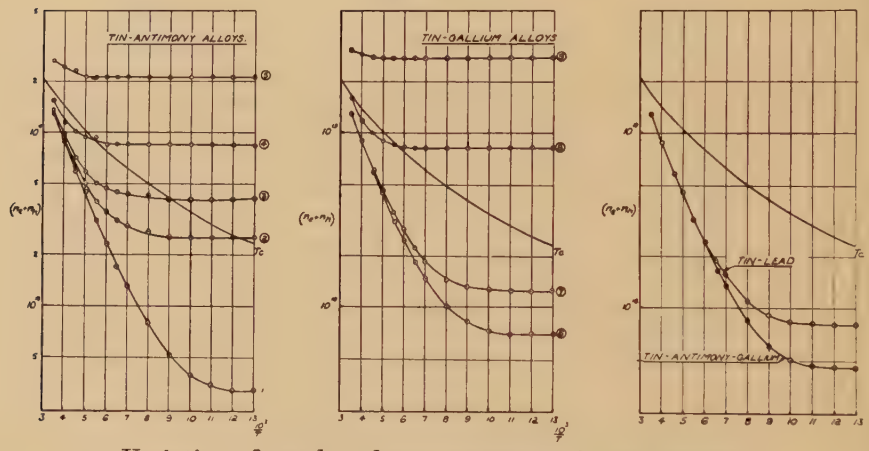

Variation of number charge-carriers with temperature.

The values obtained for n_e and n_h are not shown separately, but values of n_e+n_h are given in fig. 8. The boundary between the degenerate and non-degenerate samples is shown by plotting T_c. It is seen that the number of charge carriers increases exponentially in the intrinsic range and is constant in the impurity range.

(*e*) Using the relationships

$$\sigma=en_e\mu_e+en_h\mu_h \quad . \quad . \quad . \quad . \quad . \quad . \quad . \quad . \quad (10)$$

and

$$\mu_e=1{\cdot}3\times\mu_h \quad . \quad . \quad . \quad . \quad . \quad . \quad . \quad . \quad (11)$$

we may now calculate values for μ_e and μ_h in the lattice-scattering range. In the impurity-scattering range we must take $\mu_e=\mu_h$. For intermediate ranges we must take a weighted mean of the numerical ratios 1·3 and 1·0 (found graphically). In practice this makes only a slight difference and then only when $n_e \approx n_h$ in the intermediate range. The results are given in fig. 9.

It is seen that in the lattice-scattering range μ_e and μ_h are given by the equations

$$\mu_{eL}=11{\cdot}6\times10^6T^{-3/2}, \quad . \quad . \quad . \quad . \quad . \quad . \quad . \quad (12)$$

$$\mu_{hL}=8{\cdot}9\times10^6T^{-3/2}. \quad . \quad . \quad . \quad . \quad . \quad . \quad . \quad (13)$$

Impurity scattering gives rise to lower mobilities and the greater the number of impurity atoms the smaller the mobility.

§ 6. Discussion

6.1. *Ratio of Charge Carriers to Impurity Atoms*

In column 5 of table 1 the number of charge carriers per c.c. has been calculated from the value of the Hall constant at low temperatures. A positive value indicates that the carriers are holes, a negative value that they are electrons.

Fig. 9

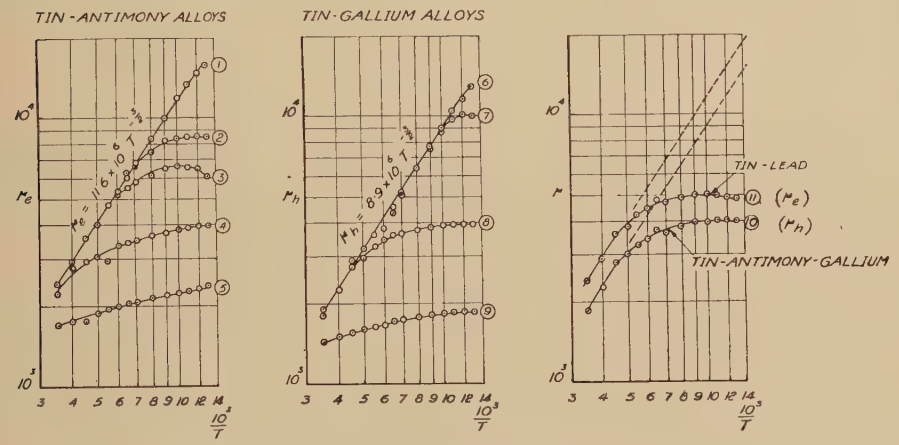

Variation of carrier mobility with temperature.

The pure sample, to which no impurity has been added, contained $3{\cdot}25\times10^{17}$ free electrons at low temperature. This represents the carriers due to impurities originally present in the 'spectroscopically pure' sample. The value of $3{\cdot}25\times10^{17}$ is therefore subtracted from the n-type samples in column 5, and added to the p-type samples, to give the values in column 7 which are the carriers due to the added impurities.

It will be noted that the values in columns 7 and 4 are not the same, and their ratio is given in column 8. If every impurity atom added gave rise to one carrier this ratio would be unity. It is less than unity because a proportion of the added impurity atoms is ineffective in giving rise to carriers. Presumably this is due to a proportion of the added impurity atoms being precipitated at crystal boundaries or elsewhere and thus not entering the grey tin lattice. It will be noted that the

more impure the sample the smaller the proportion of effective impurity atoms. In this, antimony and gallium appear to behave similarly.

In the case of lead, either only a very small proportion enters the lattice substitutionally or some other factor is operating to cut down the effectiveness. It is difficult to understand why lead should give rise to a carrier at all, as it has the same valency as tin. It does not seem likely that the carriers are due to an impurity in the lead as ' spectroscopically pure ' material was used.

6.2. *Concentrations of Electrons and Holes*

The values of n_e and n_h as functions of temperature may also be calculated without knowing the Hall constant by making use of the theoretical equation (3) for the product $n_e n_h$. The values so calculated come out to be within the limits of experimental error in the measurement of the Hall constant throughout the entire range of temperature.

In the case of silicon, Pearson and Bardeen (1949) did not obtain such close agreement and therefore cast doubt on the adequacy of the theory of the Hall effect in the intrinsic range. In the case of grey tin the theory seems to be quite adequate.

6.3. *Mobilities of Electrons and Holes*

For the non-degenerate samples the mobilities of electrons and holes approach the same values at high temperatures for all impurity concentrations. This is due to lattice scattering and it is found that μ varies as $T^{-3/2}$.

At lower temperatures impurity scattering becomes important, although the temperature range investigated did not extend sufficiently low for an accurate evaluation to be made of this effect. Making a rough comparison with the impurity scattering observed in silicon alloys by Pearson and Bardeen (1949) it is remarkable that in grey tin the scattering by impurity atoms seems to be less effective by a factor of about 100. The reason for this is not at all apparent.

For the degenerate samples the mobility should be relatively insensitive to temperature, and this is seen to be generally true, although alloy (3) which should be degenerate at low temperatures shows a significant decrease in mobility at low temperatures, i.e. it seems to behave as though it were non-degenerate.

6.4. *Tin–Gallium–Antimony Alloy*

This alloy has a comparatively large impurity content, but only a small number of charge carriers owing to the mutual neutralization of n- and p-type impurity centres. The p-type impurities are in slight excess. The conductivity-temperature relation is unusual in that the slope of $\log \sigma/T^{-1}$ is not constant in the intrinsic range (fig. 2).

The Hall constant has the value one would expect from the difference in the Sb and Ga contents. The mobility approximates to the value one

would expect from the sum of the Sb and Ga contents. It would thus appear that neutral scattering atoms are just as effective as ionized ones.

6.5. *Tin–Lead Alloy*

Although the impurity concentration is comparatively large the number of free charge carriers produced is small and the Hall constant is therefore large. The mobility corresponds to approximately what one would expect from the added impurity concentration so that a much larger proportion of the lead must go into substitutional positions than is effective as a carrier producer.

The simplest assumption to make would be that lead itself contained an impurity (e.g. antimony) which was the effective electron-producing agent, while the lead remained only a neutral scattering agent. However about 10% of impurity in the lead would be required, and in fact spectroscopically pure lead was used.

6.6. *Variation of Conductivity and Hall Constant in a Magnetic Field*

(*a*) *Conductivity*

At low fields we have

$$(\sigma_0-\sigma)/\sigma_0=\frac{9\pi}{64}\times(4-\pi)\times\mu^2H^2 \quad . \quad . \quad . \quad . \quad . \quad (14)$$

(Pearson and Suhl 1951, Estermann and Foner 1950).

Values of $(\sigma_0-\sigma)/\sigma_0$ for alloys (1) and (6) are plotted against H in figs. 4 and 5. It is seen that at low fields the H^2 law is obeyed but at higher fields the relationship falls to a lower power of H. From the values in the low-field region an estimate of the mobility of the charge carriers may be obtained. Introducing numerical values into eqn. (14) and changing from e.s.u. to practical units, we obtain

$$(\sigma_0-\sigma)/\sigma_0=0{\cdot}38\mu^2H^2\times10^{-16}. \quad . \quad . \quad . \quad . \quad (15)$$

Values of mobility calculated from this equation are given in table 2. It is seen that much higher values of mobility are obtained by this method, especially at low temperatures ; also that the mobility of holes appears to be higher than that of electrons. These effects have also been observed by Pearson and Suhl (1951) in germanium.

(*b*) *Hall Constant*

Electronic theory gives a similar formula for the variation of the Hall constant with transverse magnetic field

$$(R_0-R)/R_0=\frac{9\pi^2}{64}\mu^2H^2, \quad . \quad . \quad . \quad . \quad . \quad . \quad (16)$$

or in practical units

$$(R_0-R)/R_0=1{\cdot}38\mu^2H^2\times10^{-16}. \quad . \quad . \quad . \quad . \quad . \quad (17)$$

Values of $(R_0-R)/R_0$ for alloys (1) and (6) are plotted against H in figs. 4 and 5. It is seen that at low fields an H^2 law is obeyed, but at higher fields the relationship falls to a lower power of H (even lower than in the case of the magneto-resistance effect). From the values in

the low-field region an estimate of the mobility of the charge-carriers may be obtained, and these are given in table 2. It is seen that the values in general agree with those estimated from the magneto-resistance effect.

Table 2

Mobilities calculated from :—

1. $(R_0-R)/R_0H^2=1{\cdot}38\mu_R^2\times10^{-16}$
2. $(\sigma_0-\sigma)/\sigma_0H^2 \ =0{\cdot}38\mu_\sigma^2\times10^{-16}$
3. μ_e (from § 5 (*e*))
4. μ_h (from § 5 (*e*))
5. μ_m (mean mobility) $=(n_e\mu_e+n_h\mu_h)/(n_e+n_h)$

	Alloy (1)				Alloy (6)			
$10^3/T$	μ_R	μ_σ	μ_e	μ_m	μ_R	μ_σ	μ_h	μ_m
13	35000	35700	16000	16000	37000	41800	13000	13000
12	33400	33800	14800	14800	35000	39600	11700	11700
11	30600	32300	13300	13200	31000	36200	10400	10400
10	28100	28400	11900	11600	27500	32000	9000	9100
9	25400	25000	10000	9550	24000	27600	7500	7650
8	18000	20400	8400	7800	18500	21700	6400	6700
7	16300	16200	6800	6200	12000	15900	5200	5600
6·5	10400	13100	6300	5600		12600	4600	5100
6	6300	11200	5400	4700		10600	3800	4400
5·5	5000	7200	4750	4200		7200	3600	4000
5	4100	5600	4000	3500		5600	2950	3400
4·5	3200	4800	3600	3000	2600	4800	2750	3000
4	2100	3600	2900	2600		3400	2250	2550
3·5		2800	2400	2150		2800	1900	2100

6.7. *Activation Energy of Impurity Electrons*

The activation energies for the ionization of donators and acceptors can be estimated as approximately 0·005 ev. This follows from the Bohr formula

$$E_I=2\pi^2me^2/\kappa^2h^2.$$

Setting κ (dielectric constant) equal to 50 (Moss 1952) gives

$$E_I=13{\cdot}5/50^2=0{\cdot}005 \text{ ev.}$$

This corresponds to a temperature of 60° abs. so that we may assume that all the impurity centres are ionized throughout the temperature range investigated.

6.8. *Comparison with other Homopolar Semiconductors*

Some of the fundamental electronic properties of the homopolar semiconductors are given in table 3.

The variation of the energy gap ϵ with the crystal lattice constant a can be empirically correlated by means of the relationship

$$\epsilon=6{\cdot}2\exp[-a^{5{\cdot}5}/6400].$$

Table 3. Properties of Homopolar Semiconductors

	σ_0	ϵ	$\partial\epsilon/\partial T$	κ	$\mu_e T^{3/2}$	$\mu_h T^{3/2}$	μ_e/μ_h	a
C	$1{\cdot}2\times10^{2}$ (a)	5·2 (a)	$1{\cdot}6\times10^{-4}$ (b)	5·68 (c)	$4{\cdot}7\times10^{6}$ (d)	1×10^{6} (e)	4·7	3·56 (f)
Si	$9{\cdot}1\times10^{3}$ (g)	1·12 (g)	3×10^{-4} (g)	11·8 (g)	$1{\cdot}56\times10^{6}$ (g)	$0{\cdot}5\times10^{6}$ (g)	3·0	5·43 (f)
Ge	$3{\cdot}3\times10^{4}$ (h)	0·75 (h)	1×10^{-4} (i)	16 (f)	19×10^{6} (j)	$8{\cdot}9\times10^{6}$ (j)	2·1	5·65 (f)
Sn	$1{\cdot}6\times10^{4}$ (l)	0·064 (l)	~0 (l)	~50 (f)	$11{\cdot}6\times10^{6}$ (l)	$8{\cdot}9\times10^{6}$ (l)	1·3	6·49 (k)

(a) Wartenberg, H., 1912, *Phys. Z.*, **13,** 1123.
(b) Robertson, R., Fox, J. J., and Martin, A. E., 1934, *Phil. Trans. Roy. Soc.* A, **232,** 463.
(c) Whitehead, S., and Hackett, W., 1939, *Proc. Phys. Soc.*, **51,** 173.
(d) Klick, C. C., and Maurer, R. J., 1949, *Phys. Rev.*, **76,** 179.
(e) McKay, K. G., 1950, *Phys. Rev.*, **77,** 816.
(f) Moss, T. S., 1952, *Photoconductivity* (London : Butterworth).
(g) Pearson, G. L., and Bardeen, J., 1949, *Phys. Rev.*, **75,** 865.
(h) Bardeen, J., and Brattain, W. H., 1949, *Phys. Rev.*, **75,** 1208.
(i) Shockley, W., 1950, *Electrons and Holes in Semiconductors* (New York : Van Nostrand).
(j) Haynes, J. R., and Shockley, W., 1951, *Phys. Rev.*, **81,** 835.
(k) Brownlee, L. D., 1950, *Nature, Lond.*, **166,** 482.
(l) This paper.

This relationship is shown plotted in fig. 10 and it is seen that all the points lie exactly on a straight line. It is interesting that the substance silicon carbide, which is nearly homopolar in its properties, also lies very near the straight line. Moss (1952) gives a similar empirical relationship, but the one given here is more accurate.

Fig. 10

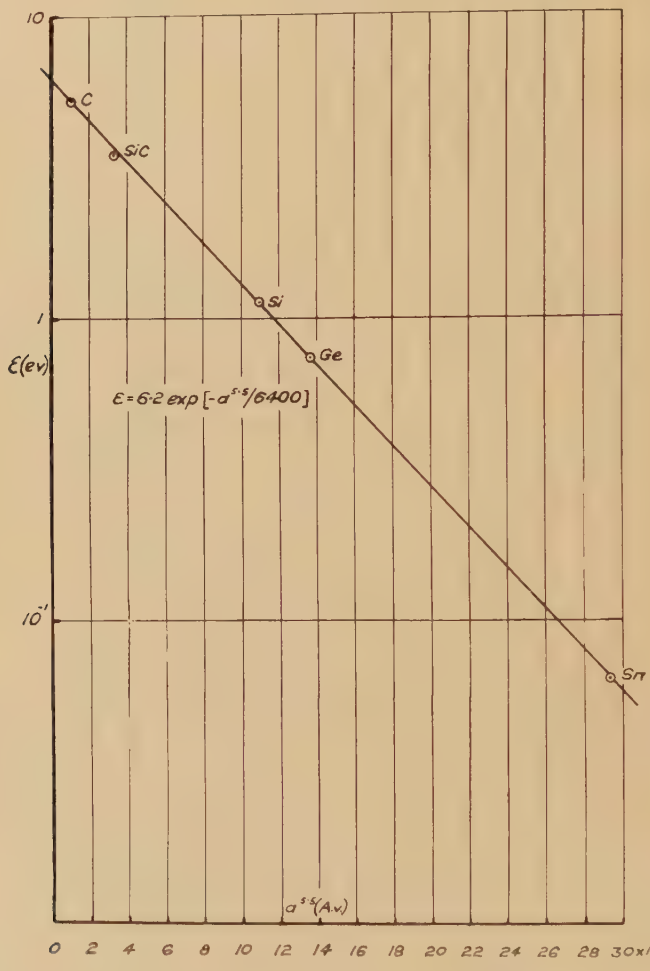

Relationship between activation energy and lattice constant,

The mobility of holes in grey tin is the same as in germanium in the lattice scattering range. The mobility of electrons is somewhat smaller. In the impurity scattering range the mobilities in grey tin are very much larger than in germanium or silicon.

In table 4 the intrinsic conductivities of the homopolar elements are compared at various temperatures. There is seen to be an enormous

variation from diamond to grey tin. In table 5 the number of free intrinsic charge carriers is similarly compared.

Table 4. Intrinsic Conductivity
(Calculated from $\sigma=\sigma_0 \exp[-\epsilon/2KT]$)

ohm^{-1} cm^{-1}				
T (°K)	C	Si	Ge	Sn
1000	$1{\cdot}2\times10^{-11}$	14	480	11000
500	$1{\cdot}3\times10^{-24}$	$2{\cdot}3\times10^{-2}$	7	7500
290	$2{\cdot}4\times10^{-43}$	$2{\cdot}1\times10^{-6}$	$1{\cdot}4\times10^{-2}$	4500
200		$9{\cdot}1\times10^{-11}$	$2{\cdot}0\times10^{-5}$	2500
100		$9{\cdot}1\times10^{-25}$	$1{\cdot}3\times10^{-14}$	400

Table 5. Number of Charge Carriers (calculated from $n=2(n_e n_h)^{1/2}=2(2{\cdot}3\times10^{31}T^3 \exp[-\epsilon/KT] \exp[\beta/K])^{1/2}$, where $\exp[\beta/K]=7{\cdot}4$ for C, 32·5 for Si, 3·5 for Ge, 1·0 for Sn)

T (°K)	C	Si	Ge	Sn
2000	$7{\cdot}6\times10^{14}$			
1000	$8{\cdot}7\times10^{7}$	$2{\cdot}8\times10^{18}$	$8{\cdot}0\times10^{18}$	$2{\cdot}2\times10^{20}$
500	$3{\cdot}3\times10^{-6}$	$1{\cdot}5\times10^{15}$	$4{\cdot}0\times10^{16}$	$5{\cdot}1\times10^{19}$
290	3×10^{-15}	$6{\cdot}0\times10^{10}$	$4{\cdot}0\times10^{13}$	$1{\cdot}3\times10^{19}$
200		$1{\cdot}6\times10^{6}$	$1{\cdot}4\times10^{10}$	$4{\cdot}3\times10^{18}$
100		$5{\cdot}5\times10^{-9}$	5·6	$1{\cdot}2\times10^{17}$
20				$8{\cdot}6\times10^{9}$

Acknowledgments

The author wishes to acknowledge the award of a Leverhulme Research Fellowship (1949–51) and to thank the Directors of Metropolitan-Vickers Electrical Co. Ltd., Manchester, for granting him extended leave of absence. He also wishes to thank Professor Willis Jackson in whose department the work has been carried out, and the D.S.I.R. for a grant of equipment.

References

Blum, A. I., and Goryunova, N. A., 1950, *Doklady Akad. Nauk.* (*S.S.S.R.*), **75,** 367.

Busch, G., Wieland, J., and Zoller, H., 1951, *Helv. Phys. Acta*, **24,** 49 and *Semiconducting Materials* (London : Butterworth), p. 188.

Estermann, I., and Foner, A., 1950, *Phys. Rev.*, **79,** 365.

Isenberg, I., Russell, B. R., and Greene, R. F., 1948, *Rev. Sci. Instrum.*, **19,** 685.

Kendall, J. T., 1950, *Proc. Phys. Soc.* B, **63,** 821.

Komar, A., 1936, *J. Exp. Theor. Phys. U.S.S.R.*, **6,** 256.

Moss, T. S., 1952, *Photoconductivity in the Elements* (London : Butterworth), p. 244.

Pearson, G. L., and Bardeen, J., 1949, *Phys. Rev.*, **75,** 865.

Pearson, G. L., and Suhl, H., 1951, *Phys. Rev.*, **83,** 768.

XIX. *A Method for the Measurement of Multiple Scattering*

By H. Överås
Fysisk Institutt, Norges tekniske högskole, Trondheim, Norway*

[Received November 5, 1953]

Summary

A new method for the determination of the multiple scattering of short, highly scattered discontinuous tracks is described.

§ 1. Introduction

For the scattering measurement in nuclear emulsions there are many methods in vogue. In most cases the Fowler coordinate method with its modifications is the best one. However, for the measuring of short, highly scattered, discontinuous tracks, e.g. from electrons near the minimum ionization, this method is not suitable. A method will be demonstrated here which, in this particular case, may be of some use.

§ 2. Theory

Imagine an infinitely long track the projection of which in the x-y-plane is represented as a Fourier integral

$$y(x)=\int_{-\infty}^{+\infty} g(\omega)\exp(i\omega x)\,d\omega.$$

Then $g(\omega)$ contains the statistical properties of the track. To this track we lay a chord of length 2λ (fig. 1). $t(s,\lambda,\xi)$ is the distance from the chord to the track, measured at a distance s from the middle of the chord, which lies at $x=\xi$. Since the angle between the chord and the x-axis is small, we can write

$$t(s,\lambda,\xi)=y(\xi+s)-\frac{\lambda+s}{2\lambda}y(\xi+\lambda)-\frac{\lambda-s}{2\lambda}y(\xi-\lambda)$$

$$=\int_{-\infty}^{+\infty} g(\omega)\exp(i\omega\xi)\left[\exp(i\omega s)-\frac{\lambda+s}{2\lambda}\exp(i\omega\lambda)-\frac{\lambda-s}{2\lambda}\exp(-i\omega\lambda)\right]d\omega.$$

By squaring and integrating with respect to ξ, using

$$|g(\omega)|^2\propto\frac{\langle\phi^2(2\lambda)\rangle}{2\lambda}\omega^{-4}$$

---

* Communicated by Dr. H. Wergeland.

(Olsen, Wergeland and Överås 1953), we obtain the mean square distance

$$\langle t^2(s,\lambda)\rangle = \frac{\langle \phi^2(2\lambda)\rangle}{2\lambda}\cdot\frac{1}{\pi}\int_0^\infty \frac{d\omega}{\omega^4}\left\{\frac{3}{2}+\frac{s^2}{2\lambda^2}-\frac{\lambda+s}{\lambda}\cos(\lambda-s)\,\omega - \frac{\lambda-s}{\lambda}\cos(\lambda+s)\omega+\frac{\lambda^2-s^2}{2\lambda^2}\cos 2\lambda\omega\right\}$$

or

$$\langle t^2(s,\lambda)\rangle = \frac{\langle \phi^2(2\lambda)\rangle}{2\lambda}\frac{\lambda^3}{6}\left(1-\left(\frac{s}{\lambda}\right)^2\right)^2 = \langle t^2(0,\lambda)\rangle\left(1-\left(\frac{s}{\lambda}\right)^2\right)^2 . \quad . \quad . \quad (1)$$

$\langle t^2(s,\lambda)\rangle$ is thus the value to be expected from measurements of the projection of many tracks or track pieces produced by electrons with equal energy.

$\langle \phi^2(2\lambda)\rangle/2\lambda$ is the characteristic quantity of the scattering process, viz. the mean square of the projected scattering angle per unit length. It is related to the mean square distance at the middle of the chord $\langle t^2(0,\lambda)\rangle$ by

$$\frac{\langle \phi^2(2\lambda)\rangle}{2\lambda} = \frac{6}{\lambda^3}\langle t^2(0,\lambda)\rangle . \quad . \quad . \quad . \quad . \quad . \quad . \quad . \quad (2)$$

Fig. 1

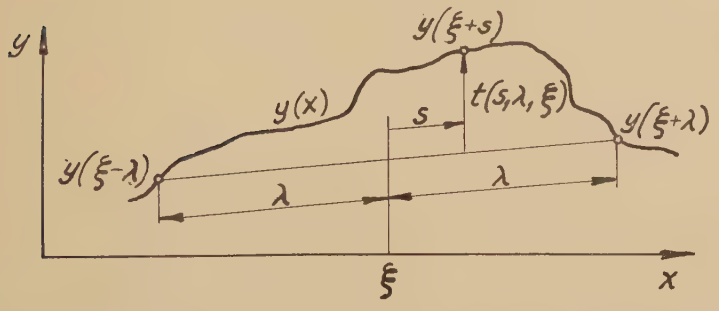

The relations (1) and (2) can also be found from the diffusion equation or by a direct method developed by H. Wergeland (unpublished).

To find $\langle t^2(0,\lambda)\rangle$ experimentally one may proceed in many ways, for instance straight forward by measuring $t(0,\lambda)$ for the tracks available. In order to get more information out of the tracks, we should rather measure all the grains in each track and use (1) to find $\langle t^2(0,\lambda)\rangle$. The same information can, however, more easily be obtained in the following way :

We imagine all the projected tracks under consideration placed in such a way that their chords of length 2λ coincide. Then the grains belonging to all these tracks will have a certain density $\rho(s,t,\lambda)$ at a point (s,t), and we may write

$$\langle t^2(s,\lambda)\rangle = \frac{\int_{-\infty}^{+\infty} t^2\rho(s,t,\lambda)\,dt}{\int_{-\infty}^{+\infty}\rho(s,t,\lambda)\,dt} . \quad . \quad . \quad . \quad . \quad . \quad . \quad . \quad (3)$$

For the reason of continuity of the paths the integral

$$\int_{-\infty}^{+\infty} \rho(s, t, \lambda)\, dt = \rho_0$$

should be independent of s.

By integrating the two expressions for $\langle t^2(s, \lambda)\rangle$, (1) and (3), with respect to s, we get

$$\int_{-\sigma}^{+\sigma} \langle t^2(s, \lambda)\rangle ds = \langle t^2(0, \lambda)\rangle 2\sigma \left[1 - \frac{2}{3}\frac{\sigma^2}{\lambda^2} + \frac{1}{5}\frac{\sigma^4}{\lambda^4}\right] = \frac{1}{\rho_0}\int_{-\infty}^{+\infty} t^2\, P(t, \lambda, \sigma)\, dt. \quad \ldots\ldots\ldots (4)$$

$$P(t, \lambda, \sigma)\, dt = dt \int_{-\sigma}^{+\sigma} \rho(s, t, \lambda)\, ds$$

is the number of grains between $-\sigma$ and $+\sigma$ ($\sigma \leqq \lambda$) in a strip dt parallel to the x-axis. We do not include the regions near the ends of the chord, because of relatively large measuring errors there. $2\sigma\rho_0$ is the total number of grains between $-\sigma$ and $+\sigma$.

$$\frac{1}{2\sigma\rho_0}\int_{-\infty}^{+\infty} t^2 P(t, \lambda, \sigma)\, dt,$$

which we shall denote by $\langle T^2(\lambda, \sigma)\rangle$, is the mean square of t, taken together for all the grains between $s = -\sigma$ and $s = +\sigma$, irrespective of their s-coordinates.

Combining (2) and (4) we then obtain

$$\frac{\langle \phi^2(2\lambda)\rangle}{2\lambda} = \frac{\langle T^2(\lambda, \sigma)\rangle}{\left[1 - \frac{2}{3}\frac{\sigma^2}{\lambda^2} + \frac{1}{5}\frac{\sigma^4}{\lambda^4}\right]}\frac{6}{\lambda^3}. \quad \ldots\ldots (5)$$

The relation (5) tells us what we should expect to find after measuring an infinite number of tracks, provided there were no measuring errors. In practice the large grain size introduces some uncertainty, so that instead of $\langle T^2(\lambda, \sigma)\rangle$ we find a value $\langle T^2(\lambda, \sigma)\rangle^*$ from the measurements. It may be shown with reasonable assumptions that

$$\langle T^2(\lambda, \sigma)\rangle = \langle T^2(\lambda, \sigma)\rangle^* - \langle \Delta^2(\sigma/\lambda)\rangle,$$

where $\langle \Delta^2(\sigma/\lambda)\rangle$ is of the order of magnitude $\langle D^2\rangle/8$, slightly varying with σ/λ. D is the grain diameter. The corrected formula is

$$\frac{\langle \phi^2(2\lambda)\rangle}{2\lambda} = \frac{\langle T^2(\lambda, \sigma)\rangle^* - \langle \Delta^2(\sigma/\lambda)\rangle}{\left[1 - \frac{2}{3}\frac{\sigma^2}{\lambda^2} + \frac{1}{5}\frac{\sigma^4}{\lambda^4}\right]}\frac{6}{\lambda^3}. \quad \ldots\ldots (6)$$

From (6) we see that the correction term in $\langle \phi^2(2\lambda)\rangle/2\lambda$ varies as λ^{-3}, and we therefore get the best determination with fairly long chords.

$\langle \Delta^2(\sigma/\lambda)\rangle$ may be estimated using two different chord lengths λ_1 and λ_2, with $\sigma_1/\lambda_1 = \sigma_2/\lambda_2 = \sigma/\lambda$

$$\langle \Delta^2(\sigma/\lambda)\rangle = \frac{\langle T^2(\lambda_1, \sigma_1)\rangle^* - (\lambda_1/\lambda_2)^3 \langle T^2(\lambda_2, \sigma_2)\rangle^*}{1 - (\lambda_1/\lambda_2)^3}. \quad \ldots\ldots (7)$$

§ 3. Experimental Verification

The relation (6) was examined experimentally by means of 40 tracks produced by 0·59 MEV electrons.

$\langle\phi^2(2\lambda)\rangle/2\lambda$ was determined from (6) for values of σ/λ ranging from 1/15 to 12/15 (table 1). Apart from statistical fluctuations the values of $\langle\phi^2(2\lambda)\rangle/2\lambda$ should be independent of σ/λ. The largest value of σ/λ gives statistically the best determination, but how the standard deviation of $\langle\phi^2(2\lambda)\rangle/2\lambda$ decreases with increasing σ/λ is not easily predicted, since measurements on the same track here are statistically dependent. If we measure N grains in each of M tracks, it can, however, be safely stated that the standard deviation lies between what would be expected for M and $N\times M$ independent observations.

Table 1

$(\sigma/\lambda)\times 15$	$\frac{\langle\phi^2(2\lambda)\rangle}{2\lambda}\times 10^4$
1	1·67
2	1·82
3	1·79
4	1·65
5	1·64
6	1·68
7	1·68
8	1·63
9	1·67
10	1·68
11	1·66
12	1·65

Table 2

$(s/\lambda)\times 15$	ρ_0
1	36
2	30
3	48
4	36
5	42
6	39
7	47
8	41
9	34
10	36
11	44
12	45

The constancy of ρ_0 was also checked (table 2). In these measurements the correction $\langle\Delta^2(\sigma/\lambda)\rangle$ was of the order of 5% of $\langle T^2(\lambda,\sigma)\rangle$*.

§ 4. The Method in Practice

For practical measurement a micrometer eyepiece as indicated in fig. 2 would be convenient. The line a is fixed and has two marks at a distance 2λ. The line b has marks at $+\sigma$ and $-\sigma$ and can be displaced in the direction of the arrows by a micrometer screw.

Before measuring, the stage of the microscope is moved until the track crosses the line a at $+\lambda$ and $-\lambda$. Then the micrometer screw is turned and reading made whenever the line b passes the centre of a grain between $+\sigma$ and $-\sigma$. Such readings are taken for all the tracks to be measured, and the mean square of all these readings gives $\langle T^2(\lambda,\sigma)\rangle$*.

The method is limited to chord lengths less than the diameter of the microscope field, but the stage needs not to be moved, except for putting a new track into position. We therefore get no stage noise.

As an example the method was used to determine the multiple scattering of 0·59 Mev electrons in nuclear emulsions, and the result obtained by Hisdal (1952) was confirmed.

Fig. 2

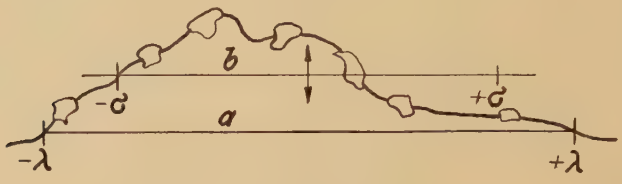

Acknowledgments

The author would like to express his gratitude to Professor H. Wergeland and Dr. H. A. Olsen for helpful discussions, to Mrs. E. Hisdal, Oslo, for providing the plates for the measurements, and to Norges almenvitenskapelige forskningsråd for a grant.

References

Olsen, H. A., Wergeland, H., and Överås, H., 1953, *D. Kgl. Norske Vidensk. Selskabs Forh.* Bd. **26,** no. 9.

Hisdal, E., 1952, *Phil. Mag.*, **43,** 790.

XX. *Some Ordering Effects in* Cu_3Au *at about* 100°C

By R. A. Dugdale and A. Green
Atomic Energy Research Establishment, Harwell, Berks*

[Received December 1, 1953]

Summary

Using the electrical resistance as an indicator for ordering it is found that Cu_3Au specimens prepared in a state of long-range order and then water quenched from 380°C (8°C below the critical temperature) show an ordering effect at about 100°C. After this has decayed a similar effect is again observed after an electron bombardment (energies of 0·5 and 1 Mev) or after a small deformation at room temperature. An activation energy $E \sim 0{\cdot}9$ ev for all three cases is determined. Attributing the ordering effect to the migration of vacancies or interstitials the experiments provide evidence that one or both of these defects are obtained in thermodynamic excess by quenching or deforming.

§ 1. Introduction

In a previous letter (Adam, Green and Dugdale 1952) the effect of a 1 Mev electron bombardment on a highly-ordered Cu_3Au specimen was reported. Using the electrical resistance at 0°C as an indicator it was shown that a further ordering at 100°C took place after the bombardment. This was attributed to the migration, at 100°C, of vacancies or interstitials, produced by the bombardment, which allowed some of the remaining wrong atoms to move to right positions. The experiment also indicated that the ' active ' defects were gradually used up.

Apart from the technique of bombardment one may hope to introduce a thermodynamic excess of vacancies into a Cu_3Au specimen by two other methods. The first of these is by quenching from a suitably high temperature. If U is the energy required to form a vacancy the equilibrium concentration at a temperature T is approximately $\exp(-U/kT)$ (see Mott and Gurney 1948). Thus, if the vacancy concentration is allowed to approach its equilibrium value at T, a rapid cool to a lower temperature should produce the desired excess. The second is by a deformation at a suitably low temperature. As indicated by Mott (1951) and Seitz (1952) the movement of dislocations occurring during deformation may be expected to generate vacancies. Thus, a

* Communicated by the Authors.

specimen deformed at a temperature low enough to prevent a rapid approach to equilibrium should contain the desired excess.*

The aim of the present experiments was to find out whether, in fact, a quench or deformation would produce an effect similar to that of electron bombardment, i.e. a low-temperature ordering at *c.* 100°C. In order that the conditions for comparing the three effects should be as nearly as possible similar all specimens were first quenched and then used for electron bombardment or deformation studies.

§2. Apparatus

The alloy used was made by Johnson, Matthey & Co., Ltd., in the form of wire of diameter 0·25 mm from specimens of Cu and Au of high purity. An analysis made by the Chemistry Division at A.E.R.E. gave $25{\cdot}8 \pm 0{\cdot}2$ atomic % Au with Ag, Fe and Si as major impurities with a concentration of 0·01 to 0·1%.

All the specimens were initially constructed as shown in fig. 1 (*a*).

Fig. 1

They were heated in an argon atmosphere at about 900°C for two hours after which coring could not be detected by x-ray diffraction methods. Specimens intended for electron bombardment were then bent into an M shape and beaten flat to a thickness of 0·025–0·05 mm as shown in fig. 1 (*b*). This shape could be circumscribed by a circle of 8 mm diameter. All specimens were annealed *in vacuo* at 600°C for half an hour to remove the effects of cold work (which, in the case of the straight specimens, occurred to some extent on their removal from the homogenizing furnace). The straight specimens (denoted by 'A') were mounted in a mica sandwich as shown in fig. 1 (*c*). The electron bombardment specimens (denoted by 'R') were attached to bakelite mounts after heat treatment. Great care was taken to avoid bending these specimens.

The critical temperature T_c, upon cooling at 1·5°C per hour, was measured on one straight specimen against a Pt—10% Pt Rh thermocouple. It was found to be 388°C according to a standard calibration table for the couple.

To obtain a high degree of order specimens were maintained at 380°C for three days and then cooled to room temperature at 20°C per hour.

* It is possible that interstitials may also be produced by these methods.

For quenching, a vertical furnace with a temperature regulation of ± 1°C was used. The temperature was measured by means of a Pt—13% Pt Rh couple permanently attached. Specimens to be quenched were placed in a small Al box and this, together with a steel plunger and some Mg ribbon to act as a getter, were sealed inside a glass tube evacuated to 10^{-2} mm Hg. The tube was attached to a wire and drawn up into the furnace from which it could be dropped into a water bath by simply cutting the wire. The presence of the steel plunger ensured an immediate breaking of the glass tube on impact with the water. The Al box, the interior of which was easily accessible to the water, prevented the specimens from being damaged. It was necessary to maintain ordered specimens for two hours at 391–392°C in this furnace before quenching to remove their super lattice lines. This is in rough conformity with the measured value of T_c for slow cooling, mentioned above, and served as a rough check on the furnace temperature measurement.

The resistance at 0°C of the specimens was measured with a precision better than ± 1 part in 20 000. They were not suitable for a determination of their resistivity ρ. However, a suitable specimen was made and after quenching from 450°C gave, for the disordered resistivity (0°C), $\rho = 11{\cdot}6\,\mu\Omega\ \mathrm{cm}^{-1}$. The values of ρ for the other specimens, in a particular state of order, could then be determined from their disordered resistance.

Isothermal curves of resistance R (0°C) *v.* time t at a temperature T were obtained by immersing the specimens in thermostated oil baths for suitable periods of time. The oil bath temperatures were measured to 0·1°C. The temperature regulation was $\pm 0{\cdot}1$°C up to 100°C and $\pm 0{\cdot}2$°C above 100°C.

A Van der Graaf machine was used for electron bombardments. The specimen was placed (in air) in a uniform beam defined by an 8 mm diameter hole in a brass plate. The temperature of the specimen (which was cooled only by convection in the air) was continuously monitored by measuring its resistance. It was not allowed to rise above 40°C. A measurement of the electron flux at the specimen was made on several occasions by replacing it by a suitably designed constant flow water calorimeter.

The displacement of atoms by electron bombardment is discussed in the Appendix.

§ 3. Experimental

(i) *The Effect of a Quench Followed by an Electron Bombardment*

An initially highly ordered specimen R1 ($\rho = 5{\cdot}4\,\mu\Omega\ \mathrm{cm}^{-1}$) was maintained at 380°C for two hours then quenched ($\rho = 9{\cdot}5\,\mu\Omega\ \mathrm{cm}^{-1}$). On heating at 130°C its resistance decreased as shown in fig. 2 (*a*). At the point B it was bombarded with 10^{17} electrons/cm^2 of 1 Mev energy. During the bombardment the resistance decreased about 0·5% as

indicated by D. Subsequent heating at 100°c and 130°c produced the fall in resistance shown.

Specimen R25 was maintained at 380°c for four days then quenched ($\rho = 7{\cdot}5\,\mu\Omega\ \mathrm{cm}^{-1}$). Subsequent heating at 100°c and 130°c produced the fall in resistance shown in fig. 2 (*b*). At the point B it was bombarded with 5×10^{16} electrons/cm^2 of energy 0·5 Mev. Subsequent heating at 100°c caused the resistance to fall as shown.

Fig. 2

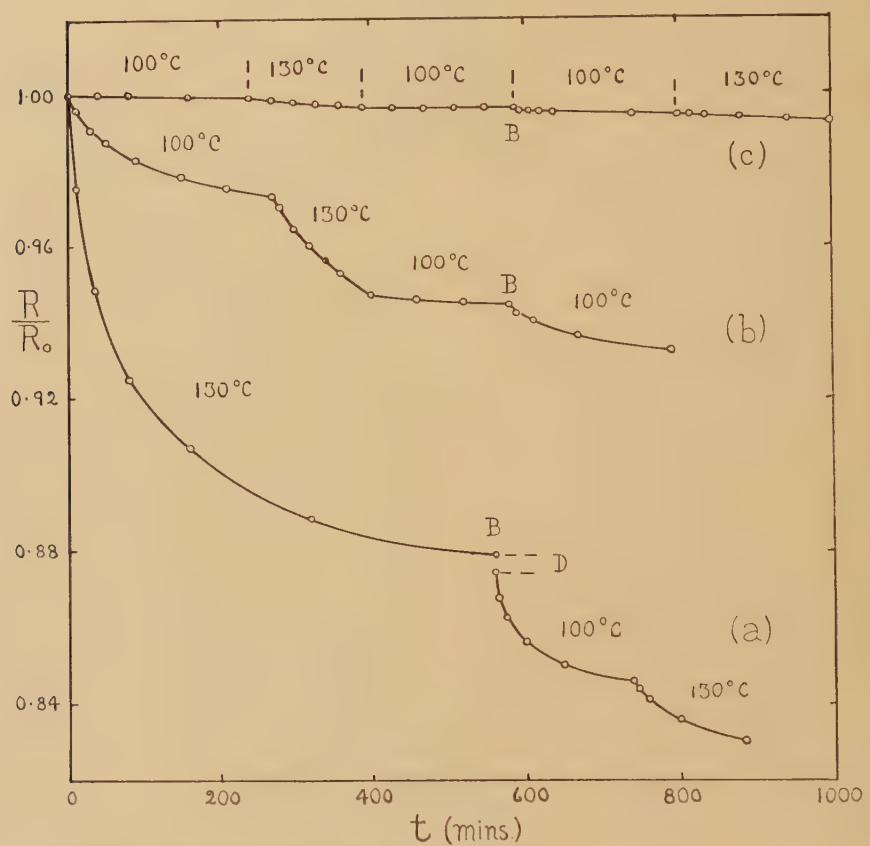

Specimen R2 was maintained at 450°c for three hours then quenched ($\rho = 11{\cdot}6\,\mu\Omega\ \mathrm{cm}^{-1}$). The small decreases in resistance shown in fig. 2 (*c*) occurred on subsequent heating at 100°c and 130°c. A bombardment with 10^{17} electrons/cm^2 of energy 1 Mev at the point B caused the further small decreases on heating at 100°c and 130°c shown.

(ii) *The Effect of a Quench Followed by a Plastic Deformation*

An initially highly ordered specimen A15 ($\rho = 5{\cdot}4\,\mu\Omega\ \mathrm{cm}^{-1}$) was maintained at 381°c for three hours then quenched ($\rho = 7{\cdot}9\,\mu\Omega\ \mathrm{cm}^{-1}$). Heating at 100°c afterwards caused R to fall as shown in fig. 3 (*a*). After 500 min at 100°c the specimen was removed from its mica sandwich

and given a small deformation at room temperature. The deformation consisted of bending the central portion of the specimen into a single loop (~8 mm diameter) and then straightening it again. The whole operation, including remounting and returning to the ice bath, took about 5 min. When R was next measured (about 30 min later) an increase of nearly 0·5% was found. Subsequent heating at 100°C for a further 500 min produced the fall in R shown.

Fig. 3

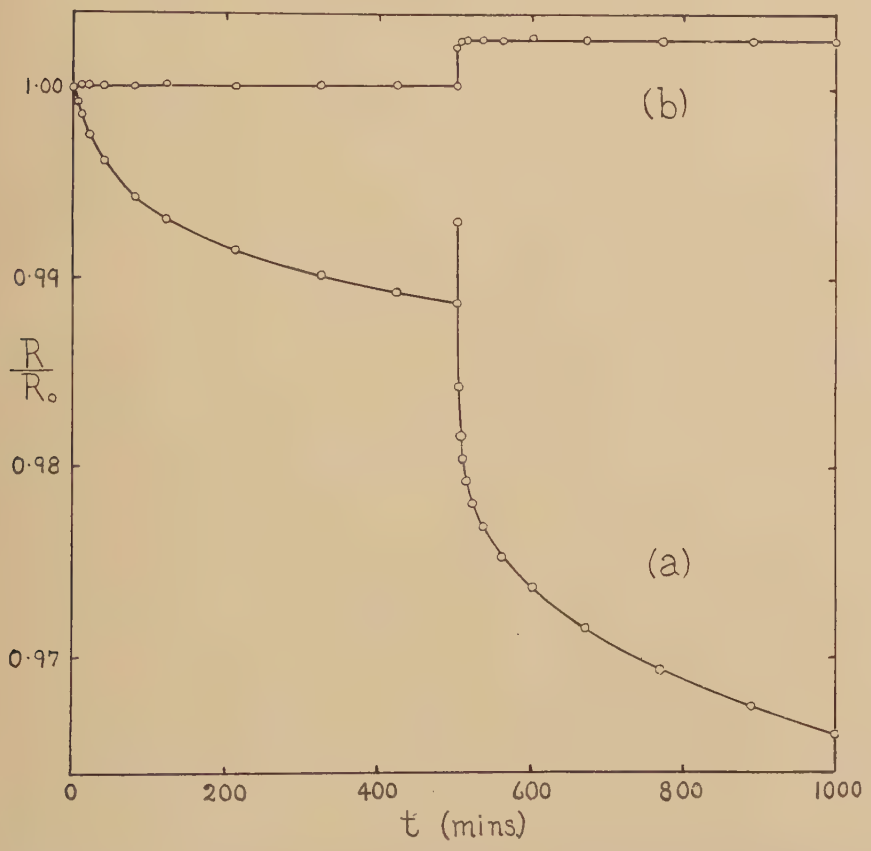

An initially highly ordered specimen A3 ($\rho = 5{\cdot}4\,\mu\Omega\,\mathrm{cm}^{-1}$) was maintained at 450°C for three hours then water quenched ($\rho = 11{\cdot}6\,\mu\Omega\,\mathrm{cm}^{-1}$). Heating at 100°C for 500 min produced hardly any change in R as shown in fig. 3 (*b*). The specimen was then deformed in the same manner as A15 with the resulting increase in R of about 0·2%. Further heating at 100°C had very little effect as shown.

(iii) *The Determination of an Activation Energy E*

The preceding experiments indicate that relatively large effects at *c.* 100°C may be induced in specimens in a state of long-range order by a quench, a bombardment or a deformation. Specimens without long-range order (those quenched from 450°C) show relatively small effects.

In this section, more detailed experiments on specimens in a state of long-range order are described. The object was to determine activation energies for the three types of effect on the assumption that

$$\frac{dR}{dt} = f(R) \exp(-E/kT) \quad . \quad . \quad . \quad . \quad . \quad . \quad . \quad (1)$$

where R is the resistance at 0°C. To obtain E it is necessary to measure dR/dt at two temperatures T_1 and T_2 for the same value of R, when, from (1)

$$E = \frac{kT_1T_2}{T_2 - T_1} \log \left[\left(\frac{dR}{dt}\right)_{T_2} \Big/ \left(\frac{dR}{dt}\right)_{T_1} \right] \quad . \quad . \quad . \quad . \quad . \quad (2)$$

if $T_2 > T_1$.

For this purpose, sets of isotherms of R (0°C) *v.* t, at several temperatures in the range 70–130°C, were obtained on two specimens, A2 and R25, after quenching from approximately 380°C. A set of activation energies was determined for each using the values of the gradients at the ends of the curves (measured with a ruler) in (2). Similarly, further sets of E were obtained from A2 after a small deformation at room temperature (similar to that, described above, for A15 and A3) and from R25 after a 1 MeV electron bombardment.*

The isotherms obtained (except those from R25 after quenching) are shown in fig. 4.† There was a considerable scatter in the values of E as exemplified by the detailed values for A2 shown in table 1 (*a*). Table 1 (*b*) shows the mean values of E for the two specimens. These all agree within the R.M.S. deviation and a figure of approximately 0·9 ev may be taken as the value of the activation energy for the low-temperature ordering process induced by the three treatments.

Some additional results on quenched specimens are now mentioned. Isotherms were obtained from three specimens, A6, A11 and A16, in the quenched ordered condition, under identical conditions and at the same time as A2. A6 had received an initial heat treatment with A2 (four days at 379°C then quenched) whereas A11 and A16, after being initially highly ordered, were maintained together at 379°C for two hours then quenched. The values of E, initial ρ and total percentage decrease in R

* The detailed treatment of these two specimens was as follows. A2 : Maintained at 379°C for four days then quenched ($\rho = 7{\cdot}3\ \mu\Omega\ \mathrm{cm}^{-1}$). After obtaining the quench isotherms, was heated at 130°C (curve 9, fig. 4 (*a*)) until dR/dt was very small, then deformed (D, fig. 4 (*a*)). R25 : Originally maintained at 380°C for four days, quenched and used in various preliminary bombardment experiments. Later, maintained at 381°C for two hours, quenched ($\rho = 7{\cdot}7\ \mu\Omega\ \mathrm{cm}^{-1}$) and heated at 130°C until dR/dt was small. Bombarded with 8×10^{16} electrons/cm² at 1 MeV (during which R decreased 0·3%) then used to obtain the bombardment isotherms. Maintained at 381°C for three hours, quenched ($\rho = 8{\cdot}3\ \mu\Omega\ \mathrm{cm}^{-1}$) and used for the quench isotherms.

† It is interesting to note that the rate of ordering at 0°C was sufficiently high for an isotherm to be obtained in a reasonable time (~6000 min) after deformation and after bombardment. This was not the case after quenching.

during the isothermal treatments obtained from these specimens are compared with those of A2 in table 2. The values of E agree, within the

Fig. 4

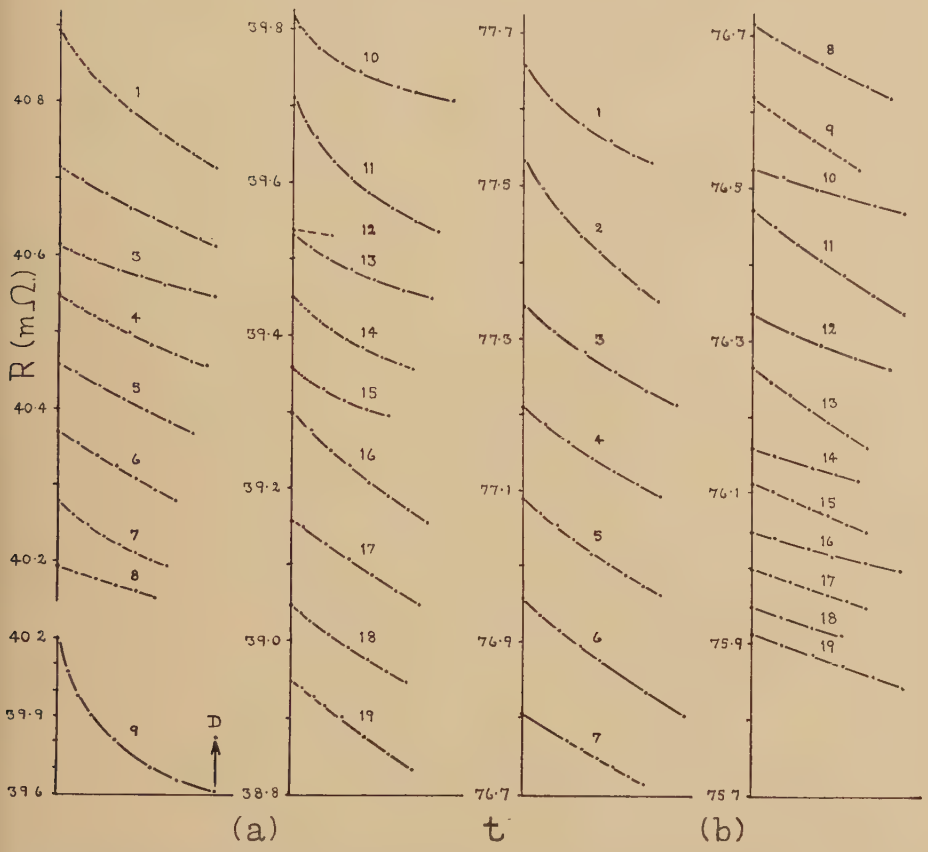

The following key to the curves gives the temperature in °C and total time in minutes at temperature.

(*a*)

Curve	T	t	Curve	T	t
1	68·8	400	11	68·8	25
2	89·4	100	12	0	3915
3	68·8	800	13	68·8	48
4	89·4	380	14	89·4	31
5	107·9	115	15	68·8	500
6	128·3	30	16	110·8	35
7	110·8	140	17	128·4	11
8	128·4	25	18	110·8	60
9	128·4	1020	19	128·5	21
10	0	4160			

(*b*)

Curve	T	t	Curve	T	t
1	0	6660	11	106·4	20
2	70·6	14	12	70·3	240
3	50·6	100	13	106·5	30
4	70·6	24	14	70·0	280
5	50·6	240	15	106·0	30
6	70·1	85	16	84·8	130
7	89·3	16	17	106·0	30
8	70·3	90	18	84·8	120
9	89·4	28	19	106·0	50
10	70·1	100			

scatter, with those already mentioned and show that E is not very sensitive to the type of heat treatment before quenching.

Table 1 (*a*). Values of E from A2

(i) After Quenching

T_1 (°C)	68·8	89·4	68·8	89·4	107·9	128·3	110·8
T_2 (°C)	89·4	68·8	89·4	107·9	128·3	110·8	128·4
E (ev)	0·77	0·91	0·79	0·95	0·92	0·88	0·94

(ii) After Deforming

T_1 (°C)	0	68·8	0	68·8	89·4	68·8	110·8	128·4	110·8
T_2 (°C)	68·8	0	68·8	89·4	68·8	110·8	128·4	110·8	128·5
E (ev)	0·86	0·91	0·90	0·87	0·96	1·16	0·81	1·14	1·04

Table 1 (*b*). Mean Values of E from A2 and R25

Specimen	Mean E (ev)	R.M.S. deviation	No. of values
A2 after quenching	0·88	±0·07	7
A2 after deforming	0·97	±0·12	9
R25 after quenching	0·88	±0·14	13
R25 after bombarding	0·84	±0·08	18

Table 2

Specimen	Initial ρ ($\mu\Omega$ cm^{-1})	$\%\Delta R$	E (ev)	R.M.S. deviation
A2	7·3	1·81	0·88	±0·07
A6	7·2	1·60	0·88	±0·04
A11	8·0	2·32	0·94	±0·06
A16	8·1	2·22	0·92	±0·10

These results also show a variation in $\%\Delta R$ between specimens given an identical preparation which may be due to insufficient precision in the quenching technique.

§ 4. Discussion

The experiments demonstrate that an appreciable resistance decay at *c.* 100°C, somewhat similar to that following an electron bombardment, does occur after quenching or deforming specimens in a state of long-range order. A plausible explanation is, as in the bombardment case, that these decays are ordering effects. The agreement between the activation energies is sufficiently good to suggest that the ordering mechanism is the

same in all three cases and therefore that a thermodynamic excess of vacancies (and/or interstitials) is indeed produced by a quench or a deformation. If the estimate made in the appendix is not too far out it would appear that these ordering effects may be brought about by a vacancy concentration of less than 1 in 10^5 or 10^6. The magnitude in the fall in resistance suggests therefore that each vacancy must, during its migration, put many wrong atoms right before it is captured.

If this explanation is correct the physical significance of $E(\sim 0{\cdot}9$ ev) possibly lies in some rate controlling process in which the vacancies are involved. The scatter in the values of E is attributed mainly to errors in R and dR/dt but these may obscure a possible fine dependence on, for instance, the type of treatment causing the effect and the degree of order of the specimen.

The small effect in specimens without long-range order (quenched from 450°C) appears to be consistent with the above explanation since one would expect their resistance to be relatively insensitive to any ordering effects which may have occurred. Indeed, Sykes and Jones (1936) showed, by observations on the specific heat, that ordering does occur at *c.* 100°C in specimens quenched from above the critical temperature without affecting the resistance appreciably.

The increase in resistance upon deforming is possibly due to three things : (i) a decrease in order (Dahl (1936) showed that an ordered Cu_3Au specimen could be completely disordered by sufficient deformation) ; (ii) an increase in the number of dislocations or similar large faults ; (iii) a change in the physical dimensions of the specimen. The two latter would seem to be the cause of an increase in R when a disordered specimen (e.g. A3) is deformed.

Acknowledgments

The authors' thanks are due to Dr. J. Adam for his x-ray studies on this alloy, to Dr. W. Wild and the Van der Graaf section for electron bombardments, to Mr. H. Sheard for his interest in the experiment and to the Director, A.E.R.E., for permission to publish this paper.

APPENDIX

The Displacement of Atoms by Electron Bombardment

The maximum recoil energy W_m which an atom can receive when its nucleus elastically scatters an electron of energy E is, very approximately,

$$W_m = \frac{2E(E+2m_0c^2)}{Mc^2} \quad . \quad . \quad . \quad . \quad . \quad . \quad . \quad . \quad . \quad . \quad (3)$$

where m_0c^2 and Mc^2 are the rest energies of electron and atom, respectively.

The number of atoms displaced in a given bombardment can be estimated if the minimum displacement energy W_0 and displacement cross section σ_D are known. W_0 can, in principle, be measured, σ_D, the

cross section for the recoil energy to lie between W_0 and W_m, may be estimated by suitably integrating the differential scattering formula of Mott (1932). Because of mathematical difficulties the integration of an approximate formula is necessary. Since, from (3), W_m for Au is about one-third that for Cu it is probable that, at low electron energies, displaced Cu atoms will predominate in Cu_3Au. Thus, only σ_D for Cu need be determined. For this purpose the following expression is used.

$$\sigma_D = 0{\cdot}25Z^2 \frac{1-\beta^2}{\beta^4}\left[\frac{W_m}{W_0} - 1 - (\beta^2 + \pi\alpha\beta)\log\frac{W_m}{W_0} + 2\pi\alpha\beta\left(\sqrt{\frac{W_m}{W_0}} - 1\right)\right] \text{barns} \quad . \quad . \quad . \quad . \quad . \quad (4)$$

where Z is the nuclear charge, $\alpha = Z/137$ and $\beta = v/c$. This formula is derived from the α^2 approximation of McKinley and Feshback (1948).

W_0 has not yet been measured. However Seitz (1949), has suggested that it will be of the order of 25 ev. That it is certainly less than 26 ev is demonstrated by the fact that ordering can be induced by a 0·5 MEV bombardment for which W_m is 26 ev for Cu. The fraction of atoms f displaced during a 1 MEV bombardment of integrated flux $\phi = 10^{17}$ electrons/cm^2 may be estimated if we assume that $W_0 = 25$ ev. From (3) $W_m = 68$ ev for Cu which gives in (4) $\sigma_D = 30$ barns. Thus

$$f = \phi\sigma_D = 3 \times 10^{-6}.$$

Dixon, Meechan and Brinkman (1953) bombarded a well-ordered Cu_3Au specimen at a temperature below −185°C with 1 MEV electrons of integrated flux $3{\cdot}4 \times 10^{19}$ electrons/cm^2. According to the above calculation this should have displaced a fraction of approximately 10^{-3} of the Cu atoms. An increase in resistance expected to be about 5% (on the basis of calculations made by Dexter (1952)) due to these displaced atoms was looked for but not found. These authors concluded therefore that many of the interstitial vacancy pairs formed must have been unstable at the temperature of the bombardment and so recombined. Thus, it is possible that the number of interstitial vacancies pairs formed during a room temperature bombardment which are capable of dissociating to form free vacancies and interstitials may be very much less than the above calculation indicates.

References

Adam, J., Green, A., and Dugdale, R. A., 1952, *Phil. Mag.*, **43**, 1216.

Dahl, O., 1936, *Zeits. f. Metallkunde*, **28**, 133.

Dexter, D. L., 1952, *Phys. Rev.*, **87**, 768.

Dixon, C. E., Meechan, C. J., and Brinkman, J. A., 1953, *Phil. Mag.*, **44**, 449.

McKinley, W. A., and Feshback, H., 1948, *Phys. Rev.*, **74**, 1759.

Mott, N. F., 1932, *Proc. Roy. Soc.* A, **135**, 429; 1951, *Proc. Phys. Soc.* B, **64**, 729.

Mott, N. F., and Gurney, R. W., 1948, *Electronic Processes in Ionic Crystals* (Oxford: Clarendon Press), p. 29.

Seitz, F., 1949, *Crystal Growth, Disc. Far. Soc.* (Gurney and Jackson), p. 29; 1952, *Advances in Physics*, **1**, 43.

Sykes, C., and Jones, F. W., 1936, *Proc. Roy. Soc.* A, **157**, 213.

XXI. *Nuclear Reactions Produced by Nitrogen and Oxygen Ions*

By K. F. Chackett, J. H. Fremlin and D. Walker
Department of Physics, University of Birmingham*

[Received November 13, 1953]

Abstract

In the production of radioactive isotopes by bombardments with ^{14}N ions accelerated in the Birmingham sixty-inch cyclotron, total initial activities of some hundreds of thousands of counts per minute have been produced in aluminium targets. The following radioactive nuclei, in order of yield, have been identified with certainty among the products :

^{32}P, ^{28}Al, ^{34}Cl, ^{38}K, ^{30}P, ^{35}S, ^{31}Si, ^{24}Na.

In addition to these isotopes, ^{27}Mg, ^{13}N and ^{11}C have been detected with certainty ; the evidence for ^{18}F, ^{38}Cl and ^{22}Na is inconclusive.

Bombardment of aluminium with ^{16}O ions was shown to give ^{38}K, ^{34}Cl, ^{30}P, ^{18}F, ^{32}P and ^{24}Na.

Most of the assignments of activity have been confirmed chemically. The experimental observations are not easily explained if the colliding nuclei simply fuse into a compound nucleus which then undergoes evaporation or fission ; it is suggested that usually only part of one nucleus sticks to the other.

§ 1. Introduction

Although in the last two decades an enormous amount of work has been done on the nuclear reactions produced by artificially accelerated particles, almost all of this has been concerned with bombarding particles no heavier than α-particles. This emphasis is natural in view of the complexity of the reactions which might be expected in bombardments by heavier nuclei, but it is also a reflection of the difficulty encountered in producing useful beams of the heavier nuclei. Considerable progress has now been made, however, in the acceleration of ions of elements such as carbon, nitrogen and oxygen, so that studies of nuclear reactions produced by such ions incident on target nuclei ranging from deuterium to uranium have become possible (Miller *et al.* 1951, Ghiorso *et al.* 1951, Wyly and Zucker 1953, Reynolds *et al.* 1953, Chackett *et al.* 1953). In a theoretical paper, Breit *et al.* (1952) have also pointed out that reactions between nuclei in the region of nitrogen might be expected to give useful information on nuclear structure.

* Communicated by the Authors.

Some of the radioactive products from the bombardment of aluminium with ^{14}N ions have already been noted (Chackett *et al.* 1953). The present paper is concerned mainly with a detailed examination of these products and possible explanations of the relative yields observed.

§ 2. Acceleration of Multiply-Charged Ions

The chief problem in accelerating heavy ions in a cyclotron is that of obtaining ions in a high state of ionization. The method we have used for accelerating ions carrying 6 electronic charges (such as $^{14}N^{6+}$ and $^{16}O^{6+}$) in the Birmingham 60 in. fixed-frequency cyclotron involves a preliminary 'third harmonic' acceleration of the ions in the 2-charged state (Walker and Fremlin 1953). Through collisions with gas atoms in the cyclotron tank the 2-charged ions become stripped to 6-charged ions. A number of experiments, described elsewhere, have been carried out on this mechanism (Walker *et al.* 1954). We give here only the data essential to an understanding of the main topic of the present paper.

All bombardments of aluminium have been made inside the cyclotron at a radius of 25 in. Here the circulating beam contains up to 10^{10} $^{14}N^{6+}$ ions per sec having energies over 50 Mev; the number of ions per unit energy interval is roughly halved for each rise of 10 Mev above 50 Mev, while the maximum possible energy is about 125 Mev. Similarly for $^{16}O^{6+}$ ions, beam intensities of 3×10^{8} ions per sec with energies over 40 Mev have been obtained, the maximum energy being about 140 Mev. The strong decrease of intensity with increasing energy means that the ions with energies not very far above the nuclear potential barrier will produce the greatest number of reactions. This will hold good at all depths in the target.

§ 3. Bombardment of Aluminium with $^{14}N^{6+}$ Ions

The choice of aluminium as a target was due mainly to simple practical considerations. Aluminium is available in thin strong foils of high purity; it consists of but a single isotope and the chemical difficulty of separating the possible products is not great. The target usually consisted of a number of foils each 12·5 μ thick, one above the other and all covered by a protective aluminium foil about 2 μ thick. This was needed because, besides the desired beam of six-charged ions, relatively large beams of slower doubly-charged particles exist, moving with energies approaching the potential barriers of elements such as carbon, which are found in the residual gas and are liable to be deposited on the target. The cover foil would reduce to negligible proportions in the main part of the target any products arising from the low-energy part of the beam. In fact, but for the single product ^{22}Na, control counts of the protective foils show no significant qualitative differences from those of the main foils, which shows also that no serious activity arises due to slow non-resonant contaminating ions.

The first few foils of the stack usually formed the 'window', about 2 cm $\times$ 1 cm, in a shielded probe (see fig. 1), any further foils being

mounted on the inner current-collector. The outer tube of the probe carried two windows, on opposite sides, so that two successive bombardments could be carried out without withdrawal, by turning the probe through 180° ; this was often useful when short well-defined bombardments were needed, as the preliminary adjustment of the ion beam could be done using one window and the main bombardment using the other. No significant radiation hazard exists, of course, with such small beams, so that the probe could be rotated by hand while the beam was present. The probe could be removed through an air lock and the foils detached and placed beneath a counter within 1½ minutes so that reaction products with half-lives down to a little less than 1 minute might be observed.

The radioactive products of the bombardments were identified by analysis of gross decay curves obtained after bombardments lasting for periods ranging from two minutes to many hours, and also by radiochemical analysis of the foils. In some cases, e.g. ^{27}Mg and ^{11}C, the evidence was entirely from chemically separated specimens.

Fig. 1

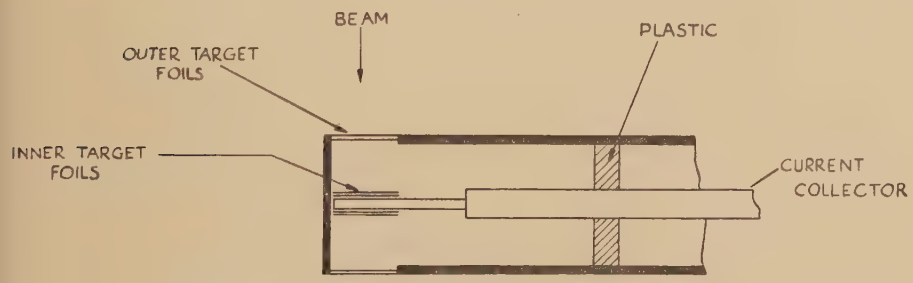

Target used in the bombardment of aluminium.

3.1. *Identification of Products by Analysis of Gross Decay Curves*

In fig. 2 is shown a typical curve for a foil bombarded for 2 min., observed with a Geiger counter with an aluminium end-window 7 mg/cm^2 thick. It will be seen that several decay periods are involved. Curve 2 has been analysed in figs. 3 (*a*) and 3 (*b*) and it will be seen that, besides longer periods, it breaks down perfectly, within the statistical errors, into a set of curves of half periods 150 min, 33 min, 7½ min and 2·3 min.

Taken in order of decreasing half-life, the products were provisionally identified as ^{32}P, ^{24}Na, ^{31}Si or ^{18}F, ^{38}Cl or ^{34}Cl, ^{38}K, and ^{28}Al or ^{30}P. While the lack of alternatives made several of these identifications seem fairly reliable, three pairs of alternative possibilities existed which could not easily be separated simply by analysis of decay curves. These were ^{31}Si and ^{18}F, ^{38}Cl and ^{34}Cl, ^{30}P and ^{28}Al. The first pair could easily be distinguished chemically, the second pair could not be so distinguished and the third pair involved some difficulty owing to their short half-life.

An elementary positron-electron discriminator was therefore made up, using a permanent magnet with a flux density of about 1800 gauss in the $1\frac{1}{2}$ in. gap between its poles. This gave a discrimination of about 7 to 1 between β-particles of opposite sign. For the sign of charge which it was desired to accept, the counting rate was reduced to about 1/5 of that obtained with the source as close as possible to the counter window in the absence of the magnet.

Positive and negative decay curves could be obtained simultaneously from this device. As an example, analysis of curves obtained from a source bombarded for 2 minutes gave the following information. Firstly, both positive and negative curves showed a weak activity of 2–3 hours half-life, suggesting that both ^{18}F and ^{31}Si were present. Secondly, not

Fig. 2

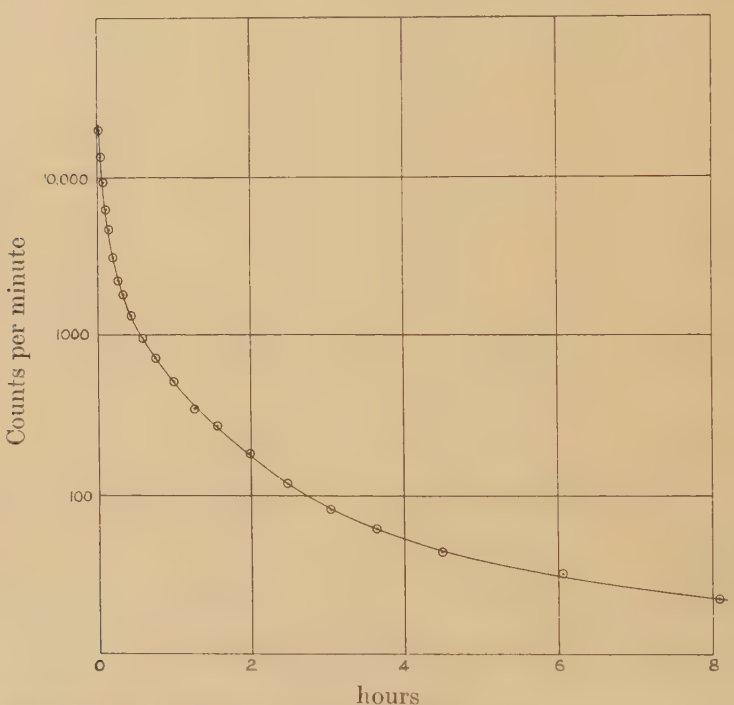

Decay of activity in aluminium bombarded for 2 minutes by ^{14}N ions.

only the $7\frac{1}{2}$ minute activity but also the 33 minute activity was 100% positive (probable error under 5%) showing that the main, if not the only, chlorine isotope was ^{34}Cl. Thirdly, the $2\frac{1}{2}$ minute activity was 90 ± 5% negative, thus confirming that the main $2\frac{1}{2}$ minute activity was ^{28}Al but suggesting the possible presence of a trace of a short-lived positron emitter, presumably either ^{30}P or ^{15}O.

This charge-discriminator was also used to check the sign of the particles emitted by each of the chemically separated fractions mentioned below except for the short-lived aluminium and phosphorus fractions.

The possible occurrence of ^{22}Na calls for special comment. The first curve analysed showed an extraordinarily large quantity, the yield in number of atoms formed being 10 times that of any other isotope. This curve, however, was derived from the first long bombardment, in which no precautions were taken to protect the foil from surface contamination. The next bombardment, performed with a cover foil as already described, showed a yield less than 1/500th as great. By counting also the cover foil itself, it was found that almost all of the ^{22}Na appears in the top 2 μ of target. This may be due to any of several causes irrelevant to the main

Fig. 3 (*a*)

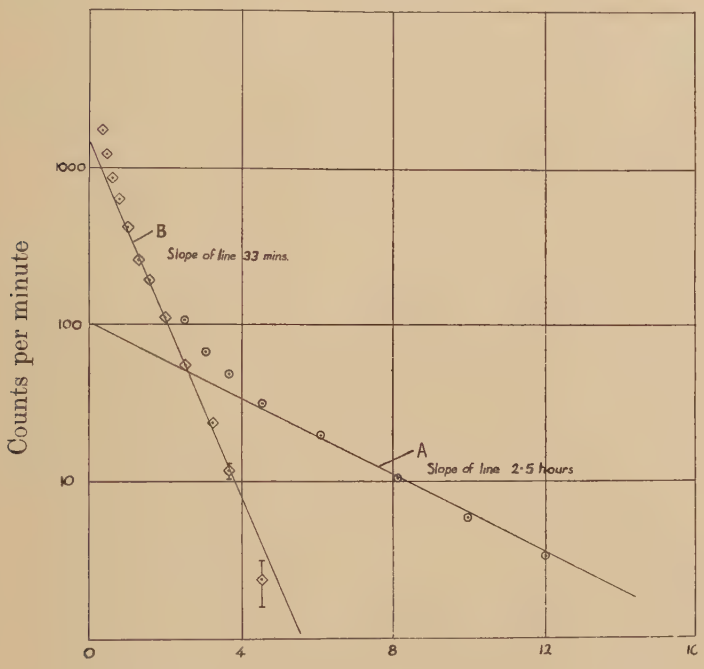

Analysis of the later part of fig. 2.

Curve A shows points obtained after subtraction of the activities due to ^{32}P and ^{24}Na from the gross decay curve. The straight part represents ^{31}Si with a trace of ^{18}F.

Curve B shows the points obtained after subtraction of the activity due to $^{31}Si + ^{18}F$ from curve A. The straight part (about 6 half-lives) represents ^{34}Cl.

investigation. The two most likely are (1) that ^{22}Na is sputtered from the dees, which are almost certainly contaminated, as some 40 mC of this isotope have been made in the cyclotron in the last two years, or (2) that it is produced by the interaction of the very large current of 14 MeV $^{14}N^{2+}$ ions with carbon from the pump oils. A serious discoloration due to the latter is always observed on the cover-foil after long runs.

Absorption measurements have been made of the radiations from a four-month-old target foil which had been properly protected from such

sources of contamination. This, on analysis, showed some 10 counts/min. from ^{32}P, about 20 counts/min from ^{35}S and less than 2 counts/min of ^{22}Na. If indeed this last isotope is produced at all, therefore, by the bombardment of aluminium by the high energy $^{14}N^{6+}$ ions, the yield must be less than 0·003 of the ^{32}P yield.

3.2. *Chemical Identifications*

Standard radiochemical methods were used in the identification of the radioactive products, the only unusual feature of the investigation being

Fig. 3 (*b*)

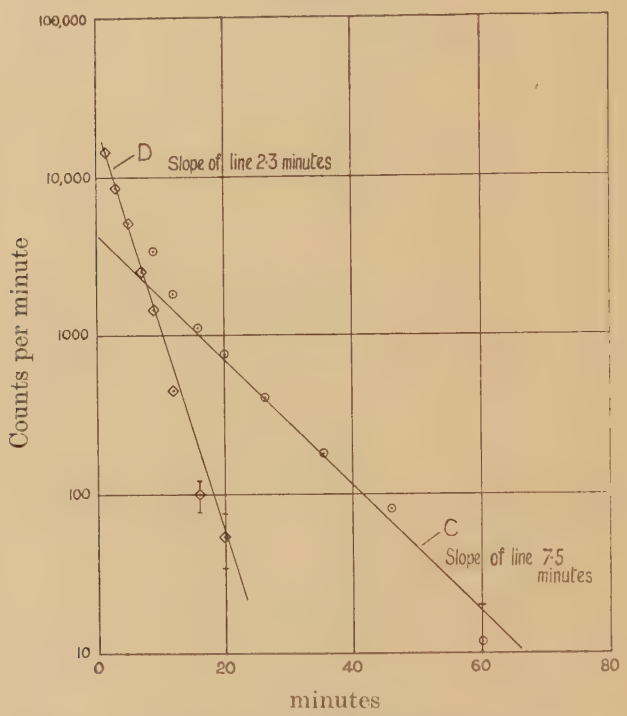

Further analysis of fig. 2.

Curve C shows the result of subtracting activities due to ^{32}P, ^{24}Na, $^{31}Si + ^{18}F$, and ^{34}Cl from the original gross decay curve. The straight part (about 6 half-lives) represents ^{38}K.

Curve D shows the result of subtracting the activity due to ^{38}K from Curve C. The straight part (about 8 half-lives) represents ^{28}Al with a trace of ^{30}P.

the devising of successful methods for the separation of the various activities from such a wide variety of radioactive products in this part of the Periodic System. Fortunately aluminium is dissolved very rapidly by both hot caustic soda solution and by hydrochloric acid. Radiochemical analysis of the solutions so obtained, after adding suitable carriers, as well as of the gases evolved during solution, clearly indicated the presence of radioactive isotopes of the following elements (in order of increasing Z).

(1) Carbon (^{11}C) : counted as $K_2{}^{11}CO_3$. This activity is present in the gases evolved when a bombarded foil is dissolved in hot sodium hydroxide solution. The ^{11}C is presumably carried as a hydrocarbon which, after combustion with excess of oxygen, is converted to $^{11}CO_2$ and may now be trapped on powdered potassium hydroxide.

(2) Nitrogen (^{13}N) : counted as $(^{13}NH_4)_2SO_4$. This activity also appears in the gas phase on dissolving bombarded foils in boiling sodium hydroxide solution. It may be trapped and counted on a filter pad moistened with dilute sulphuric acid.

Fig. 4

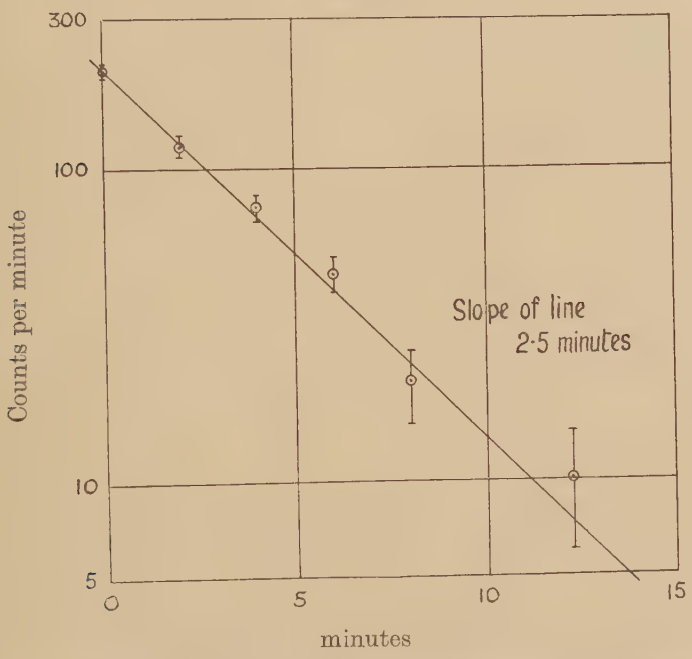

Decay of activity in $Zr(HPO_4)_2$ (after subtraction of ^{32}P) showing ^{30}P.

(3) Fluorine (^{18}F) : precipitated and counted as CaF_2 from neutral solutions after removal of the aluminium as hydroxide.

(4) Sodium (^{24}Na) : counted as NaCl. Here no specific test was applied but a solution of a bombarded foil was treated to remove all cations other than the alkali metals and then evaporated to dryness. The residue showed a clear 14·5 hour decay characteristic of ^{24}Na.

(5) Magnesium (^{27}Mg) : precipitated and counted as $Mg(NH_4)PO_4$, care being taken to remove nitrogen and phosphorus activities.

(6) Silicon (^{31}Si) : precipitated and counted as SiO_2 from acid solutions, and also as Cs_2SiF_6 after distillation of SiF_4.

(7) Phosphorus (^{30}P and ^{32}P) : precipitated and counted as $Zr(HPO_4)_2$; ^{32}P also as $(NH_4)_3PO_4 . 12\,MoO_3$, from solutions of bombarded foils in aqua regia. (For decay of a zirconium phosphate sample see fig. 4.)

(8) Sulphur (^{35}S) : precipitated and counted as $BaSO_4$.

(9) Chlorine (^{34}Cl) : precipitated and counted as AgCl. The decay of one sample was followed over twelve half-lives but the slope remained very constant, indicating again that the proportion of ^{38}Cl is quite small—probably below 5% (fig. 5).

(10) Potassium (^{38}K) : precipitated and counted as $KClO_4$.

In addition to the above, activities in calcium were looked for but not found ; activities in argon, neon, oxygen and beryllium have not been looked for as yet.

Fig. 5

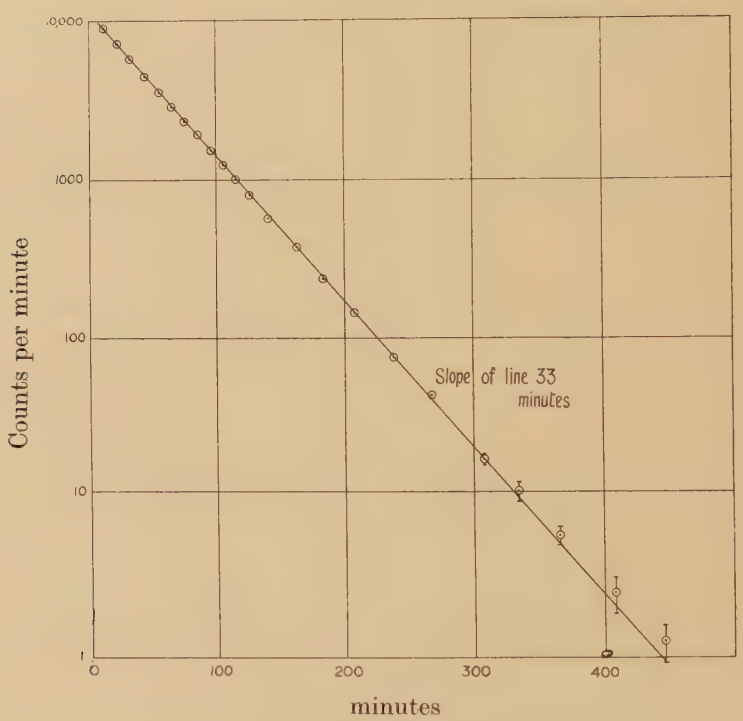

Decay of activity of AgCl, showing ^{34}Cl.

3.3. *Relative Yields of the Radioactive Products*

Several stacked-foil bombardments have been carried out for different bombardment times, and the relative yields of the main radioactive products have been calculated from the resolved gross decay curves of the individual foils. The relative yields are the same within a factor two for all the foils examined (down to 50 μ below the target surface), and are shown in table 1. They are expressed as numbers of atoms formed per 100 of ^{34}Cl. This isotope is chosen as an arbitrary standard as, owing to its suitable half-life and high yield, it was usually determined with greatest accuracy.

Both ^{27}Mg and ^{11}C must be formed in relatively low yield as their activities are not detected in the gross decay curves. However, if their yields (in numbers of atoms formed) were 10% of the ^{38}K or ^{34}Cl yields, they could easily be missed as their half-lives lie between these two (^{38}K 7·5 min, ^{27}Mg 9·5 min, ^{11}C 20 min, ^{34}Cl 33 min). Similarly, the yield of ^{18}F must be considerably less than that of ^{31}Si (^{18}F 112 min, ^{31}Si 157 min). It is in fact difficult to be sure whether ^{18}F is a true reaction product at all, since some trial experiments in which various oxygen compounds were bombarded with ^{14}N showed very strong yields of ^{18}F, and it is possible that the ^{18}F observed in bombardments of aluminium foil arose from a surface layer of oxide.

Table 1. Yield of Active Nuclei Observed and to be Expected on Various Assumptions, from the Bombardment of Aluminium with ^{14}N

Evaporation				*Buckshot*	
Observable nucleus	Evaporated particles	Q (MEV)	Whether observed	*Group* 1	Actual Yield (^{34}Cl≡100)
				^{32}P	300
^{32}P	p 2α	— 2·1	Yes	^{28}Al	140
^{35}S	2p α	— 2·6	Yes	^{24}Na	12†
^{38}Cl	3p	— 6·4	No	*Group* 2	
^{38}K	2n p	— 9·0	Yes	^{38}K	75
^{31}Si	2p 2α	—10·7	Yes	^{34}Cl	100
^{28}Al	p 3α	—12·0	Yes	^{30}P	25
^{34}Cl	2n p α	—16·4	Yes	*Group* 3	
^{33}P	n 3p α	—20·4	No	^{35}S	25
^{27}Mg	2p 3α	—21·6	Yes	^{31}Si	15
^{30}P	2n p 2α	—22·5	Yes	^{27}Mg	small (<10)
^{24}Na	p 4α	—22·9	Yes	*Group* 4	
^{29}Al	n 3p 2α	—31	No	^{22}Na	⩽2
^{22}Na	2n p 4α	—42·3	No	^{13}N	Undetermined*
^{25}Na	n 3p 3α	—44	No	^{11}C	small
^{15}O	2n 6α	—47·8	?	The following should be rare	
^{18}F	2n p 5α	—50·8	?	^{15}O ^{17}F	No other
^{11}C	2n 7α	—58·1	Yes	^{18}F ^{25}Na	nuclei
^{17}F	3n p 5α	—59·9	No	^{38}Cl ^{29}Al	observed but
^{13}N	3n p 6α	—65·7	Yes	^{33}P	unconfirmed possibility of ^{18}F.

† See discussion in text of the special case of ^{24}Na.

* The total yield of this isotope may be considerable, but the ^{13}N nuclei appear to have a large velocity after formation, the amount found in any foil not being simply related to the amount produced therein. This point is being further investigated.

§ 4. Bombardment of Magnesium by ^{14}N Ions

The lack of active calcium isotopes from the bombardment of aluminium was believed to be due to the lack of β-emitters of suitable half-life. It was realized, however, that it might be difficult to avoid the loss of one or

more charged particles from a compound nucleus with as small a potential barrier as ^{41}Ca, so it was thought desirable to make a specific search for ^{38}K in magnesium bombarded by nitrogen ions. The possible products of complete fusion of the ^{14}N with the isotopic target nuclei are ^{38}K, ^{39}K and ^{40}K ; to give ^{38}K one of the latter two must be able to get rid of its excitation energy by neutron loss alone.

Four ten-minute bombardments were carried out and in each case the potassium, chemically extracted as before, showed an activity of about the expected half-life. In one case the charge discriminator was used to confirm that the particles emitted were positrons. Complete confirmation was thus obtained that all seven protons could be made to ' stick ', though the yield was very small, less than 5% of the ^{34}Cl yield.

§ 5. Other Experimental Evidence concerning the Kinds of Reaction Produced by Nitrogen Ions

A preliminary examination has been made of some 250 nuclear interactions observed in an Ilford C2 emulsion bombarded by ^{14}N ions of 60–140 Mev.

As was found by Miller (1951) using ^{12}C ions, the commonest events apart from simple scattering are three-pronged stars. Most of the prongs are α-particles but a large number of our stars show one proton track. With two possible exceptions, no cases of fission are observed in the emulsion either of the heavier compound nuclei formed from silver and bromine or of the lighter ones formed from carbon, nitrogen and oxygen. (The fairly common elastic collisions which occur at low energy can readily be distinguished by the fact that the centre-of-mass energies are well below the Coulomb barrier concerned.)

This suggests strongly that fission processes are rarely, if ever, involved in the production of the active bodies identified in the work described in previous sections.

§ 6. Discussion of the Reactions Produced in Aluminium by Nitrogen Bombardment

In reactions produced by light particles of moderate energies, only a few reaction products are energetically possible. In the reactions described here, however, there is enough energy to produce almost every one of the known nuclides lighter than ^{41}Ca.

In fact, by no means all of the energetically-possible nuclei appear in appreciable quantity and a particular feature stands out very strongly. This is the prominence of β^+ emitters among the products (see table 1), particularly ^{32}P, although the earlier Berkeley work on the bombardment of heavier elements with carbon ions showed a high probability of neutron evaporation (Miller *et al.* 1950).

Let us consider some of the possible ways in which reactions may take place. The simplest assumption is that the whole of both nuclei first combine into a single excited compound nucleus, ^{41}Ca. This will be des-

cribed as the 'fusion' nucleus to distinguish it from other possible compound nuclei involving parts only of the initial pair. The excitation energy can then be lost by fission or by evaporation of heavy particles. (This excitation energy, calculated from the ^{14}N energy distribution, will usually be in the range 35–50 MEV.) Evaporation and fission processes are not of course completely distinct; fission here will be taken to mean a disintegration in which both fragments are heavier than alpha particles.

In their paper Wyly and Zucker (1953) tacitly assume fission; Miller (1951) appears rather to favour evaporation. We believe that fission may generally be regarded as improbable on the basis of the photographic emulsion evidence in § 5. It does not seem very likely that such reactions could be markedly more frequent with aluminium than with any of the elements common in photographic emulsions.

A multiple evaporation, particularly of α-particles, would be consistent with the photographic plate evidence and energetically is entirely possible. The production of ^{38}K, for example, could well occur by loss of $p+2n$ from ^{41}Ca, and that of ^{34}Cl and ^{30}P by the same process with loss of one or two extra α-particles respectively. It seems curious, however, that the chief product of the ^{14}N reaction should be ^{32}P, which involves the evaporation of two α-particles and a proton without loss of a neutron at all, and still more difficult to believe in the production of ^{31}Si (two α-particles and two protons) or ^{24}Na (four α-particles and one proton) by this means. Even if such a production were possible it is difficult to see why the yields (see table 1) should be so nearly comparable over the whole range from ^{24}Na to ^{38}K. The fair yields of ^{11}C and ^{13}N are further awkward facts.

The evidence is strong, then, that even if evaporation processes account for the heavier positron emitters, they cannot alone be involved.

The next possible process which will be considered is a simple 'stripping' process in which a neutron is removed by either nucleus from the other without significant interaction of the remaining parts of the nuclei. This process might well be favoured at low energies as the charged parts of the nuclei would not need to penetrate the full Coulomb barrier. This process would give rise to the following reactions:

$$^{14}N+{}^{27}Al \rightarrow {}^{15}N+{}^{26}Al$$

$$^{14}N+{}^{27}Al \rightarrow {}^{13}N+{}^{28}Al$$

possibly followed by

$$^{26}Al \rightarrow {}^{22}Na+\alpha$$

$$^{28}Al \rightarrow {}^{24}Na+\alpha$$

which might account for ^{13}N, ^{22}Na, ^{24}Na, ^{28}Al. There remain ^{11}C, ^{27}Mg, ^{31}Si, ^{32}P and ^{35}S not fitting either of the above supposed processes.

An explanation which fits the facts observed so far is as follows. It was noticed that the energy required to overcome the Coulomb barrier of aluminium in these reactions (17·4 MEV for $^{14}N+{}^{27}Al$ in the centre-of-mass system) was comparable with the energy required for the disintegration $^{14}N \rightarrow 3\alpha+n+p$, which is 19·77 MEV. Let us suppose that the incident

^{14}N nucleus might be thought of, at least in the field of target nucleus, as three independent α-particles, a proton and a neutron. The target could then be visualized as being struck, not by a single bullet, but rather by a shower of buckshot. (If the nuclei are of comparable mass, of course. both might be regarded at the instant of collision as composed of largely independent particles.)

It is not intended to imply that the undisturbed ^{14}N must be already divided up in this way or that the paths of the individual particles are parallel. The internal velocities of the particles must be quite comparable with the velocity of the whole nucleus. The separation visualized may be regarded as a virtual one only, unless one or more of the particles is actually captured by the target nucleus.

If we consider this picture, it is easy to see that only when the impact parameter is small will there be a good chance of all the separate particles being captured by the target nucleus. If the impact parameter is large, some particles may be captured but others will miss and be deflected away. On simple geometrical grounds it can then be seen that the chances of capture of one, two or three α-particles would all be comparable.

A difference of behaviour between the α-particles and the odd proton and the odd neutron is to be expected, for the neutron will find no potential barrier against its capture. The deflecting force in fact will be even more important for the proton than it will be for an alpha particle, which for a given velocity has four times the kinetic energy and has to surmount only twice the potential barrier. The groups of particles escaping capture by the aluminium, then, would have the following order of probability :

(1) $x\alpha+\mathrm{p}$,

(2) $x\alpha+\mathrm{n}+\mathrm{p}$,

(3) $x\alpha$,

(4) $x\alpha+\mathrm{n}$,

where x may be 0, 1, 2 or 3, though $x=3$ may be regarded as a special case.

It is reasonable to suppose, where considerable energies are involved, that radiative capture is less likely than capture with subsequent emission of a heavy particle. Potential-barrier considerations would favour neutron emission but discourage proton emission. In the region of the periodic table concerned, the binding energy of either nucleon is fairly large, often larger than that of an alpha particle. The energy *per nucleon* needed by an alpha particle is thus a good deal less. We shall thus regard the emission of either a neutron or an alpha particle as more favoured than emission of a proton. It is worth noting that this will be particularly important where $x\alpha+\mathrm{n}$ have just been captured, as the energy required to extract a proton will then be higher than that required for either of the other particles.

On this basis, then, we can readily explain the large production of ^{32}P, as follows :

$$^{27}\mathrm{Al}+\mathrm{n}+2\alpha \rightarrow {}^{36}\mathrm{Cl} \rightarrow {}^{32}\mathrm{P}+\alpha.$$

The complete set of this class of reactions, with the *favoured* modes of breakdown, are as follows :

$$^{27}\mathrm{Al}+\mathrm{n} \rightarrow {}^{28}\mathrm{Al} \begin{cases} \nearrow {}^{27}\mathrm{Al}+\mathrm{n}-7{\cdot}7 \text{ MEV} \\ \searrow {}^{24}\mathrm{Na}+\alpha-10{\cdot}9 \text{ MEV} \end{cases}$$

$$^{27}\mathrm{Al}+\alpha+\mathrm{n} \rightarrow {}^{32}\mathrm{P} \begin{cases} \nearrow {}^{31}\mathrm{P}+\mathrm{n}-7{\cdot}9 \text{ MEV} \\ \searrow {}^{28}\mathrm{Al}+\alpha-9{\cdot}9 \text{ MEV} \end{cases}$$

$$^{27}\mathrm{Al}+2\alpha+\mathrm{n} \rightarrow {}^{36}\mathrm{Cl} \begin{cases} \nearrow {}^{35}\mathrm{Cl}+\mathrm{n}-8{\cdot}5 \text{ MEV} \\ \searrow {}^{32}\mathrm{P}+\alpha-8{\cdot}3 \text{ MEV} \end{cases}$$

$$^{27}\mathrm{Al}+3\alpha+\mathrm{n} \rightarrow {}^{40}\mathrm{K} \begin{cases} \nearrow {}^{39}\mathrm{K}+\mathrm{n}-7{\cdot}8 \text{ MEV} \\ \searrow {}^{36}\mathrm{Cl}+\alpha-5{\cdot}6 \text{ MEV} \end{cases}$$

(The reaction-energies listed refer only to the second steps of these processes.)

There are thus three observable radioactive products, ^{24}Na, ^{28}Al and ^{32}P. In the parent of ^{32}P alone α emission is energetically favoured as against neutron emission, which may well account for the yield being greater than that of ^{28}Al. For the first case, ^{24}Na, it may well be that the capture of a single neutron, from a bound state of similar energy, does not usually leave enough excitation energy for α emission and either gives ^{27}Al or contributes directly to the ^{28}Al yield.

The group of nuclei produced by adding $x\alpha$ particles to aluminium comes next, giving us ^{39}K, ^{35}Cl and ^{31}P. The previous situation is now reversed ; emission of an α-particle in each case leaves a stable nucleus while emission of a neutron gives ^{38}K, ^{34}Cl and ^{30}P. Table 1 shows that these are in fact the next group experimentally, with quite similar yields.

The next group, in which $x\alpha$+n+p are captured, gives us ^{29}Si, ^{33}S, ^{37}A and ^{41}Ca. Emission of either a neutron or an alpha particle from any of these leads to a stable nucleus except for ^{37}A which is a K-capturer and not observable by the methods used. In the final group, $x\alpha$+p are supposed to be captured. This gives rise to ^{28}Si, ^{32}S, ^{36}A and ^{40}Ca. In every case α emission gives rise to a stable isotope and n-emission to an isotope too short-lived for our observation.

We have next ^{27}Mg, ^{31}Si and ^{35}S, each of which requires a *proton* emission from one of the readily-produced Al+$x\alpha$+n nuclei. It will be seen that the yield increases more rapidly with mass than in the other series. This may reasonably be regarded as due to the higher excitation needed for proton emission, which is more likely to occur when more particles have been captured. Finally, we have ^{13}N and ^{11}C. These may arise from the uncaptured particles, when these are not permanently separated.

In table 1 are shown all of the observable nuclei which could be produced by evaporation, with the corresponding values of Q. There is some correlation between the Q's for evaporation and the observed yield but there are some striking discrepancies such as the large yield of ^{34}Cl and the so-far unobservably small yield of ^{38}Cl. The same table shows the nuclei which would be expected on the buckshot picture, in the expected order of yield, and the observed values. No attempt is made to predict the relative probabilities of the inverse reactions ; i.e. those in which nucleons are captured by the lighter nucleus from the heavier. Most of the nuclides

produced in this way would be stable and unobservable, and the photographic emulsion evidence suggests that reactions leaving two heavy nuclei are rare.

It will be seen, however, that an excellent qualitative fit exists between the nuclei predicted by the proposed 'buckshot' picture and those observed. Although no observed nucleus requires the emission of more than one heavy particle from the primary compound nucleus, it is not suggested that multiple emission cannot occur at all.

Thus two neutrons might well be emitted by the first group of compound nuclei mentioned (^{28}Al, ^{32}P, ^{36}Cl and ^{40}K), adding to the yield of ^{30}P, ^{34}Cl and ^{38}K obtained from the second group. It must be remembered, however, that in the lighter compound nuclei the level of excitation will not ordinarily be very large. The more-or-less exponential energy distribution above 50 Mev of the ^{14}N ions in the cyclotron, already mentioned, ensures that, at any point within the target, the majority of the ions energetic enough to cause a reaction have energies not very far above the barrier. This explains why the relative yields of different products seldom vary very much with depth in the stack of foils. An estimate based on the energy spectrum of the ions indicates that almost three-quarters of the ions reaching the target with energies over 26 Mev are still below 45 Mev. A ^{14}N ion with 45 Mev energy in the laboratory system will carry into the compound nucleus an energy of only about 2 Mev per nucleon in the centre-of-mass system. To take a specific instance, consider the production of ^{36}Cl by capture of two alpha particles and a neutron from a ^{14}N ion with 20 Mev available energy (i.e. 30 Mev in lab. system). Of this, since 9 nucleons are captured, on the average about 13 Mev will go towards exciting the compound nucleus. Since the Q of the reaction

$$^{27}\mathrm{Al}+{}^{14}\mathrm{N}-\mathrm{p}-\alpha\rightarrow{}^{36}\mathrm{Cl}$$

is only about 6 Mev, the total excitation of the ^{36}Cl will be about 19 Mev. This is only a little above the binding energy of two alpha particles (16 Mev) and is actually below that of two neutrons (22 Mev). At such an excitation two-particle emission is, therefore, likely to be uncommon even from this relatively heavy compound nucleus. It can probably be neglected altogether in the lighter ones.

This slightly surprising result is, of course, due to the fact that the particles are captured from a bound state in the ^{14}N nucleus of potential energy not very dissimilar to that in the compound nucleus.

While not ruling out the possibility of fusion followed by evaporation for the heavier nuclei formed, or of neutron-stripping for the nuclei close to the original ones, the partial capture picture seems satisfactorily to cover the whole range of products; it may be noted, of course, that the other possibilities in fact arise naturally as limiting special cases of this.

Now if there is any substance in these considerations, an immediate experimental test suggests itself. If we use as our bombarding nucleus, instead of ^{14}N, a pure α-particle nucleus such as ^{12}C or ^{16}O, a very different set of products should appear. $^{12}C^{6+}$ is less convenient as it is very difficult to avoid heavy contamination from the cyclotron with $^{2}D^{+}$ or $^{4}He^{2+}$, but

the resonance of $^{16}O^{6+}$ lies well away from any possible interfering particles and this was chosen.

In the next section the results obtained with this are discussed.

§ 7. Bombardment of Aluminium with ^{16}O Ions

The best oxygen beams at present obtainable are some 50 times less than the best nitrogen beams, but are nevertheless quite adequate to give fair activities.

Several bombardments of various durations have been carried out. A very marked difference from the nitrogen decay curves was observable. The oxygen decay curves could be analysed perfectly clearly into :

(1) a weak 14 day activity (^{32}P),
(2) a weak 15 hour activity (^{24}Na),
(3) a weak 112 min activity (^{18}F),
(4) a 33 min activity (^{34}Cl),
(5) a $7\frac{1}{2}$ min activity (^{38}K),
(6) a $2\frac{1}{2}$ min activity (^{30}P).

No activities longer than 14-days half-life have yet been observed, although this would not rule out the possibility of ^{22}Na being formed in yield comparable to that of the other nuclei mentioned, as its counting rate would be very low owing to its long half-life. Chemical experiments proved conclusively that the 112-minute decay was due to ^{18}F, as a weak but definite activity of this period was found to be associated with a precipitate of calcium fluoride obtained from a solution of a bombarded foil in hydrochloric acid after addition of suitable carriers. On the other hand, a precipitate of silica was completely inactive indicating the absence of ^{31}Si among the reaction products. These results are in contrast to those obtained with ^{14}N bombardments, in which the ^{31}Si activity was much stronger than that of ^{18}F. Separations of zirconium phosphate demonstrated the $2\frac{1}{2}$ minute activity as being due to ^{30}P. The magnetic discriminator showed that the activities ascribed to ^{34}Cl, ^{38}K and ^{30}P were in fact due to positrons ; any real negative electron activity could not have been more than 5% of the positron activity observed in each case. In view of the clear resolution of the decay curves we have therefore considered further identifications unnecessary.

The relative yields are shown in table 2, again taking ^{34}Cl as 100.

It will be seen that, as expected in the ' buckshot ' picture, there is a complete change-over of the relative activities from the nitrogen yields. As we can no longer add anything but $x\alpha$, and emission of protons or α-particles from the resulting nuclei leads always to stable products, to a first approximation we should expect the only observable reactions to be :

$$^{27}Al + \alpha \rightarrow {}^{31}P \rightarrow {}^{30}P + n$$
$$^{27}Al + 2\alpha \rightarrow {}^{35}Cl \rightarrow {}^{34}Cl + n$$
$$^{27}Al + 3\alpha \rightarrow {}^{39}K \rightarrow {}^{38}K + n$$

^{26}Al and ^{42}Sc being unobservable.

Table 2. Active Isotopes Observed to be Produced from Bombardments of Aluminium with Oxygen

Active Nucleus	Yield relative to $^{34}Cl \equiv 100$
^{38}K	115
^{34}Cl	100
^{30}P	35
^{18}F	17
^{32}P	5
^{24}Na	3
No other product observed	

In fact these are not the only, but are outstandingly the most important, products. The very small yield of ^{32}P may involve the emission of the less-likely particle ^{3}He, which is known to be produced from various high-energy reactions. The yields of ^{18}F and ^{24}Na may be made by the inverse reactions in which ^{16}O abstracts the stray nucleons from the ^{27}Al, e.g.

$$^{27}Al + ^{16}O \rightarrow ^{24}Mg + ^{19}F$$
$$^{19}F \rightarrow ^{18}F + n$$

(none of the simple particles emitted from ^{24}Mg will leave an observable product).

$$^{27}Al + ^{16}O \rightarrow ^{25}Mg + ^{18}F$$
$$^{25}Mg \rightarrow ^{24}Na + p$$

the small yield of ^{17}F produced from ^{18}F not being observable in the presence of the heavy yield of ^{30}P.

§ 8. Conclusion

The great contrast between the ^{14}N and ^{16}O results, which appears as a natural consequence of the 'buckshot' hypothesis, is very difficult to explain on the basis of fission and not immediately easy on the basis of evaporation from the fusion nuclei ^{41}Ca and ^{43}Sc. It would be surprising that evaporation at moderate energies from the former should lead to such an excess of β^- emitters and from the latter of β^+ emitters.

We believe that the data described here, while they are far from proving that the 'buckshot' picture is correct, do show that it is a helpful conception when trying to see a pattern in the observed facts, and further that it may be useful in predicting the likely outcome of this very complicated kind of nuclear reaction. The results predicted do not differ very greatly from those to be obtained from the evaporation model if, after the first particle emitted, evaporation of α particles is very strongly preferred, but, where they do differ, our picture seems to be in closer accord with the experimental results.

Acknowledgments

We are much indebted to several members of the laboratory for occasional assistance with the counting of active samples, and to our wives for their patience in bearing the inconvenience caused by the all-night counting which was sometimes required.

We are grateful also to Professor Moon and to Professor Burcham for valuable criticism and discussions.

References

Breit, G., Hull, M. H., and Gluckstern, R. L., 1952, *Phys. Rev.*, **87,** 74.

Chackett, K. F., Fremlin, J. H., and Walker, D., 1953, *Proc. Phys. Soc.* A, **66,** 495.

Ghiorso, A., Thompson, S. G., Street, K., and Seaborg, G. T., 1951, *Phys. Rev.*, **81,** 154.

Miller, J. F., Hamilton, J. G., Putnam, T. M., Raymond, H. R., and Rossi, G. B., 1950, *Phys. Rev.*, **80,** 486.

Miller, J. F., 1951a, *Thesis*, University of California ; 1951b, *Phys. Rev.*, **83,** 1261.

Reynolds, H. L., Scott, D. W., and Zucker, A., 1953, *Proc. Nat. Acad. Sci.*, **39,** 975.

Walker, D., and Fremlin, J. H., 1953, *Nature, Lond.*, **171,** 189.

Walker, D., Fremlin, J. H., Link, W. T., and Stephens, K. G., 1954, *Brit. Journ. App. Phys.* (in the press).

Wyly, L. D., and Zucker, A., 1953, *Phys. Rev.*, **89,** 524.

XXII. *Nuclear Disintegrations Caused by* 50–125 MeV *Protons: II*

By P. E. Hodgson*
Imperial College of Science and Technology, London, S.W.7†

[Received November 4, 1953]

Summary

A method of separating nuclear disintegrations caused in photographic emulsion by 50–125 MeV protons into those in the light and those in the heavy nuclei of the emulsion is described. It is used to determine the characteristics of the disintegrations of the light and the heavy nuclei. These results show that about thirty per cent of the low energy particles emitted from nuclear disintegrations are the result of a nuclear cascade initiated by the primary particle.

Introduction

In a previous paper (Hodgson 1953, referred to as I) the results of measurements on nuclear disintegrations caused by 50–125 MeV protons in Ilford C2 emulsion were described. These measurements refer to the disintegrations in the mixture of elements constituting the emulsion, and are consequently difficult to interpret theoretically. In Part I of this paper, a method is described by which it is possible to separate, with quite a high efficiency, the disintegrations reported in I into those in the light (carbon, nitrogen and oxygen) and those in the heavy (silver and bromine) nuclei of the emulsion.

Part II summarizes the main characteristics of the nuclear disintegrations in the light and heavy nuclei determined by measurements on events separated according to the procedure described in Part I. In Part III several models of the collision and disintegration process are compared with the experimental results for the heavy elements.

Part I.—The Separation Procedure

§1. Introduction

The method of separation uses some well-established characteristics of nuclear disintegrations in the light and heavy elements to divide the observed events into the two categories. Several possible characteristics were tried before the energy of the emitted alpha-particles was finally

* Communicated by the Author.
† Now at University College, London, W.C.1.

selected as the most suitable. In addition, several subsidiary criteria were used to allocate those events from which no alpha-particles were emitted.

The first attempt was made with the method based on the length of the shortest track which had previously been used with success to separate the disintegrations caused by the cosmic radiation (Hodgson 1952 b). This method depends on the results of Harding (1949 b) who showed that most of the stars caused by the cosmic radiation and having recoil fragments are due to the disintegration of the heavy elements, while most of the stars without recoil fragments are formed in the light elements. When this method was applied to the present group of stars it did not effect the desired separation. This is because the average energy of the disintegrations is much less than that of those studied by Harding, with the result that a considerable proportion of the stars in the heavy elements have no visible recoil fragment.

The separate procedure used is described and justified in the following section.

§ 2. The Separation Criteria

The separation procedure used here is based essentially on the fact that very few, if any, alpha-particles emitted from moderately excited silver and bromine nuclei have energies less than 9 MeV.

This is to be expected from the potential barriers of silver and bromine, which are about 14 and 12 MeV respectively in the unexcited state, when allowance is made for slight lowering of the barrier due to the nuclear excitation. It has been confirmed by calculations of the emission process by Puppi (1953), who found a sharp low energy cut-off at about 9 MeV in energy spectrum of the alpha-particles from such nuclei. The first experimental proof of this was given by Perkins (1949), who showed by subtracting the energy distribution of the alpha-particles from light nuclei (obtained by the gelatin sandwich method) from that of a corresponding number of disintegrations in normal emulsion that " practically all alpha-particles of energies below 10 MeV can be attributed to light nuclei ". This conclusion was confirmed by Menon, Muirhead and Rochat (1950), who measured the energy distribution of the alpha-particles from one-track stars caused by the nuclear absorption of slow π^--mesons and found two peaks, one at about 2 MeV corresponding to the light elements and one at about 10–12 MeV corresponding to the heavy elements, with a marked minimum in the range 8–10 MeV. Further support is provided by the measurements of Lees, Morrison, Muirhead and Rosser (1953) and of Hodgson (1953) who find a peak at about 12 MeV in the energy distribution of alpha-particles emitted from one- and two-track stars caused by 110–146 and 50–125 MeV protons respectively, and by measurements of Hodgson (1952 b) of the energy distribution of the alpha-particles from disintegrations caused by the cosmic radiation.

To establish a rigid set of criteria, it is necessary to distinguish between tracks due to nuclear recoils and those due to alpha-particles of very low

energy. These cannot be distinguished by their ionization, and so this must be done by their range. The range distribution of short tracks from all the disintegrations was therefore determined, and it was found to consist of a sharp peak at very small ranges, which may be ascribed to the nuclear recoils, superimposed on a broad distribution extending to greater ranges which may be ascribed to the low energy alpha-particles. The tracks comprising the sharp peak were all less than four microns long, which agrees with approximate calculations of the range of nuclear recoils. All particles making heavily ionizing tracks longer than four microns were therefore counted as alpha-particles. After the stars had been assigned to the light and heavy elements, tracks shorter than four microns in stars in the heavy elements were counted as nuclear recoils, while those in stars in the light elements were counted as alpha-particles.

All events with one or more tracks of alpha-particles of energy less than 9 Mev were assigned to the light elements, and events with all alpha-particles of energy more than 9 Mev to the heavy elements. As alpha-particles are very frequently emitted from nuclear disintegrations, the majority of the events were allocated by means of this criterion.

The energy distribution of the protons from the remaining events was then compared with that of the protons from the stars already assigned to the light or to the heavy elements. It was found to be indistinguishable from that of the protons from the heavy elements and significantly different from that of those from the light elements. All the remaining events were therefore assigned to the heavy elements, with the exception of two types of events noted below.

Firstly, events with two or more tracks with range less than four microns are almost certainly due to the disintegration of a light nucleus, as fission of the residual nucleus from the disintegration of a heavy nucleus is most unlikely at such low excitation energies. Secondly, although the emission of low energy protons from heavy nuclei may be explained by the process discussed by Le Couteur (1950) by which there is a probability of 0·3 that the last proton evaporated from an excited heavy nucleus has an energy between 0·5 and 3·5 Mev, the emission of two such protons from a heavy nucleus is very unlikely. Such events were therefore assigned to the light elements.

In this way each event was assigned either to the light or to the heavy nuclei. After this had been done, the tracks made by nuclear recoils from the disintegration of heavy nuclei were no longer included in the star size. Thus a star of two protons in a heavy element is called a two-track star whether it has a visible nuclear recoil or not, in contrast to the classification in I, in which all tracks, including nuclear recoils, were included in the star size. The advantage of the new classification is that the assignment of star size no longer depends on whether a very short track is observed or not. As these tracks are difficult to see, and their visibility depends on the type and degree of development of the emulsion, this should facilitate the comparison of results obtained by different observers.

The separation procedure outlined above is not infallible but it is sufficiently reliable for a determination of the main features of the disintegrations of light and heavy nuclei to be made. Its efficiency is clearly greater for some types of events than for others, and this must be taken into consideration during the evaluation of results. Thus, for example, it is very reliable for stars of four or more tracks but quite unreliable for stars consisting of only one proton.

§3. Comparison with other Separation Procedures

The method described in the last section may be compared with two others designed to achieve the same object. Lees, Morrison, Muirhead and Rosser (1953) have compared the disintegrations produced by 130 MEV protons in normal G5 emulsion with those in emulsion containing more than the usual proportion of gelatin. By suitable subtractions they find the characteristics of the light and heavy elements separately. The main advantage of this method over the present one is that there is less possibility of systematic error, but this is offset to some extent by the low statistical accuracy resulting from the subtraction procedure and the extra labour of calibrating and processing multigel plates.

Blau, Oliver and Smith (1953) and Germain (1953) have applied the gelatin sandwich method of Harding (1949 a) to the study of the disintegrations of the light elements caused by artificially accelerated particles. This method has the advantage that every event observed to originate in the gelatin layer certainly occurs in a light element. One of its disadvantages is that the number of events per unit volume of emulsion is much lower for comparable conditions of exposure than that obtained by other methods, which increases the scanning time per event. Further, some particles, especially those of short range, remain wholly in the gelatin layer and must be allowed for in the evaluation of results.

These three methods are in many respects complementary, and the best one to use depends on the problem being studied. The main advantage of the method described here is that results can be obtained more rapidly than by either of the other methods.

Part II.—The Disintegrations of the Light and Heavy Nuclei

§1. The Size Distributions

The distributions of star sizes are given in table 1 for the four energies of incident protons.

These distributions are considerably more peaked than those calculated from Poisson's Law. They are remarkably insensitive to the energy of the incident protons, and the mean star size increases slowly with increasing E_p.

§ 2. The Relative Numbers of Secondary Protons and Alpha-Particles

The proportion P_α of alpha-particles among the emitted particles from stars in the light nuclei showed no significant variation with E_p for stars of the same size. P_α is plotted in fig. 1 as a function of star size.

Table 1

Proton Energy E_p	Number of tracks											
	Light Nuclei							Heavy Nuclei				
	1	2	3	4	5	6	7	1	2	3	4	5
45	1	16	34	40	7	—	—	59	33	8	2	—
68	1	9	25	17	9	1	—	78	55	5	—	—
94	2	7	14	21	13	1	—	48	82	11	1	—
122	1	10	20	21	11	3	1	33	55	37	6	2

Fig. 1

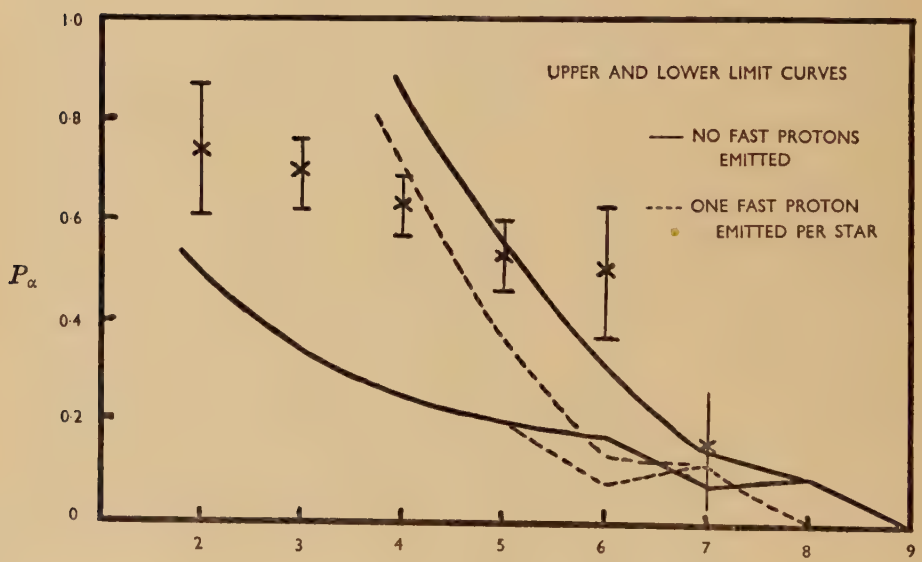

Variation of P_α with star size for the disintegrations of the light nuclei.

Upper and lower limits to P_α can be calculated from elementary considerations. The upper limit is set by the number of charged nucleons in the target nucleus and is the reason why P_α decreases with increasing star size. If we assume that the nucleus disintegrates completely into alpha-particles and protons only, then the numbers of alpha-particles and protons, and

hence P_α, are fixed by the charge on the target nucleus and the size of the star. The upper limit was calculated in this way as a function of star size by combining the disintegrations in carbon, nitrogen and oxygen in the proportions in which they are present in the emulsion and assuming that the cross-section for star production follows an $A^{2/3}$ law.

The lower limit to P_α is set by the fact that if a light nucleus disintegrates into a few particles, at least one of these must have charge greater than or equal to two, and so be classed among the alpha-particles. Thus $[P_\alpha]_{\min}=1/n$ for an n-track star when $n\leqslant 5$. It is of course possible that the heavily charged particle makes too short a track to be visible, but this happens so rarely that the lower limit given by the formula above is not materially affected.

These calculations will be affected if one or more fast secondary particles were emitted and not counted among the tracks of the star. They were therefore repeated assuming that one such particle was emitted from each star.

The results of these calculations are plotted in fig. 1 and are consistent with the experimental results.

The proportion of alpha-particles among all the particles emitted from heavy nuclei was found to have no significant variation either with the energy of the incident proton or with the star size. Its mean value over all the stars is $0{\cdot}22\pm0{\cdot}02$.

§3. The Proportions of Stars with Different Numbers of Protons and Alpha-Particles

The proportions of stars with different numbers of protons and alpha-particles were found to be independent of the energy of the incident proton. Results for all energies are therefore grouped together in the following table.

Table 2. Numbers of Stars with N Alpha-particles

Star size \ N	Light Nuclei							Star size	Heavy Nuclei					
	0	1	2	3	4	5	6		0	1	2	3	4	5
2	1	24	17	—	—	—	—	1	160	58	—	—	—	—
3	1	20	39	32	—	—	—	2	150	69	6	—	—	—
4	0	12	36	38	11	—	—	3	24	32	3	2	—	—
5	1	1	19	13	8	0	—	4	2	3	2	1	1	—
6	0	0	0	6	0	0	0	5	0	0	1	0	0	1

These distributions were compared with those given by Bernouilli's Law, which corresponds to the case when the emission of one particle does not affect the probability of emission of another similar particle (Hodgson 1952 a), and no significant difference was found between them.

§4. The Energy Distributions of the Secondary Alpha-Particles and Protons

The energy distributions of the secondary alpha-particles and protons were found to have no significant variation with the energy of the incident protons. The variation of the energy distribution of the alpha-particles from the light elements with star size is shown by figs. 3 (*a*)–3 (*d*) of I if the

Fig. 2

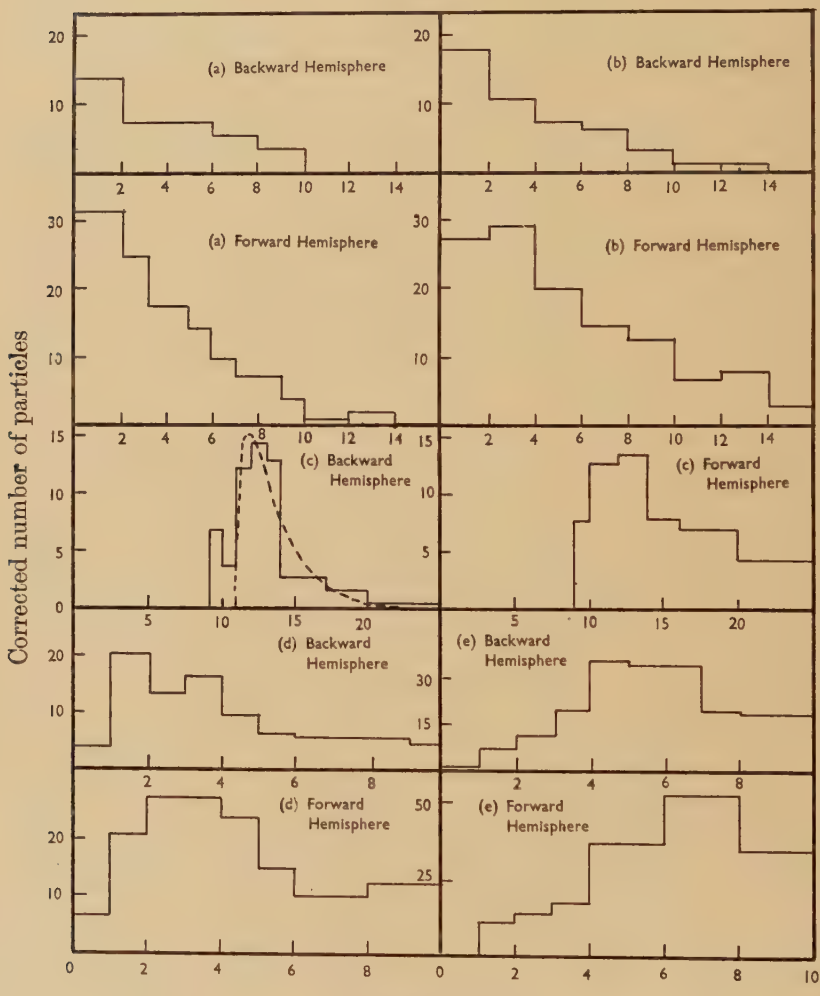

Energy distributions of protons and alpha-particles from light and heavy nuclei. (*a*) Alpha-particles from 1 to 3 track stars in light nuclei. (*b*) Alpha-particles from 4 to 7 track stars in light nuclei. (*c*) Alpha-particles from heavy nuclei. (*d*) Protons from light nuclei. (*e*) Protons from heavy nuclei. – – – – Fitted evaporation curve.

peak at 10–12 MEV in fig. 3 (*a*) due to alpha-particles from the heavy elements is omitted. The energy distributions of the alpha-particles emitted in the forward and backward hemispheres with respect to the incident particles are shown in fig. 2 for the light and heavy nuclei. The energy distribution of the alpha-particles emitted in the backward direction from the heavy nuclei was fitted by the best curve of the form

$$P(T)\,dT = \frac{(T-V')^{l-1}}{\Gamma(l)\tau^{*l}} \exp\left[-\frac{T-V'}{\tau^*}\right] dT$$

where V' is the effective potential barrier height and τ^* the nuclear temperature, which is approximately equal to 11/12 τ (Le Couteur 1952). The experimental values were $V'=11$ MEV, $\tau=2$ MEV.

These results can be used to check Le Couteur's relation $U=A\,\tau^2/11$ between the excitation energy U and the nuclear temperature τ. Inserting the known values of τ and A, we obtain $U=34$ MEV which is of the correct order of magnitude for a group of disintegrations caused by 50–125 MEV protons.

The alpha-particles emitted in the forward hemisphere contain a considerable proportion of direct knock-ons (see Part III) and so they were excluded from the above comparison.

The energy distributions of the protons did not vary significantly with star size and are shown in fig. 2 for all stars together, the distributions in the forward and backward hemispheres being shown separately. They were found from those protons ending in the emulsion, and so do not extend beyond 10 MEV.

In all cases the usual corrections for particles passing out of the emulsion were made.

§ 5. The Angular Distributions of the Secondary Alpha-Particles and Protons

The angular distributions of the secondary alpha-particles and protons were found to have no significant variation either with the energy of the incident protons or with the star size. The results for all stars together are therefore plotted in fig. 3. The particles ending in the emulsion and those leaving it before coming to rest, which correspond roughly to the lower and higher energy particles, are shown separately in these figures. The angle ψ plotted is the projection on the plane of the emulsion of the angle between the direction of emission of the secondary particle and that of the incident protons. Isotropic emission therefore corresponds to a uniform distribution of ψ.

§ 6. The Proportion of Stars in the Heavy Nuclei

The proportion of all stars that are assigned to the heavy nuclei is plotted in fig. 4 as a function of incident proton energy for each star size. The lines are drawn through the experimental points to emphasize the

Fig. 3

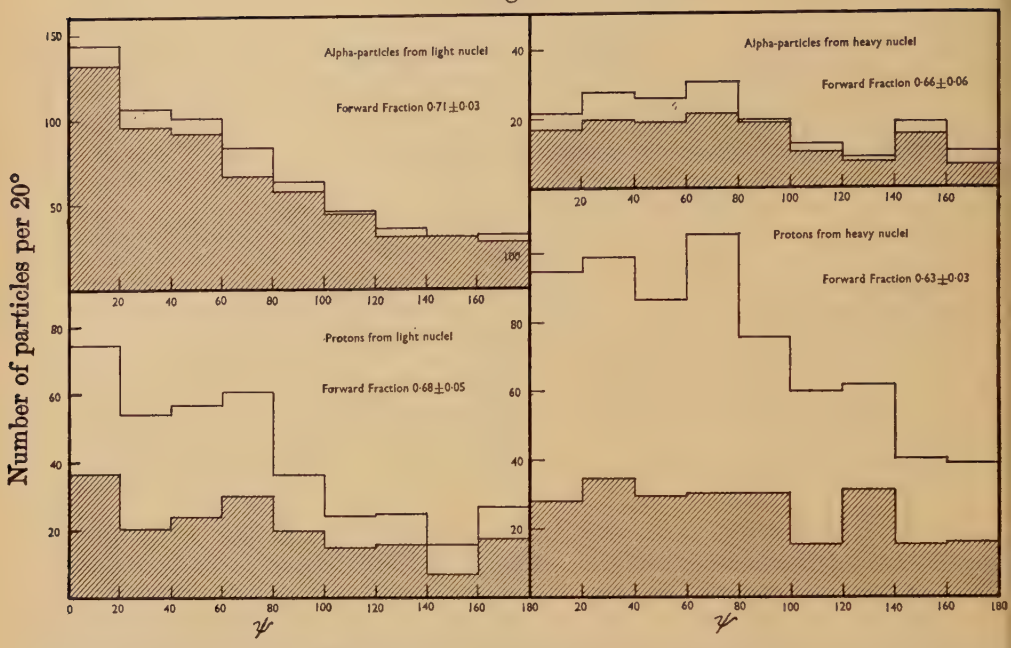

Projected angular distributions of protons and alpha-particles from light and heavy nuclei. The shaded portions correspond to particles ending in the emulsion and the unshaded to those leaving the emulsion.

Fig. 4

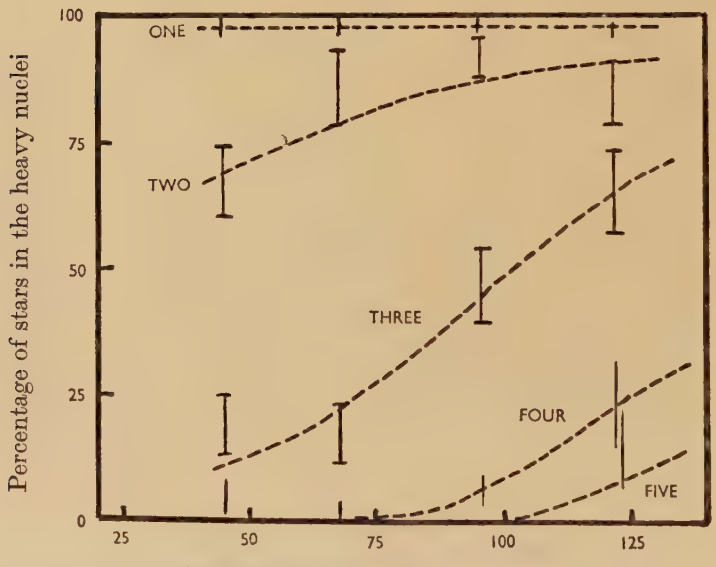

Percentage of stars in the heavy nuclei as a function of star size and energy of incident proton.

main trends but, owing to the considerable statistical uncertainties, their positions are known only approximately. It can be seen that the proportion of stars in the heavy nuclei increases with the energy of the incident protons for each star size. The results of Blau, Oliver and Smith (1952), who investigated the disintegrations of light nuclei by 300 MEV neutrons using gelatin sandwich emulsions show that this trend continues to higher energies, for they found that only 17% of all the events occurred in light nuclei. These results also agree with those of Lees, Morrison, Muirhead and Rosser (1953) who examined disintegrations produced by 130 MEV protons.

This diagram shows that a considerable preliminary separation of the events into those in the light and those in the heavy nuclei may be effected by selecting the incident proton energy and the size of the stars examined.

PART III.—INTERPRETATION

§ 1. INTRODUCTION

In this Part, the results given above are compared with those predicted by simple models of the collision and disintegration process.

The simplest model of the process is to suppose that the incident proton enters the target nucleus and is brought to rest inside it by a series of nucleon–nucleon collisions, thus transferring all its energy and momentum to it. The target nucleus then moves forward with a momentum equal to that of the incident proton, and evaporates secondary particles until it returns to the ground state.

If this were so, the excitation energy of the nucleus would be proportional to the energy of the incident proton, so that the mean energy of the emitted particles or the mean star size or both would increase markedly with primary energy. This is in disagreement with the results of Part II, which indicate that the primary particle often emerges from the target nucleus with a large fraction of its initial energy. This is confirmed by observation of the tracks of high energy particles emitted from many of the disintegrations and by numerous experiments on the attenuation of beams of particles through various materials.

The simplest development of this model is to suppose that only the primary particle goes on with high energy, while all the other particles are emitted at low energy by an evaporation process. The ability of this model to account for the observed features of the disintegration of the heavy elements is investigated in the next section.

§ 2. THE SECOND MODEL OF THE COLLISION PROCESS

Suppose that the primary particle gives the target nucleus sufficient momentum to give it a velocity V, and let $P(v)\,dv$ be the number of secondary particles with velocities in the range v to $v+dv$, with

$$\int_0^\infty P(v)\,dv=1.$$

Then it may easily be shown that the forward fraction F for the low-energy particles is given by

$$F=\frac{1}{2}\int_V^\infty \left(1+\frac{V}{v}\right) P(v)\,dv+\int_0^V P(v)\,dv.$$

In the case of the heavy elements $V \ll \bar{v}$, and so F is very insensitive to the assumed value of the momentum transfer. If rough values of V and v are inserted in the above relation, it may be shown that the mean value of F lies between 0·50 and 0·51, and even if extreme assumptions are made does not much exceed 0·52.

These figures are inconsistent with the observed values of $0{\cdot}66\pm0{\cdot}06$ and $0{\cdot}63\pm0{\cdot}03$ for alpha-particles and protons respectively, which indicates that a considerable proportion of the low energy particles are not emitted by an evaporation process. A modified model of the collision process by which this can be taken into account is discussed in the next section.

§ 3. Modified Model with Nuclear Cascade

Suppose that the incident proton initiates a nuclear cascade in the target nucleus, as a result of which a number of neutrons, protons and alpha-particles are emitted. When the cascade has finished, the nucleus returns to the ground state by evaporation as before.

This model of the collision process is similar to one proposed by Bernardini, Booth, and Lindenbaum (1952) to account for their observations of the disintegrations of heavy nuclei caused by 350 Mev protons. These investigators, however, used G5 emulsion and so they were unable to distinguish between low energy alpha-particles and protons. They were therefore unable to establish the participation of alpha-particles in the cascade process and so in their calculations they take account only of the neutrons and protons. The present results, however, provide strong evidence that the alpha-particles take part as well. This can be interpreted as implying the existence of alpha-particles in the nucleus, or it may be due to the nucleons of the cascade picking up further nucleons on their way out of the nucleus.

The detailed calculations of this cascade process are best treated by the method of Goldberger, but a few preliminary results can be obtained by making some simple assumptions.

Assume that all the particles of the nuclear cascade are emitted in the forward hemisphere in the laboratory system. This is likely to be very nearly the case, although it is possible that a few particles are emitted in the backward direction as a result of multiple collisions within the target nucleus. As a result of this assumption, the calculated percentage of all the emitted particles that are emitted in the cascade is too low. The forward fraction for the evaporated particles can, without sensible error, be taken as 0·5.

Let C be the proportion of charged cascade particles among all the emitted charged particles, and let $p_\alpha{}^C$ and $p_\alpha{}^E$ be the proportions of alpha-particles among the cascade and evaporated particles respectively.

Then we have

$$F_\alpha = \frac{Cp_\alpha^C + \frac{1}{2}(1-C)p_\alpha^E}{Cp_\alpha^C + (1-C)p_\alpha^E},$$

$$F_p = \frac{C(1-p_\alpha^C) + \frac{1}{2}(1-C)(1-p_\alpha^E)}{C(1-p_\alpha^C) + (1-C)(1-p_\alpha^E)},$$

$$P_\alpha = Cp_\alpha^C + (1-C)p_\alpha^E.$$

Substituting the experimental values of F_α, F_p, and P_α, we obtain $C = 0{\cdot}26 \pm 0{\cdot}06$; $p_\alpha^C = 0{\cdot}27 \pm 0{\cdot}14$ and $p_\alpha^E = 0{\cdot}20 \pm 0{\cdot}05$. Thus about 25% of the low energy particles are emitted as the result of a nuclear cascade in the target nucleus. This is probably a little low for reasons pointed out above. The results also show no significant difference between the proportions of alpha-particles among the cascade and evaporated particles. These results may be compared with those of Bernardini, Booth and Lindenbaum (350 MEV protons) who estimate that "at least 25% of the black prongs from AgBr are knock-ons" and with those of Blau, Oliver and Smith (300 MEV neutrons) who conclude that "at most, 70% of black prongs in heavy elements are due to nuclear evaporation".

The existence of the nuclear cascade means that the velocity of the excited nucleus cannot be calculated from the forward fraction F, although this has often been done.

These calculations cannot be applied to the disintegrations of the light nuclei because the number of nucleons in the nuclei is so small that the distinction between cascade and evaporation particles can no longer be made.

ACKNOWLEDGMENTS

I would like to thank the Director of the Atomic Energy Research Establishment, Harwell, for permission to work there, Dr. D. M. Skyrme, Dr. J. M. Cassels and the Harwell cyclotron operators for assistance during the exposures, Professor S. Devons for a valuable discussion, Dr. A. J. Herz for developing the plates, and the Department of Scientific and Industrial Research for a Senior Research Award.

REFERENCES

BERNARDINI, G., BOOTH, E. T., and LINDENBAUM, S. J., 1952, *Phys. Rev.*, **85,** 826 ; **88,** 1017.
BLAU, M., OLIVER, A. R., and SMITH, J. E., 1953, *Phys. Rev.*, **91,** 949.
GERMAIN, L. S., 1953, private communication.
HARDING, J. B., 1949 a, *Nature, Lond.*, **163,** 440 ; 1949 b, *Phil. Mag.*, **40,** 530.
HODGSON, P. E., 1952 a, *Phil. Mag.*, **43,** 190 ; 1952 b, *Ibid.*, **43,** 934 ; 1953, *Ibid.*, **44,** 1113.
LEES, C. F., MORRISON, G. C., MUIRHEAD, H., and ROSSER, W. C. V., 1953, *Phil. Mag.*, **44,** 304.
Le COUTEUR, K. J., 1950, *Proc. Phys. Soc.* A, **63,** 259; 1952, *Ibid.*, **65,** 718.
MENON, M. C. K., MUIRHEAD, H., and ROCHAT, O., 1950, *Phil. Mag.*, **41,** 583.
PERKINS, D. H., 1949, *Phil. Mag.*, **40,** 601.
PUPPI, G., 1953, private communication.

XXIII. *Distance Correlations in an Ideal Fermi–Dirac Gas*

By A. B. Lidiard
Department of Physics, University of California*

[Received November 3, 1953]

Summary

The antisymmetry of the total wave function of a Fermi–Dirac gas leads to an apparent repulsion between the gas particles. In other words, the average probability that two particles will be found at a distance r from one another falls to zero as r tends to zero. This pair distribution function, $D(r)$, is calculated (§ 2) at all temperatures by means of a variation method founded on a minimum property of the free energy. It is not possible to make a straightforward calculation using Fermi–Dirac statistics on account of the integrals which arise. Instead we use an approximation which has already been employed to meet a similar difficulty in the problem of finding the influence of exchange energy on the specific heat of electrons in metals.

§ 1. Introduction

It is well known that the distance correlations between the molecules of an ideal Fermi–Dirac or Bose–Einstein gas are due to the symmetry properties of the wave functions (see for example the review article by de Boer 1949, especially § 6(iii)). One may summarize the known results by saying that there is an apparent attraction between Bose–Einstein particles and an apparent repulsion between Fermi–Dirac particles. Thus Uhlenbeck and Gropper (1932) showed that in the limit of high temperatures and low densities, the probability of finding a particle within a distance interval $(r, r+dr)$ of a given particle is $4\pi r^2 D(r)dr$, where

$$D(r)=\frac{N}{V}\{1\pm\exp(-2\pi r^2/\lambda^2)\}, \quad . \quad . \quad . \quad . \quad . \quad (1.1)$$

in which the + sign is taken with Bose–Einstein statistics and the − sign with Fermi–Dirac statistics. Here N denotes the number of particles in a volume V and λ is the de Broglie wavelength corresponding to the temperature T,

$$\lambda=\hbar/(2\pi m\boldsymbol{k}T)^{1/2}.$$

At lower temperatures it is no longer possible to handle both cases together and in the present paper we shall consider only a Fermi–Dirac gas. The Bose–Einstein case has been treated by London (1943).

* Communicated by F. Booth.

The expression for $D(r)$ in the opposite limit of very low temperatures and high densities was obtained by Wigner and Seitz (1933).

$$D(r)=\frac{N}{V}\left\{1-9\left(\frac{k_0 r\cos k_0 r-\sin k_0 r}{(k_0 r)^3}\right)^2\right\}, \quad . \ . \ . \quad (1.2)$$

where $k_0=\pi(6N/\pi V)^{1/3}$. The one-particle wave-functions ψ are plane waves normalized over a volume V, i.e. $\psi_{\mathbf{k}}=V^{-1/2}\exp i(\mathbf{k}\,.\,\mathbf{r})$, and the quantity k_0 is the wave number of the highest occupied level at absolute zero.* It is related to the Fermi energy ϵ_0 through the equation $\epsilon_0=\boldsymbol{h}^2k^2_0/8\pi^2m$.

Now although we have these expressions (1.1) and (1.2), valid at very high and very low temperatures respectively, there are no calculations which bridge the gap between these limits. Bhatnagar and Singwi (1949) have, however, shown that (1.1) and (1.2) are the leading terms in two different series and have calculated additional terms in these expansions, thereby approaching the region of intermediate temperatures simultaneously from both limits. Their starting point is a general formula for $D(r)$ namely

$$D(r)=\frac{N}{V}\left[1-\frac{1}{N^2}\left\{\left(\Sigma_{\mathbf{k}} f_{\mathbf{k}}\frac{\sin kr}{kr}\right)^2-\Sigma_{\mathbf{k}} f_{\mathbf{k}}^2\right\}\right], \quad . \ . \ . \quad (1.3)$$

where $f_{\mathbf{k}}$ is the average occupation number of the state $\psi_{\mathbf{k}}$. (As usual we shall replace these sums by integrals, assigning $Vd\mathbf{k}/(2\pi)^3$ states to each volume $d\mathbf{k}$ of $\mathbf{k}$-space.) At the present time it is not possible to evaluate (1.3) at all temperatures, if for $f_{\mathbf{k}}$ we use the exact Fermi–Dirac distribution function. In particular the region of intermediate temperatures around $\boldsymbol{k}T/\epsilon_0\sim 1$ is covered neither by the high nor by the low temperature series. It therefore seemed of interest to calculate $D(r)$ using an approximate distribution function, one which would allow closed expressions to be obtained at all temperatures. Previous work (Lidiard 1951 a and 1951 b, particularly § 2 and appendix A) has already shown how even quite a crude form for $f_{\mathbf{k}}$ can give reliable results if the specifying parameters are chosen so as to minimize the free energy (Lidiard 1953). The details of the calculation are described in the next section and numerical results are exhibited graphically in fig. 2.

§ 2. Calculation of $D(r)$

First we discuss the approximate distribution function to be used. We note, to begin with, that the free energy function, F, of an ideal Fermi–Dirac gas may be expressed in terms of the distribution function as follows:

$$F=\frac{\boldsymbol{h}^2V}{16\pi^4m}\int_0^\infty f(k)\,k^4\,dk+\frac{\boldsymbol{k}TV}{2\pi^2}\int_0^\infty\left\{f\ln f+(1-f)\ln(1-f)\right\}k^2\,dk. \quad (2.1)$$

* We are assuming that only one particle at a time can be in the state $\psi_{\mathbf{k}}$. It is a trivial matter to generalize the equations to the case where the occurrence of spin degeneracy allows more than one particle per state.

The first term in (2.1) is the total kinetic energy of the gas and the second term is $-T$ multiplied by the entropy. The total number of particles is fixed, so we must have

$$N = \frac{V}{2\pi^2}\int_0^\infty f(k)\, k^2\, dk, \quad . \quad . \quad . \quad . \quad . \quad . \quad . \quad (2.2)$$

whichever form we choose for $f(k)$. If we make F an *absolute* minimum by setting the variation δF equal to zero, subject only to the condition (2.2) then, as is to be expected, one finds that $f(k)$ must be the usual Fermi–Dirac function. It is however, possible to obtain approximate equations (which remain thermodynamically consistent) even if we place

Fig. 1

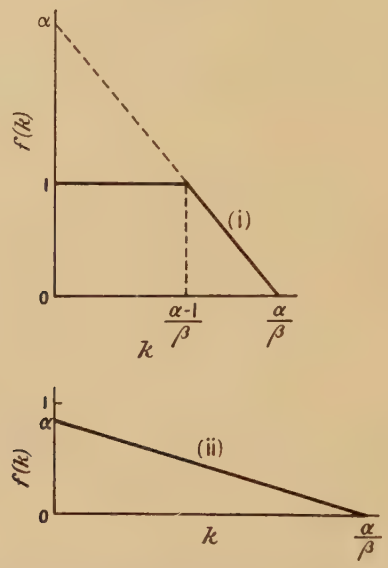

Approximate forms for $f(k)$ in place of the Fermi–Dirac function: (i) $\alpha \geqslant 1$; (ii) $\alpha \leqslant 1$.

additional restrictions on the form of $f(k)$ which enable us to evaluate (2.1), (2.2) and (1.3) without difficulty. This has already been demonstrated for the function shown in fig. 1 (Lidiard 1951 b); we adopt this function here too, i.e. for $x \equiv 1/\alpha \leqslant 1$ we take,

$$\begin{aligned} f(k) &= 1, && 0 \leqslant k \leqslant (\alpha-1)/\beta, \\ &= \alpha - \beta k, && (\alpha-1)/\beta \leqslant k \leqslant \alpha/\beta, \\ &= 0, && k \geqslant \alpha/\beta, \quad . \quad . \quad . \quad . \quad . \quad . \quad . \quad . \end{aligned} \quad (2.3)$$

while for $x \geqslant 1$,

$$\begin{aligned} f(k) &= \alpha - \beta k, && 0 \leqslant k \leqslant \alpha/\beta, \\ &= 0, && k \geqslant \alpha/\beta. \quad . \quad . \quad . \quad . \quad . \quad . \quad . \quad . \end{aligned} \quad (2.4)$$

Substitution of (2.3) and (2.4) into (2.2) gives

$$N=\frac{V}{6\pi^2}\left(\frac{\alpha}{\beta}\right)^3\left(1-\frac{3x}{2}+x^2-\frac{x^3}{4}\right), \quad x\leqslant 1, \quad . \quad . \quad . \quad (2.5)$$

$$=\frac{V}{24\pi^2}\left(\frac{\alpha}{\beta}\right)^3\frac{1}{x}, \quad x\geqslant 1. \quad . \quad . \quad . \quad . \quad . \quad . \quad . \quad . \quad (2.6)$$

Similarly the evaluation of (2.1) with the elimination of (α/β) by (2.5) and (2.6) yields

$$\frac{F}{N\epsilon_0}=\frac{3}{5}A(x)-\frac{3\boldsymbol{k}T}{2\epsilon_0}C(x), \quad . \quad . \quad . \quad . \quad . \quad . \quad (2.7)$$

where $A(x)$ and $B(x)$ are the following functions of x, in which

$$P=(1-3x/2+x^2-x^3/4)^{-1},$$

$$A(x)=P^{5/3}\,[1-(1-x)^6]/6x, \quad x\leqslant 1,$$

$$=2^{7/3}\,x^{2/3}/3, \quad x\geqslant 1,$$

$$C(x)=P\,(x-x^2+11x^3/36), \quad x\leqslant 1,$$

$$=\frac{2}{3}\ln x-\frac{2}{3}(x-1)^4\ln\left(\frac{x}{x-1}\right)+\frac{26x}{9}-\frac{7x^2}{3}+\frac{2x^3}{3}, \quad x\geqslant 1.$$

Finally we fix the value of x by using the condition that F should be a minimum, i.e. $\partial F/\partial x=0$. This gives the implicit equation

$$\boldsymbol{k}T/\epsilon_0=2A'(x)/5C'(x), \quad . \quad . \quad . \quad . \quad . \quad . \quad (2.8)$$

where the prime denotes differentiation with respect to x. Limiting forms of these equations have been given previously in the paper cited above and will not be repeated here. This paper also contains a comparison of the approximate with the accurate functions computed by Stoner (1939), using the tables of Fermi–Dirac integrals previously drawn up by McDougall and Stoner (1938). Unfortunately there are no tables available which could help us to evaluate (1.3) accurately. We shall proceed with the calculation of $D(r)$ using (2.3) and (2.4) for $f(k)$ with (α/β) and x given by (2.5), (2.6) and (2.7). The integrations are perfectly straightforward and abbreviating $k_0 r$ by ρ we find that,

$$D(r)=\frac{N}{V}(1-\Delta^2)$$

where, $$\Delta\,(x,\rho)=\frac{3}{x\rho^3}[(1-x)\sin\{\rho(1-x)P^{1/3}\}-\sin\{\rho P^{1/3}\}$$

$$+2\rho^{-1}P^{-1/3}\cos\{\rho(1-x)\,P^{1/3}\}$$

$$-2\rho^{-1}P^{-1/3}\cos\{\rho P^{1/3}\}], \quad x\leqslant 1, \quad . \quad . \quad . \quad . \quad . \quad (2.9)$$

$$=\frac{3}{x\rho^3}\left[-\sin\{4^{1/3}x^{1/3}\rho\}+\frac{2}{4^{1/3}x^{1/3}\rho}(1-\cos\{4^{1/3}x^{1/3}\rho\})\right],$$

$$x\geqslant 1. \quad . \quad . \quad . \quad . \quad . \quad . \quad . \quad . \quad . \quad . \quad . \quad . \quad . \quad (2.10)$$

The parameter x is related to the temperature through equation (2.8). $VD(r)/N$ as calculated from (2.9) and (2.10) is plotted as a function of ρ

in fig. 2 for five different temperatures, namely $\boldsymbol{k}T/\epsilon_0 = 0{\cdot}0$, $0{\cdot}5$, $1{\cdot}0$, $2{\cdot}0$ and $4{\cdot}0$. The oscillatory behaviour which one would expect from the presence of the sine and cosine functions is too strongly damped to show up in a drawing of the scale of fig. 2.

Fig. 2

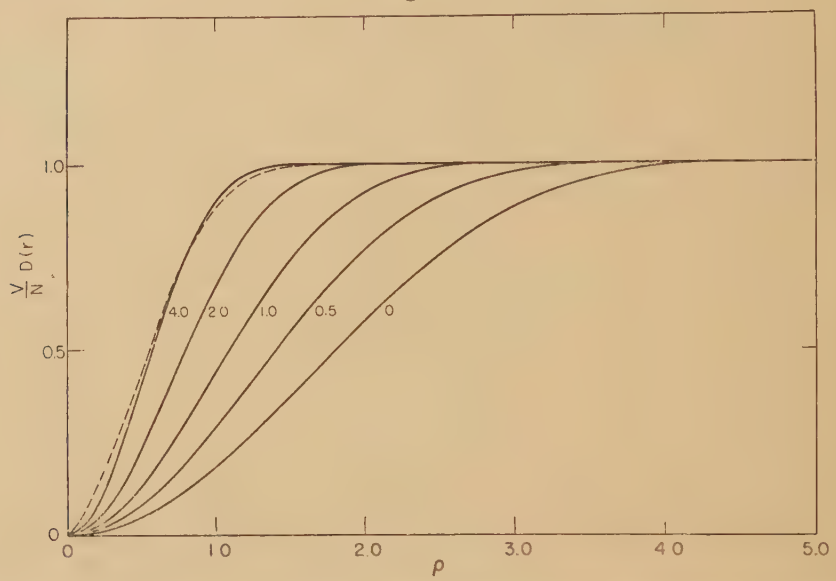

The pair distribution function for a perfect Fermi–Dirac gas at several different temperatures. The numbers on the curves are the corresponding values of $\boldsymbol{k}T/\epsilon_0$ and the variable ρ is $k_0 r$, where k_0 is the radius of the Fermi sphere at absolute zero. The dashed line for $\boldsymbol{k}T/\epsilon_0$ equal to $4{\cdot}0$ has been calculated from the high temperature expansion given by Bhatnagar and Singwi.

It is not difficult to find a simple limiting form for $D(r)$ at very low temperatures. In this region $x = 3\boldsymbol{k}T/\epsilon_0$ and when $x\rho \ll 1$ we obtain,

$$D(r) = \frac{N}{V}\left[1 - 9\left\{\frac{(1-(\rho \boldsymbol{k}T/\epsilon_0)^2/24)(\sin\rho - \rho\cos\rho)}{\rho^3}\right\}^2\right]. \quad . \quad (2.11)$$

Except for the occurrence of $3\boldsymbol{k}T/\epsilon_0$ in place of $\pi\boldsymbol{k}T/\epsilon_0$ this expression is identical with the low temperature formula derived by Bhatnagar and Singwi (1949, eqn. (19)) by means of the Sommerfeld lemma (note that our k_0 is equal to their $2\pi k_0$).

§ 3. Discussion

The replacement of $\pi\boldsymbol{k}T/\epsilon_0$ by $3\boldsymbol{k}T/\epsilon_0$ in formula (2.11) appears to be a general consequence at low temperatures of the use of the approximate function (2.3); for it is known to occur also with the formulae for the specific heat (Wohlfarth 1950) and electron spin paramagnetism (March and Donovan 1953). We may be sure therefore that formula (2.9) is accurate to a few per cent in the region $0 < \boldsymbol{k}T/\epsilon_0 < 0{\cdot}3$. Unfortunately it is difficult to form an estimate of the general accuracy at high temperatures

since (2.10) does not go over into any simple form which could be compared directly with (1.1). The following observations are however, relevant :

(1) The accurate curve for $\boldsymbol{kT}/\epsilon_0=4{\cdot}0$, calculated from eqn. (12) of the paper by Bhatnagar and Singwi, lies across that calculated from (2.10)—being greater for small values of ρ.

(2) Nevertheless at higher temperatures the approximate and the accurate curves come into coincidence for small ρ. Thus expanding (2.10) we get

$$D(r)=\frac{N}{V}\left[\frac{1}{2}\left(\frac{\boldsymbol{kT}}{\epsilon_0}\right)\rho^2-\frac{101}{896}\left(\frac{\boldsymbol{kT}}{\epsilon_0}\right)^2\rho^4\ldots\right], \quad . \quad . \quad . \quad (3.1)$$

whereas (1.1) becomes

$$D(r)=\frac{N}{V}\left[\frac{1}{2}\left(\frac{\boldsymbol{kT}}{\epsilon_0}\right)\rho^2-\frac{1}{8}\left(\frac{\boldsymbol{kT}}{\epsilon_0}\right)^2\rho^4\ldots\right]. \quad . \quad . \quad . \quad (3.2)$$

(3) $\Delta^2(x,\rho)$ has roughly the same shape as the accurate expression $\exp(-\boldsymbol{kT}\rho^2/2\epsilon_0)$ (except for the suppressed oscillations) and we may calculate the second moment of Δ^2 with a view to finding an equivalent Gaussian form $\exp -Y\rho^2$. In this way we obtain $\Delta^2\sim\exp(-\boldsymbol{kT}\rho^2/1{\cdot}76\epsilon_0)$ compared with $\exp(-\boldsymbol{kT}\rho^2/2\epsilon_0)$.

We conclude from (2) and (3) that the accurate and approximate expressions are in reasonable agreement at high temperatures although our equations predict that Δ^2 falls to zero too rapidly. The radius of the Fermi hole which (2.10) gives as

$$\begin{aligned}\rho_F&=2\pi/4^{1/3}\,x^{1/3},\\&=\frac{4\pi}{\sqrt{15}}\left(\frac{\epsilon_0}{\boldsymbol{kT}}\right)^{1/2}\quad\text{for}\quad\left(\frac{\boldsymbol{kT}}{\epsilon_0}\right)\gg 1, \quad . \quad . \quad . \quad . \quad (3.3)\end{aligned}$$

seems to agree well with (1.1).

Acknowledgments

The work reported here was carried out while the author was at Kings College, London. He wishes to thank Prof. C. A. Coulson and Mr. F. Booth for their interest and encouragement and also to acknowledge the benefit of a number of helpful discussions with Mr. G. V. Chester. Financial support was provided by the D.S.I.R. ; thanks are also due to the Control Research Fund of London University for the loan of a calculating machine.

References

Bhatnagar, P. L., and Singwi, K. S., 1949, *Phil. Mag.*, **40,** 917.
de Boer, J., 1949, *Rep. Prog. Phys.*, **12,** 305 (London : Physical Society).
Lidiard, A. B., 1951 a, *Phil. Mag.*, **42,** 1325 ; 1951 b, *Proc. Phys. Soc.* A, **64,** 814 ; 1953, *Ibid.* A, **66,** 392.
London, F., 1943, *J. Chem. Phys.*, **11,** 203.
March, N. H., and Donovan, B., 1953, *Proc. Phys. Soc.* A (in the press).
McDougall, J., and Stoner, E. C., 1938, *Phil. Trans. Roy. Soc.* A, **237,** 67.
Stoner, E. C., 1939, *Phil. Mag.*, **28,** 257.
Uhlenbeck, G. E., and Gropper, L., 1932, *Phys. Rev.*, **41,** 79.
Wigner, E., and Seitz, F., 1933, *Phys. Rev.*, **43,** 804.
Wohlfarth, E. P., 1950, *Phil. Mag.*, **41,** 534.

XXIV. *Experiments with Thin Films of Silver Sulphide, Silver and Gold*

By J. H. Burrow and J. W. Mitchell
H. H. Wills Physical Laboratory, University of Bristol*

[Received December 31, 1953]

Abstract

An account is given of experimental work on the reaction between bromine and (1) thin films of silver sulphide, (2) composite thin films of silver sulphide with silver and gold. It has been established that, under these conditions, silver sulphide reacts with bromine to form silver and a sulphur bromide before silver or gold is attacked. Hickman postulated the existence of this reaction in 1927 to account for the increase in sensitivity which follows the digestion of photographic emulsions with sulphur sensitizers. On the basis of the experimental observations, a new mechanism is advanced for the formation of the latent image in modern high speed negative emulsions.

§ 1. Introduction

The discovery by Sheppard (1925) and his co-workers that the sensitivity of washed silver halide emulsions could often be considerably enhanced by digesting them at temperatures up to 65°c with suitable sulphur compounds represented a great advance in photographic science. They deduced from their experiments that silver sulphide was formed during digestion and favoured the hypothesis that it was present on the surfaces of the crystals of silver halide in the form of discrete specks which provided centres for the concentration of silver atoms produced by the action of light (see Sheppard 1928 a). Gurney and Mott (1938) later described a two stage mechanism for the concentration of the silver atoms, which could be applied to Sheppard's hypothesis if it were assumed that silver sulphide trapped electrons.

An alternative explanation of the action of silver sulphide in increasing sensitivity was advanced by Hickman (1927) who suggested that it acted as a halogen acceptor by the liberation of metallic silver and the formation of sulphur monobromide. He was unable to obtain any experimental evidence to support this assumption, but wrote: "Even so, it is possible that, when the reaction takes place on the small scale governing latent image formation, the bromine liberated atom by atom by light in contact with an excess of silver sulphide may indeed liberate metal." He demonstrated the feasibility of his ideas by making experiments with

* Communicated by the Authors.

pieces of sensitive photographic materials which had been visibly darkened by immersion in a dilute solution of sodium sulphide. Strips were exposed to light until a print-out image was produced and then immersed in a solution of sodium thiosulphate and potassium ferricyanide, which dissolves silver bromide and metallic silver but not silver sulphide. The silver sulphide was found to have disappeared from the exposed parts. This would scarcely be expected if the only role of the silver sulphide was to concentrate photolytic silver atoms, and Hickman concluded that bromine liberated by light attacked the silver sulphide. This conclusion was not generally accepted. In the discussion following the presentation of Hickman's paper to the Royal Photographic Society, Renwick remarked that " Dr. Hickman could not expect anyone to accept his hypotheses, contrary as they were to many experimental facts, without fresh evidence in their favour ". Sheppard (1928 a) also rejected this interpretation of the sensitizing action of silver sulphide, although he admitted the importance of halogen removal to which Hickman had drawn attention. Sheppard expressed the opinion that the molecules of gelatine around the silver halide crystals would combine with the extremely small amount of halogen liberated during an exposure of the duration necessary to form a latent image and this viewpoint was also taken by Gurney and Mott.

The purpose of this paper is first to describe experiments which were designed to test Hickman's hypotheses and then to describe further experiments which appear to lead directly to a possible new mechanism for the formation of the latent image in modern high speed negative emulsions. We have observed that a thin film of silver sulphide is converted into a thin film of silver by treatment with bromine at a very low vapour pressure. The sulphur combines with bromine, apparently quantitatively, to form a sulphur bromide. The silver film which is formed is attacked by the sulphur bromide or by excess bromine at a slower rate and is then converted into silver bromide. This work lends direct support to one of the hypotheses advanced by Hickman.

Prior to Sheppard's work, Lüppo-Cramer (1921, 1927) had proposed that the digestion of washed emulsions with gelatine resulted in the formation of particles of colloidal silver which were adsorbed to the surfaces of the silver halide crystals. That this was the cause of the increase in sensitivity during digestion came to be widely accepted, because it was reasonable to assume that the particles could increase in size during exposure and thus be converted into development centres. This conception, however, gradually faded into the background following Sheppard's discovery and interpretation of the sensitizing action of sulphur compounds. Clark (1927) presented evidence in favour of composite sensitivity specks consisting of silver and silver sulphide, but his experimental technique was criticized by Sheppard (1928 b). Sheppard (1928 a) nevertheless admitted that sensitivity specks might consist of silver and silver sulphide; at the same time, he insisted that their principal function was to concentrate silver atoms liberated during exposure.

Interest in chemical sensitization by silver has recently been revived by the publication of a series of papers by Mitchell (1948), Mueller (1949), Lowe, Jones and Roberts (1951), Hedges and Mitchell (1953) and Wood (1953). Of these, the one most relevant to the present work is that by Lowe and his co-workers, who showed that, with a positive emulsion of the type which they used, the effects of sulphur sensitization and silver sensitization were additive. The increased sensitivity may be attributed to the formation of layers adsorbed at the surfaces of the crystals of silver halide in which atoms of silver and molecules of silver sulphide are closely associated. We therefore studied the action of bromine on superimposed thin films of silver and silver sulphide and found that bromine at very low vapour pressures removed the sulphur from the silver sulphide with the formation of a sulphur bromide and left a thin film of silver of increased thickness. This film was itself attacked at a slower rate by sulphur bromide or by excess bromine.

Modern negative emulsions owe their high speed to the sensitizing action of complex salts of monovalent gold such as ammonium or alkali aurous thiocyanates or thiosulphates which was discovered by Koslowsky (1951) in 1936 in the Agfa Laboratories at Wolfen, Germany (see also Chilton 1946, Mueller 1949). Although Hedges and Mitchell (1953) have demonstrated that a crystal of silver bromide can be sensitized for the formation of a surface latent image by the deposition of a thin film of gold on its surface, it is most probable that composite layers consisting of adsorbed atoms of gold and molecules of silver sulphide are formed on the surfaces of the microcrystals during the digestion of the emulsion with these added sensitizers. For this reason, the action of bromine at very low vapour pressures on composite films of silver sulphide and gold was studied. It was found that the silver sulphide again reacted with bromine to form a sulphur bromide and that a composite metallic film of silver and gold remained which reacted much more slowly with the sulphur bromide or with excess bromine to form a mixture of silver bromide and aurous bromide.

The possible application of these observations to the discussion of the formation of the latent image in high speed negative emulsions will be considered in a later section. The important conclusion is that the reaction between silver sulphide and bromine occurs in two stages, the first resulting in the formation of a sulphur bromide and metallic silver and the second in the formation of silver bromide. Fresh evidence has thus been obtained in favour of Hickman's hypothesis that silver sulphide reacts with bromine during the exposure of sensitized silver halide crystals to liberate silver and form a sulphur bromide.

§ 2. Experimental Methods

The thin films of silver and gold which were used in all the experiments were deposited on the inner surfaces of highly evacuated thin walled spherical bulbs of Hysil glass, 10 cm in diameter, by heating beads of the

metals supported on tungsten filaments near the centres. The beads were prepared and processed by the methods described by Mitchell and Mitchell (1951). About one third of the experiments were done with bulbs which had a single bead mounted on a pinch with two tungsten leads. Two beads were required for all the experiments with composite films. They were screened from each other with a disc of molybdenum and the two tungsten filaments supporting them were spot welded to four tungsten leads passing through a pinch. This pinch was sealed in so that the disc was at the centre of the bulb. The two beads were symmetrically spaced on opposite sides of it so that the shadow of the disc cast by each bead covered approximately one third of the internal surface; this meant that each component film covered one third of the area of the bulb while the composite film covered the remaining third where the two films overlapped. With this arrangement, it was possible to make reliable estimates of the relative rates of many reactions. A side arm opposite the pinch was drawn down to a long fine capillary through which liquids could conveniently be admitted to the evacuated bulb. The bulbs were provided with two other side arms and one of these was sealed to the high vacuum system through a constriction. This carried several glass bubble seals, through which the bulb could be sealed for re-pumping after the admission of gases, and also a long plain tube and a U tube either or both of which could be immersed in liquid air to condense volatile reaction products. Tubes with breakable tips containing bromine, sulphur monobromide, hydrogen sulphide, air and nitrogen were sealed to the opposite side arm as required. Short lengths of iron rod or ball bearings, sheathed in glass, were used for breaking the tips and the glass bubbles.

Hydrogen sulphide was prepared in the usual way and purified by fractional distillation. Nitrogen was obtained from a cylinder of the oxygen-free gas. Analar bromine supplied by B.D.H. was used throughout the experimental work. The tubes with breakable tips were filled with small quantities of bromine, using an all glass apparatus which was evacuated while the side arm containing the supply of bromine was immersed in liquid air and then sealed from the pumping system. Sulphur bromide was prepared by reacting an excess of vacuum sublimed Analar sulphur with Analar bromine in a previously evacuated all glass apparatus. There was no significant evolution of heat when the reactants were mixed and, after a period of refluxing, the product was fractionated by immersing the side arms in turn in liquid air while the bulb containing the product was at room temperature. When a fraction had been collected, this bulb was also immersed in liquid air to reduce the vapour pressure to a negligible value before the side arm was sealed off. The sulphur bromide which was used appeared to be a product of definite composition. Bromine could not be separated from it by slow vacuum fractional distillation at low temperatures and no residue of sulphur remained after the complete distillation of a sample between room temperature and the temperature of liquid air. Every possible precaution was taken to ensure that it did not contain free bromine.

The completed bulbs were pumped for several hours and repeatedly torched during this period. The beads were meanwhile heated to a temperature just below that at which the metal would have begun to evaporate at a significant rate. When the pressure had fallen to 10^{-7} mm Hg, a bead was heated until the metal began to evaporate slowly from it. The thickness of a film was judged visually from its colour by transmitted light and deposition was interrupted when the required thickness was reached. If composite films were being prepared, the second bead was heated and the corresponding film deposited before the bulb was sealed from the pumping system.

After sealing off, the films could be exposed to hydrogen sulphide by breaking the tip of the tube containing it. The bulb was heated and the excess hydrogen sulphide was then condensed as far as possible by immersing the tube in liquid air before it was sealed off. The bulb itself was then sealed to the pumping system through one of the glass bubbles which was broken when the pressure in the system had fallen to 10^{-6} mm Hg and pumping continued until the pressure had fallen to 10^{-7} mm Hg. The second component of a composite film could then be deposited and the bulb again sealed from the pumping set.

Films of silver sulphide, silver and gold, and composite films of silver sulphide and silver, silver sulphide and gold, and of silver and gold were prepared by these methods and their reactions with bromine and sulphur bromide both under good vacuum conditions and in the presence of dry and moist air and nitrogen at pressures up to one atmosphere were investigated. In all the experiments the tube containing the bromine or sulphur bromide was immersed in liquid air before the tip was broken. It was then allowed to warm up very slowly in the space above the surface of the liquid air in a deep Dewar vessel and, as soon as the appearance of the film began to change, was plunged back into liquid air so that the vapour pressure fell rapidly. The tube was often sealed from the spherical bulb as soon as the conversion of silver sulphide to silver appeared to be complete. The sulphur bromide could then be condensed in the plain side arm cooled in liquid air and fractionated at a low temperature. If the bulb had previously been filled with air or nitrogen, it could be sealed to the vacuum system at this stage through a glass bubble seal, pumped out through the U tube which was cooled in liquid air, and then sealed off again. The volatile reaction products could then be condensed either in the side arm or in the U tube.

§ 3. Experimental Observations

The colour transmitted by a thin film of silver passes through the sequence, pale yellow, yellowish brown, reddish violet, bluish violet, and blue fading into bluish grey as the mass of silver deposited per unit area of the substrate is increased. The bluish violet films are the first in the sequence to give a white metallic reflection. The bulk of the experimental work described in this paper was done with unannealed reddish violet or

bluish violet films of silver which could be deposited reproducibly and showed the most pronounced colour changes when they reacted with other substances. Bromine attacked thin films of silver rapidly at room temperature to form clear films of silver bromide which recrystallized on heating becoming pale yellow and opalescent. Reddish or bluish violet films of silver were converted instantly into yellowish brown films of silver sulphide by exposure to hydrogen sulphide. Films of silver sulphide prepared in this way were stable and could be heated in vacuum to 300°C without any condensation of sulphur in a side arm cooled in liquid air. Thin films of silver were attacked by sulphur monobromide with the formation of silver bromide and sulphur. The sulphur could be condensed in a side arm cooled in liquid air by warming the bulb.

The films of silver sulphide reacted with bromine at a very low vapour pressure to form films of silver and a sulphur bromide. The films of silver produced by this reaction had the same colour as those which had been converted into silver sulphide for the experiment. The sulphur bromide could be partially condensed in a side arm cooled in liquid air or else completely dissolved out by admitting dry benzene, chloroform, or carbon tetrachloride to the bulb through the capillary. The solution of silver nitrate produced by dissolving the silver film remaining in the latter case in hot nitric acid gave no precipitate with barium nitrate, showing that the sulphur had been removed within the limits of the test. A precipitate of barium sulphate was obtained when a control experiment was run with a film of silver sulphide. If the tube containing the bromine was not immersed in liquid air and sealed off, immediately the transformation of the film of silver sulphide to silver appeared to be complete, the film of silver was slowly attacked by the sulphur bromide and by bromine and converted to silver bromide. In many experiments dry or moist air or nitrogen was admitted to the bulb at pressures up to one atmosphere before the tip of the bromine tube was broken. The presence of air or nitrogen did not appear to influence the primary phenomena in any way.

The reaction between a thin film of silver sulphide and sulphur monobromide was next studied. Sulphur monobromide appeared to react catalytically with silver sulphide to form silver and sulphur at a rate which was not very different from the rate of reaction between silver sulphide and bromine. The same result was obtained when the bulb was filled with dry air or nitrogen before the admission of the sulphur monobromide. An excess of sulphur monobromide reacted with the silver to form silver bromide and sulphur.

Following these experiments with thin films of silver and silver sulphide, a composite film of silver and silver sulphide was prepared as described in the previous section. A reddish violet thin film of silver was first deposited over two thirds of the inner surface of the bulb and converted to a yellow brown film of silver sulphide by exposure to hydrogen sulphide. The bulb was then exhausted and another reddish violet film of silver was deposited from the second bead so that it overlapped half the area of the silver

sulphide film. The bulb was evacuated or else filled with air or nitrogen in the different experiments of this series. The introduction of bromine at a very low vapour pressure into the system converted the yellow brown film of silver sulphide back to a reddish violet film of silver before it had affected the reddish violet film of silver on the other side of the bulb in any way. The composite film of silver and silver sulphide was changed from a dull greyish violet to a clear blue violet by exposure to bromine corresponding to the formation of a thicker film of silver. When more bromine was admitted, it was observed that the silver film derived from the silver sulphide was attacked at the same rate as the other silver film with the formation of silver bromide. The rate at which the thicker silver film derived from the composite film was attacked was not sensibly different. These experiments were repeated many times.

We turned now to the investigation of the properties of thin films of gold. With increasing mass of gold per unit area, the colour transmitted by the films passed through the sequence, reddish violet, bluish violet, blue, bluish green with a white reflection, and bluish green with a golden yellow reflection. When such films were heated to temperatures above 150°c, they were transformed into pink films which showed the same colour by transmitted as by reflected light. The latter are known from other work to have an infinite electrical resistance and to consist of discrete particles of gold. These thin films, whether previously converted to pink films by heating or not, reacted with bromine to form clear pale green films of aurous bromide and then yellowish brown opalescent films of auric bromide. If the tube containing the bromine was immersed in liquid air and the bulb was heated to a temperature in the neighbourhood of 120°c, the film of auric bromide broke down forming first a green film of aurous bromide and then a pink film of gold. Coloured thin films of gold of all thicknesses were changed irreversibly into pink films by reaction with bromine followed by thermal decomposition of the gold bromides. No conditions could be found under which thin films of gold would react with hydrogen sulphide, which is in striking contrast to the immediate reaction which occurs with silver films. The reaction between bromine and a reddish violet film of silver, a bluish violet film of gold and a deep violet composite film of silver and gold was next studied to determine whether, under identical conditions, there was any significant difference in the rates of attack. It was found that all three films were attacked at the same rate by bromine with the formation of silver bromide and aurous bromide. Experiments with sulphur monobromide instead of bromine led to a similar conclusion. The same observations were made when the bulb was filled with air or nitrogen before the admission of the bromine.

The reaction of composite films of silver and gold with hydrogen sulphide was studied in the next series of experiments. In half of them, the gold was superimposed on the silver and in the other half, the silver was superimposed on the gold. The silver films were bluish violet by transmitted light and the gold films were bluish green and showed a white

reflection. The composite films were a deep bluish violet. Treatment of either type of film with hydrogen sulphide produced exactly the same result : the silver was converted to silver sulphide and the gold remained unaffected. The whole of the area covered by the gold film became blue green by transmitted light and the boundary between the gold film and the composite film almost vanished. The bulb was then evacuated and sealed off or else filled with air or nitrogen. Exposure to a very low vapour pressure of bromine caused the film of silver sulphide and the film in the composite area to return to the colours which they had before treatment with hydrogen sulphide and sulphur bromide could be condensed in the side arm cooled in liquid air. The gold film was unaffected at this stage. Further reaction with bromine transformed the silver into silver bromide and the gold into aurous bromide and finally, with excess bromine, into auric bromide. The same changes were observed whether the silver or the gold of the composite film was deposited first and whether the bulb was evacuated or filled with air or nitrogen before the admission of the bromine. In later experiments, sulphur bromide was admitted to the bulb instead of bromine. The same changes were observed but auric bromide was not formed. For the last group of experiments, a composite film of silver sulphide and gold was prepared in a different way. A thin film of silver was deposited over two thirds of the surface of the bulb and converted to silver sulphide. A thin film of gold was then deposited to cover one half the film of silver sulphide. The appearance of the bulbs was the same as in the previous series and when bromine and sulphur bromide were admitted the same changes were observed.

§ 4. Discussion of the Experimental Results

In recent years, the properties of thin films of silver and other metals have been extensively investigated at Bristol (see, for example, Holloway 1951, Dorling 1953). The accumulated evidence has led to the working hypothesis that the unannealed conducting films are built up from crystalline granules consisting of small groups of atoms. The pink non-conducting films mentioned above have larger discrete groups of atoms. We have therefore good grounds for assuming that, in the thin films of silver and gold which we have used for our experiments, surface atoms of metal are adsorbed to the glass substrate in the same way as atoms of silver and gold are adsorbed to the surfaces of the crystals of silver halide in a sensitized photographic emulsion. For this reason, results obtained with thin films of silver and gold may be directly applicable to the discussion of the formation of the latent image in the photographic system.

A granular film of silver is most probably converted into a granular film of silver sulphide by treatment with hydrogen sulphide. In striking contrast to the immediate reaction which occurs with a thin film of silver, a thin film of gold does not react with hydrogen sulphide. Particles of gold may also be stable in a photographic emulsion under conditions

where particles of silver would be converted into silver sulphide, as, for example, when sodium thiosulphate is added to an emulsion at a p_H greater than 7·5 and at a temperature of about 60°c. The experiments in which composite films of silver and gold were treated with hydrogen sulphide and found to react in the same way whether the silver or the gold was deposited first provide further evidence for the existence of a granular structure. If the films were continuous, it would be anticipated that an overlying gold film would protect a silver film from attack by hydrogen sulphide.

The observations on the reactions of films of silver sulphide, and of composite films of silver sulphide and silver, and silver sulphide and gold with bromine, are all consistent with the assumption that they have a granular structure. Silver sulphide whether present by itself or in association with silver or gold is converted into silver by reaction with bromine at very low vapour pressure. The sulphur of the silver sulphide reacts to form a sulphur bromide. This reaction occurs under conditions where particles of silver or of gold are not attacked. The experimental conditions approximate very closely to those which are likely to hold at the interface between a crystal of silver bromide and the gelatine during a normal photographic exposure. We may therefore conclude that the increase in sensitivity of a photographic emulsion which results from sulphur sensitization is at least partly due to the formation of silver sulphide which can liberate silver when it reacts with bromine as was suggested by Hickman in 1927. The details of his mechanism for the formation of the latent image require revision, however, in the light of modern knowledge and this will be attempted in the next section.

There is no experimental evidence that sulphur monobromide is the primary product of the reaction between silver sulphide and bromine. The primary product could equally well be sulphur dibromide which could subsequently condense with itself to form sulphur monobromide and bromine. The reaction between sulphur monobromide and silver sulphide is of considerable interest. The sulphur monobromide was most carefully freed from excess bromine and could be distilled unchanged in vacuum at room temperature. It is, nevertheless, possible that it suffered heterogeneous catalytic thermal decomposition on the surfaces of the films in the spherical bulb into sulphur and bromine. Bromine would then be made available for reaction with the films and sulphur would be deposited on the surface. The results seem to suggest that a thin film of silver sulphide might be converted into silver and sulphur by catalytic reaction involving less than the equivalent amount of bromine or sulphur monobromide. This matter requires further detailed investigation. Sulphur monobromide reacts more rapidly with silver sulphide than with particles of silver or gold of approximately the same size under the same conditions.

All the experiments involving bromine were carried out using both bulbs which had been evacuated before the admission of bromine and bulbs which had been filled with air or nitrogen at pressures up to one

atmosphere. No difference in the primary reactions due to the presence of these gases was ever observed. The primary reactions were also not affected by the presence of traces of water vapour. The experimental results may therefore be applied with some confidence to the photographic system. When finely divided sulphur is produced in a reaction, it is likely that it will react with oxygen in the presence of moist air to form sulphur dioxide and, ultimately, sulphuric acid but this was not established in the present series of experiments.

§ 5. The Application of the Results to the Photographic Process

The material of this section is inevitably speculative and has therefore been separated from the account of the experimental results. Any satisfactory theory of the formation of the latent image must explain how the most sensitive crystals of a modern high speed negative emulsion become developable after the absorption of very few quanta. With the results of the present series of experiments, it is possible to account for this. It is also possible to explain the function of the two main components of the sensitizing layer, silver sulphide and gold, and the effectiveness of gold sensitization in reducing high intensity reciprocity failure (see, Mueller 1949).

For purposes of discussion, we shall assume that the sensitizing substance forms a layer, perhaps a monolayer, of molecules of silver sulphide with atoms of gold in addition, principally at the surface of the sensitivity centre (see Mitchell 1953) during the digestion of the washed emulsion with appropriate amounts of sodium thiosulphate and aurous thiocyanate. In the first stage of the formation of the latent image in a microcrystal, the quanta may be absorbed (1) by the lattice of the silver bromide, (2) by bromide ions at the surface of the crystal or (3) by atoms or molecules of the products of chemical sensitization. (2) and (3) are responsible for the inherent long wave or red sensitivity of the emulsion. Positive holes and electrons, both of which can diffuse through the crystal are liberated in the first case (1). The absorption of a quantum by a surface bromide ion liberates an electron and leaves a bromine atom and an excess silver ion at the site of absorption. An electron may be ejected from an atom of gold or of silver by the absorption of a quantum leaving an aurous or a silver ion behind. By the absorption of a quantum of the appropriate energy an electron may also be ejected from a molecule of silver sulphide. The positively charged molecule may then dissociate into a silver ion, a silver atom and a sulphur atom.

We shall first consider the case where the absorption of a quantum of relatively short wavelength liberates a positive hole and an electron. Mitchell (1953) has recently pointed out that the lifetime of the hole is probably less than that of the electron. The hole is most likely to be trapped either by a bromide ion at the surface of the sensitivity centre or by an atom or molecule of a product of chemical sensitization. The trapping of a hole by a bromide ion produces a bromine atom and creates a local positive charge in the form of an excess silver ion. The electron

will be held in the neighbourhood by electrostatic attraction but cannot immediately combine with the excess silver ion (see Mitchell 1953); neither can it combine with the bromine atom once the vibrational excitation energy of that atom has been dissipated. The bromine atom may, on the other hand, combine with a molecule of silver sulphide to release a silver atom and form a molecule of silver sulpho-bromide, AgSBr, which may subsequently break down into a molecule of silver bromide and an atom of sulphur. The silver atom may now combine with a gold atom to form a pair of atoms which may in turn associate themselves with the excess silver ion to form a positively charged triple aggregate. The positive charge of this aggregate can then be neutralized by the electron so that a neutral aggregate consisting of two silver atoms and one gold atom can result from the absorption of a single quantum. This aggregate may then combine with a silver ion from the surface of the silver halide crystal to form a positively charged aggregate of four atoms, probably in a tetrahedral arrangement, which could trap an electron directly and by a succession of similar processes continue the building up of the latent image. The positively charged aggregate of four atoms may also satisfy the minimum requirements for a development centre. The mechanism outlined here does not involve any long range motion of silver ions for the neutralization of space charges and may therefore be of the greatest significance under high intensity conditions of exposure.

The same sequence of events would follow the absorption of a quantum of lower energy by a bromide ion which was adsorbed or occupied a kink site at the surface. If a quantum of suitable wavelength is absorbed by a molecule of silver sulphide, an electron may be ejected leaving a positively charged molecule which may break down into a silver ion, a silver atom and a sulphur atom. Here, the observations of Rigollet (1895) are of interest; he found that electrons could be released from a thin film of silver sulphide in contact with silver by the absorption of radiations with wavelengths between $1{\cdot}32\,\mu$ and $0{\cdot}45\,\mu$. Should electrons be ejected from molecules of silver sulphide, the mechanisms already discussed would apply: the silver ion and the silver atom could associate with the electron and a gold atom to form a neutral aggregate of three atoms which could then combine with a further silver ion to form a positively charged aggregate of four atoms. This mechanism would also operate if the positive hole resulting from the absorption of a quantum by the silver bromide lattice were trapped by a molecule of silver sulphide. The ejection of an electron from an atom of silver or of gold by the absorption of a quantum could only result in the formation of a pair of metallic atoms. This would also apply if the positive hole were trapped by an atom of silver or gold, either in an emulsion which had been sensitized with silver sulphide and silver or gold, or in an emulsion which had been sensitized only with silver or gold. In dye sensitized emulsions, the quanta are absorbed by the dyestuff,

which is adsorbed in the form of a monolayer over the whole surface of the crystal and the excitation energy is transferred, with greatest probability, either to bromide ions occupying surface sites of low positive electrostatic potential (for example, kink sites) at the sensitivity centre, or else to atoms or molecules of the products of chemical sensitization also at the sensitivity centre; electrons are then ejected. The exciton must move about in the adsorbed layer of dyestuff until this happens, unless the excitation energy is degraded to thermal energy. The subsequent processes are the same as if the electron had been ejected from the bromide ion or from the sensitizing atom or molecule by the direct absorption of a quantum and have already been discussed.

We shall next consider the formation of the latent image in crystals of silver bromide, which have been subjected to both sulphur and reduction sensitization but have not been gold sensitized. Lowe, Jones and Roberts (1951) have shown that the sensitivity of certain relatively fine grained emulsions which have been sensitized with sulphur compounds can be considerably enhanced by subsequent sensitization with suitable reducing agents. We shall assume that, in this case, the sensitizing layer consists of a close association of molecules of silver sulphide and atoms of silver. The sequence of events already described for a gold sensitized emulsion would lead to the formation of a pair of silver atoms, followed by a positively charged aggregate of three silver atoms which could then combine with the electron to form a neutral triple aggregate.

We are naturally led to inquire why the treatment of such an emulsion with a gold salt which will only replace the silver atoms by gold atoms produces a very considerable increase in sensitivity. It is important to remember here that the same increase in sensitivity is obtained whether the emulsion is treated before or after exposure with a salt of monovalent gold (see Mueller 1949, James 1948, James, Vanselow and Quirk 1949), so that at least part of the explanation must be concerned with the mechanism of development. As a result of their work with large single crystals of silver bromide, Keith and Mitchell (1953) suggested that chemical development results from a combination of two processes: first, the transference of silver ions from the surface of the silver bromide crystal to the metallic nucleus produced during exposure and, secondly, the transference of electrons from molecules of the developer to the positively charged nucleus. The same mechanism applies to physical development, but here the silver ions are derived from the solution.

There seems to be no reason why a group of three silver atoms should not be formed during the exposure of an emulsion which has been both sulphur and reduction sensitized following the absorption of a single quantum by exactly the same mechanisms as in an emulsion which has been sulphur and gold sensitized. In seeking an explanation of the fact that a triple nucleus which includes a gold atom is more effective in initiating development than a nucleus consisting entirely of silver atoms, we have therefore to consider the next step in the mechanism

in which the nucleus combines with a silver ion from the surface of the crystal to form a positively charged aggregate of four atoms. The compensating negative charge will reside on the surface probably in the form of two adjacent kink sites both occupied by bromide ions. The question is whether more energy is liberated when a silver ion combines with a triple nucleus containing gold atoms than when the nucleus consists solely of silver atoms. When the aggregates are positively charged, the energy of van der Waals interaction must make an important contribution to the cohesive energy. This component will be greater when the aggregate contains gold atoms than when it consists only of silver atoms because the polarizability of an aurous ion is greater than that of a silver ion. We may therefore conclude that an aggregate including gold atoms will have a greater tendency to become positively charged at a smaller size than an aggregate of silver atoms. This could account for the enhanced developability of the latent image which is formed under conditions of minimum high intensity exposure in gold sensitized emulsions compared with reduction sensitized emulsions. It could also account for the post-exposure latensifying action of gold salts on the latent image formed in emulsions which have not been gold sensitized.

We have finally to consider the formation of the latent image in emulsions which have been sensitized with a sulphur compound under conditions which give a minimum of reduction sensitization. We shall assume that the sensitizing material consists only of molecules of silver sulphide adsorbed at the surfaces of the crystals. The sequence of changes which we have already discussed will now lead to the formation of a pair of silver atoms which will be much less likely to combine with a silver ion from the surface than a triple aggregate. This seems to account for the lower sensitivity of emulsions which have been sensitized only with sulphur compounds.

We have assumed that isolated atoms of silver and gold are produced mainly at the surface of the sensitivity centre during reduction and gold sensitization. There is no experimental justification for this and pairs or larger aggregates might equally well be formed. Although a pair of silver atoms might dissociate at room temperature, a pair of gold atoms should form a stable unit (see Mitchell 1953). The absorption of a single quantum by a microcrystal of silver halide which had a distribution of molecules of silver sulphide and pairs of atoms of gold at the sensitivity centre could lead to the formation, under the most favourable circumstances, of a neutral group of four metallic atoms. We have so far restricted the discussion to the formation of the latent image under conditions of minimum exposure and it will be convenient at this point to summarize the conclusions. After the absorption of a single quantum by a microcrystal of a non-sensitized silver halide emulsion, not more than one silver atom can separate at the surface. When molecules of silver sulphide are present, the absorption of a quantum can give rise to a

pair of silver atoms. If single atoms of silver or gold are associated with molecules of silver sulphide in the sensitizing layer, groups of three metallic atoms can result from the absorption of a single quantum. Such triple groups can then combine with silver ions from the surface of the crystal during or after exposure or when the crystal is immersed in a developer to form positively charged groups of four metallic atoms which can function as development centres. Positively charged groups containing gold atoms should be more stable than groups consisting only of silver atoms. These considerations provide a reasonable explanation of the progressive increases in sensitivity which follow the application of the different types of chemical sensitization. If the mechanisms proposed are indeed applicable to the photographic system, it should not be possible to obtain the same increases in sensitivity by digesting a pure silver iodide emulsion with a sulphur compound because iodine does not combine with sulphur to form a stable sulphur iodide. The adsorbed silver sulphide molecules would therefore have either to absorb quanta which would cause the ejection of electrons or else to trap positive holes before their silver atoms could contribute to the formation of the latent image. It might also be predicted that it would not be possible to optically sensitize a sulphur sensitized silver iodide emulsion as efficiently as a pure silver bromide emulsion. The excitation energy of the dyestuff would have to be transferred directly to molecules of silver sulphide before the sensitization could be effective at the longer wavelength. For the same reasons, the efficiency with which silver bromo-iodide emulsions can be sensitized for longer wavelengths by a combination of sulphur sensitization and dye sensitization should be decreased as the concentration of iodide increased because an ever increasing proportion of kink sites would be occupied by iodide ions.

It must be emphasized that the speculations of this section apply to only one aspect of a very complex problem. They are concerned with the detailed behaviour of the products of chemical sensitization during exposure and are supplementary to one of the author's recent speculations on photographic sensitivity (Mitchell 1953). These products are most likely to be concentrated at the surfaces of the sensitivity centre which is, according to Mitchell, the region of maximum localized imperfection in the crystal. In a tabular crystal, the sensitivity centre will be the part of the crystal in the immediate neighbourhood of the inevitably imperfect nucleus from which the crystal grew and will consequently usually be located near the centre of the crystal. Now, if a molecule of bromine were formed there as a result of a rapid succession of events during a normal exposure, it would be able to react with a molecule of silver sulphide to form a pair of silver atoms and a molecule of sulphur dibromide. After dissociation, this molecule could then react with a further molecule of silver sulphide and the process could be continued so that under favourable circumstances the absorption of at least two quanta might cause the liberation of silver atoms from more than two

molecules of silver sulphide. This type of reaction would probably only occur at the surface of the sensitivity centre where bromine atoms are most likely to be formed by the trapping of holes and where there is the greatest surface concentration of products of chemical sensitization. The silver atoms together with gold atoms, silver ions and electrons would then condense to form development nuclei. It is perfectly clear that the formation of the latent image under average conditions of exposure in a fully sensitized modern high speed silver bromo-iodide negative emulsion is likely to be an extremely complicated process.

References

Chilton, L. V., 1946, *B.I.O.S.*, Final Report No. 1355, 35 and 68.

Clark, W., 1927, *Brit. J. Phot.*, **74,** 227 and 243.

Dorling, E. B., 1953, *Ph.D. Thesis*, University of Bristol.

Gurney, R. W., and Mott, N. F., 1938, *Proc. Roy. Soc.* A, **164,** 151.

Hedges, J. M., and Mitchell, J. W., 1953, *Phil. Mag.* [7], **44,** 357.

Hickman, K. C. D., 1927, *Photo. J.*, **67,** 34.

Holloway, D. G., 1951, *Ph.D. Thesis*, University of Bristol.

James, T. H., 1948, *J. Coll. Sci.*, **3,** 447.

James, T. H., Vanselow, W., and Quirk, R. F., 1948, *P.S.A.J.*, **14,** 349.

Keith, H. D., and Mitchell, J. W., 1953, *Phil. Mag.* [7], **44,** 877.

Koslowsky, R., 1951, *Z. wiss. Phot.*, **46,** 65.

Lowe, W. G., Jones, J. E., and Roberts, H. E., 1951, *Fundamentals of Photographic Sensitivity* (London : Butterworth), p. 112.

Lüppo-Cramer, C., 1921, *Kolloidchemie und Photographie*, 2nd Edn. (Dresden : Steinkopf) ; 1927, Die Grundlagen der Photographischen Negativverfahren, *Eder's Handbuch der Photographie*, **2,** Part 1 (Halle : Knapp).

Mitchell, E. W. J., and Mitchell, J. W., 1951, *Proc. Roy. Soc.* A, **210,** 70.

Mitchell, J. W., 1948, *Sciences et Industries Photographiques* (2), **19,** 361 ; 1953, *J. Photo. Sci.*, **1,** 110.

Mueller, F. W. H., 1949, *J. Opt. Soc. Amer.*, **39,** 494.

Rigollet, H., 1895, *Compt. Rend.*, **121,** 164.

Sheppard, S. E., 1925, *Photo. J.*, **65,** 380 ; 1928 a, *Ibid.*, **68,** 397 ; 1928 b, *Brit. J. Phot.*, **75,** 207.

Wood, H. W., 1953, *J. Photo. Sci.*, **1,** 163.

XXV. CORRESPONDENCE

Observations on the Fatigue Fracture of Copper

By N. J. Wadsworth and N. Thompson
H. H. Wills Physical Laboratory, University of Bristol

[Received December 21, 1953]

In the course of experiments on fatigue, we have made some observations which seem pertinent to the question of the origin of the fatigue crack.

The experiments were done on pure copper fully annealed, and tested at constant stress in push-pull at about 1000 cycles per second. The diameters of the cylindrical specimens were 3·8 mm, and the grain size was about 0·1 mm. The specimens were carefully prepared so as to be free from a cold-worked surface layer, and were finally electro-polished. When tested at stresses which gave a fatigue life of the order of 10^6–10^7 cycles, the surface showed, at a very early stage of the test, a number of slip bands. These became more numerous, and some of them became more intense, as the test proceeded.

It was noticed that the eventual fatigue crack frequently appeared to have originated at such an intense slip band. The course of the crack in both directions from this centre point was marked by an abnormally high density of slip bands, while the centre itself was comparatively clean. Similar features were observed on other, smaller cracks, when these were present.

The detection of a small crack under the microscope is made more difficult by the high general density of slip markings. Accordingly the expedient was adopted of electro-polishing the specimen some time before failure was expected. This removed the slip bands and revealed the presence of markings which we believe to be incipient cracks. Figure 1 (Pl. 2, figs. 1–7), for example, shows a photograph taken after $2{\cdot}8\times10^6$ cycles. This crack spread and eventually caused fracture after a total of $3{\cdot}65\times10^6$ cycles.

In an attempt to establish the point at which such cracks could first be detected, a specimen was electro-polished at intervals throughout a test, and photographs were taken each time of a number of fields. Figure 2 shows the appearance of one area after $2{\cdot}7\times10^5$ cycles; this was on the same specimen which failed, elsewhere, after $3{\cdot}65\times10^6$ cycles. Figure 3 is the same field after electro-polishing to remove a layer about 2 microns thick from the surface. It will be seen that most of the surface markings have been removed, but a few of the more intense bands remain. A second electro-polish, removing about the same amount as before, left

the appearance substantially unchanged. Further periods of stressing in the fatigue machine, followed by electro-polishing, showed the same marks persisting, and new ones of similar character appearing. Some of these persistent slip bands began to spread into neighbouring grains (see fig. 1) and eventually gave rise to unmistakable fatigue cracks. One of these would grow in length more rapidly than the others, perhaps joining up with another in the process, and eventually giving rise to the fatigue fracture.

One fatigue test was stopped when the above technique revealed about a dozen such incipient cracks, ranging in length from 3 to 10 grain diameters, together with a considerable number of the persistent slip band markings only one grain long. This specimen was then given a 5% slow tensile extension. All the ' cracks ' opened out in the manner shown in figs. 4 and 5, but none of them showed any tendency to increase in length. The marks confined to a single grain were difficult to locate on the deformed surface, but it can safely be said that their tendency to open out in the above manner was very much less, and perhaps not present at all.

At what stage a persistent slip band can be called a crack is perhaps rather a question of nomenclature. The above observations show the presence of persistent slip band markings after less than 10% of the fatigue life, and of the indubitable cracks into which they develop at about 60% of the life. The markings cannot simply be large steps on the surface, since such steps, which are produced in abundance by moderate unidirectional strains (say 10%), were removed by the electro-polishing treatment used. Again, it was found that, if a specimen were subjected to alternating stress for, say, 10% of its estimated fatigue life and then polished to show the persistent markings, and finally vacuum annealed at 600°C for 1 hour and re-polished, the same markings were still present. These results suggest a possible explanation of the observation of Sinclair and Dolan (1952) that a (brass) specimen can be annealed repeatedly during a fatigue test without any significant effect on the fatigue life. This conclusion is supported qualitatively by a few results obtained by us on the copper specimens used in the above work.

Preliminary observations on single crystals suggest a similar pattern of behaviour. A broad slip band, visible at, say, 10% of the life, will be removed by electro-polishing except for a number of localized regions (figs. 6 and 7). One or more of these, on further stressing, will eventually appear as an obvious crack. The crack, although thus starting in the slip band, will later deviate from it, to pursue its more usual course approximately in the plane normal to the tensile axis.

The observations are being continued, and a fuller account will be published in due course.

Reference

Sinclair, G. M., and Dolan, T. J., 1952, *Proc. 1st Nat. Cong. Appl. Mech.*, p. 647.

Fig. 1

Fig. 4

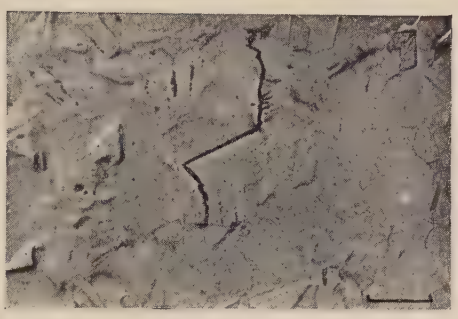

Fig. 2

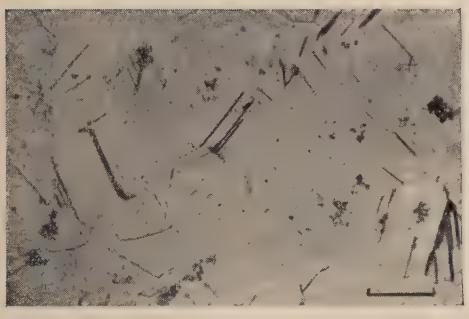

Fig. 5

Fig. 3

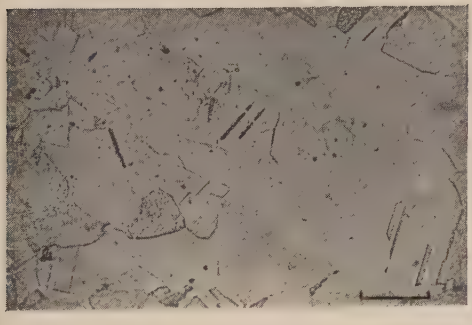

Fig. 6

Fig. 7

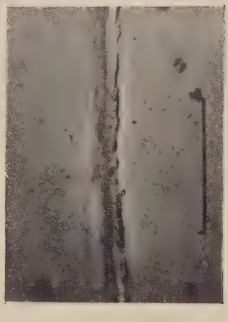

The markers on the diagrams are all 0·1 mm long.

The Quantum Yield of the F→Z_1 Conversion in KCl *with* Sr *Impurity*

By P. Camagni,* G. Chiarotti, F. G. Fumi* and L. Giulotto
Istituto di Fisica, Università di Pavia, Italy

[Received December 15, 1953]

To study the interaction as electron traps of the Schottky defects and of the impurities in the alkali halides, we have investigated in detail the conversion of the F band to the simplest colour-centre band connected with the presence of positive divalent impurities, the Z_1 band (Pick 1939, Seitz 1951). KCl crystals with a small quantity of Sr^{++} added as $SrCl_2$ ($5{\cdot}5\times10^{-5}$ mole fraction) were coloured either additively in Na vapours or by irradiation with x-rays at room temperature and then exposed to the action of the 5461 Å line of Hg, which falls in the spectral region common to the F and Z_1 bands.

In additively coloured crystals we found that practically only Z_1 band is formed while the F band decreases. Therefore we assumed the equality between the numbers per cm^3 of Z_1 centres formed and of F centres destroyed at the end of the conversion in a given crystal, and determined in this way the oscillator strength for the Z_1 band using Smakula's formula (Seitz 1940). The value of 0·84† that we obtain is very close to the oscillator strength for the F band (Kleinschrod 1936), as it is reasonable it should be (Seitz 1951).

Figure 1 gives the numbers of F and Z_1 centres per cm^3 as functions of the number of quanta absorbed in an additively coloured crystal. The numbers of centres are determined directly from the height and width of the F and Z_1 bands using the oscillator strengths. The quantum yield for the destruction of F centres (or the formation of Z_1 centres) at the beginning of the conversion is about 0·15 in our crystals, and goes gradually to zero during the conversion as the Z_1 band reaches a saturation value.

The initial absence of the Z_1 band can be justified through the thermal instability of the Z_1 centre (Pick 1939). To explain the observed saturation of the Z_1 band, which is practically stable under Z_1 light, we suppose that at saturation all the Sr^{++} which are not associated to a positive-ion vacancy (free Sr^{++}) have formed a Z_1 centre by capturing an electron and that the associated Sr^{++} do not act as effective electron traps at room temperature (Harten 1950)‡ : the number of unassociated

---

* Gruppo di Fisica dei Solidi, Sezione di Milano dell'Istituto Nazionale di Fisica Nucleare.

† To be exact, this value is a lower limit for the oscillator strength of the Z_1 band since we neglect the very small R and M bands which actually form during the conversion.

‡ This interpretation is confirmed by the total conversion to Z_1 band of a small initial F band.

ions should not change rapidly at room temperature owing to the values of the association energy and of the jump frequency for free positive-ion vacancies. To investigate the validity of our interpretation we have exploited some of its consequences.

If we assume that the only efficient electron traps are F and Z_1 traps and that each photon frees an electron from an F centre (Mott and Gurney 1938), the quantum yield for the conversion can be written

Fig. 1

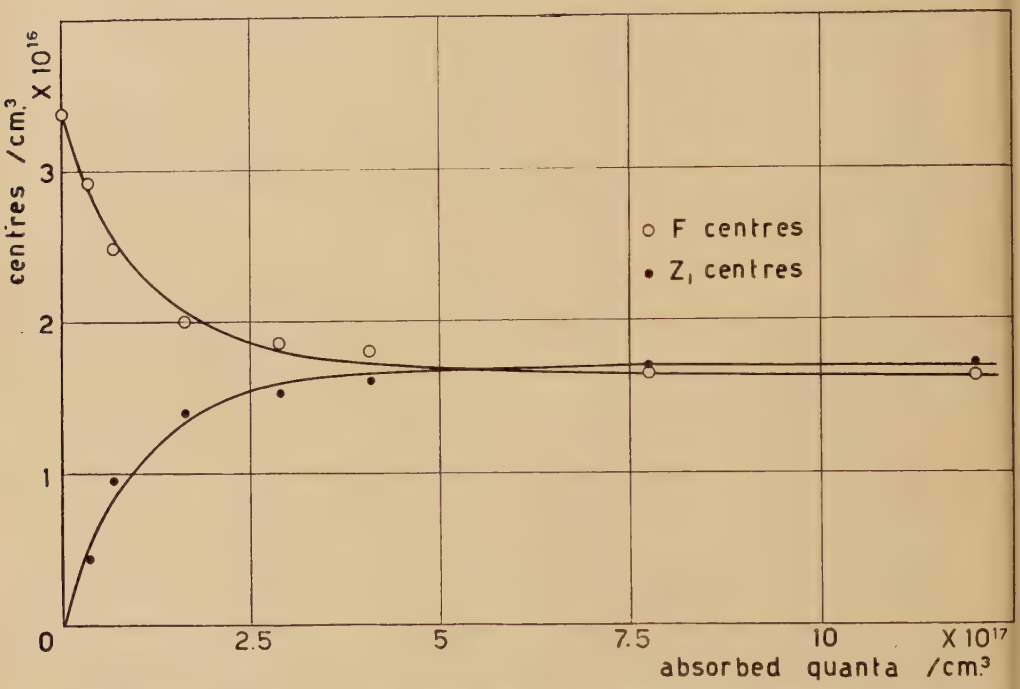

The numbers of F and Z_1 centres/cm^3 as functions of the number of absorbed quanta/cm^3 (Hg 5461Å) in a crystal of KCl containing 9×10^{17} Sr^{++}/cm^3 coloured additively.

$$\eta=\frac{(N^{++}-N_{Z_1})\sigma_{Z_1}}{(N_v-N_F)\sigma_F+(N^{++}-N_{Z_1})\sigma_{Z_1}} \quad . \quad . \quad . \quad . \quad . \quad (1)$$

where N^{++} is the number of free Sr^{++}/cm^3 and thus the number of Z_1 centres/cm^3 at saturation : N_v, N_F, N_{Z_1} are respectively the numbers of negative-ion vacancies, F centres and Z_1 centres per unit volume ; σ_F and σ_{Z_1} are the capture cross sections for electrons of a negative-ion vacancy and of a free divalent ion. The behaviour of η during the conversion as a function of N_{Z_1} is found to be nearly linear and this indicates that σ_F/σ_{Z_1} is of the order of unity. If one takes $\sigma_F/\sigma_{Z_1}=1$, one obtains $N_v\simeq 1{\cdot}4\times10^{17}$/cm^3. These results appear plausible but must be considered approximate.

The knowledge of the concentration of strontium and of free Sr^{++} in the crystal allows us to determine also the association energy of the complex $+ + \oplus$ which is related to the equilibrium constant K of the association reaction through the equation

$$K = 12 \exp(W/kT). \quad . \quad . \quad . \quad . \quad . \quad . \quad . \quad . \quad (2)$$

Using $T = 300°K$, we obtain $W \simeq 0{\cdot}3$ ev : this value is somewhat smaller than the theoretical value (0·39 ev) (Bassani and Fumi, see following paper), as it should be (Lidiard). A cause of inaccuracy of our method for determining W is the uncertainty in the equilibrium temperature T.

Fig. 2

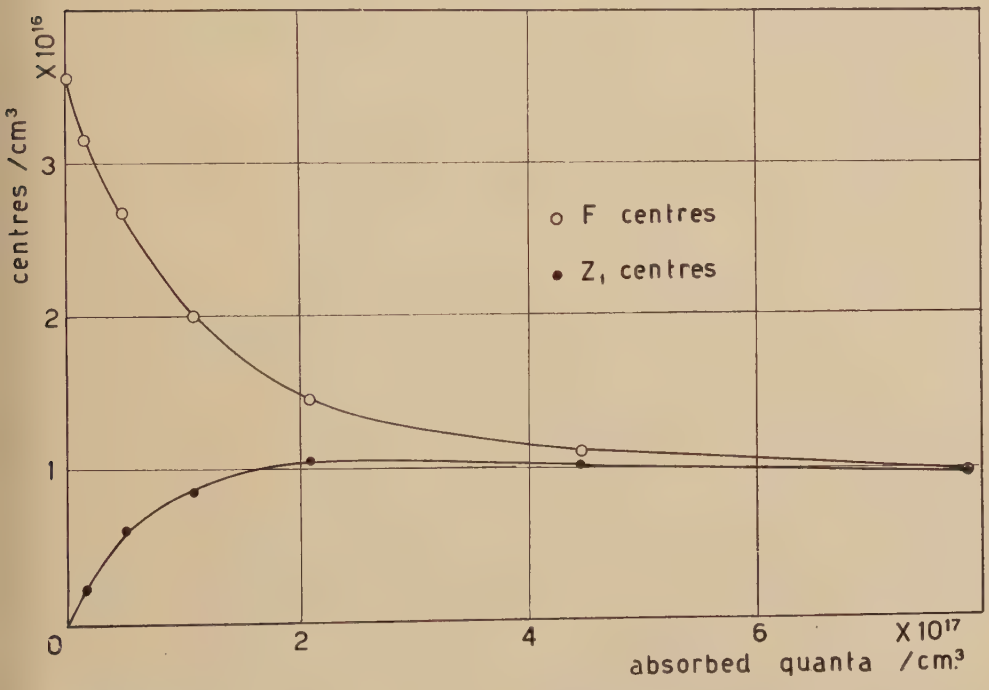

The numbers of F and Z_1 centres/cm³ as functions of the number of absorbed quanta/cm³ (Hg 5461Å) in a crystal of KCl containing 9×10^{17} Sr^{++}/cm³ coloured by x-rays.

Figure 2 refers to the F→ Z_1 conversion in a crystal coloured by x-rays. The general behaviour of the curves can be understood in relation with fig. 1 if one allows for the presence of holes. The observed very slow decrease of the Z_1 band is possibly due to a small ionization probability of the Z_1 centre under Z_1 light : this probability, however, appears so small that the equilibrium to which it would lead in the F→ Z_1 conversion in additively coloured crystals would practically correspond to the saturation of the available Z_1 traps. The apparent initial absence of

the Z_1 band may be rationalized if one considers that σ_F and σ_{Z_1} are approximately equal and that the irradiation with x-rays introduces vacancies (Esterman, Leivo and Stern 1949, Sakaguchi and Suita 1952).

A description of the apparatus used and a detailed discussion of the results obtained will appear soon in *Il Nuovo Cimento*.

The writers are indebted to Professor F. Seitz for useful correspondence. This research was supported by the Consiglio Nazionale delle Ricerche.

References

Bassani, F., and Fumi, F. G., 1954, *Phil. Mag.* **45,** 228 (following paper).
Estermann, I., Leivo, W. J., and Stern, O., 1949, *Phys. Rev.*, **75,** 627.
Harten, H. U., 1950, *Nachr. Akad. Wiss. Göttingen*, 15.
Kleinschrod, F. G., 1936, *Ann. Physik*, **27,** 97.
Lidiard, A. B., *Phys. Rev.* (to appear).
Mott, N. F., and Gurney, R. W., 1948, *Electronic Processes in Ionic Crystals* (Oxford : Clarendon Press), pp. 129, 136.
Pick, H., 1939 a, *Ann. Physik*, **35,** 73 ; 1939 b, *Z. Physik*, **114,** 127.
Sakaguchi, K., and Suita, T., 1952, *Tech. Rep. Osaka Univ.*, **2,** 177.
Seitz, F., 1940, *Modern Theory of Solids* (New York : McGraw-Hill), p. 664, eqn. 8 ; 1951, *Phys. Rev.*, **83,** 134.

The Association Energy between Positive Divalent Impurities and Positive-Ion Vacancies in NaCl *and* KCl *Crystals*

By F. Bassani* and F. G. Fumi*
Istituto di Scienze Fisiche, Università di Milano, Italy

[Received December 15, 1953]

The experimental data available at present on the properties of the alkali halides containing positive divalent impurities give a rather incoherent picture of the dependence of association between divalent impurities and positive-ion vacancies on the nature of the impurity and of the crystal. This situation suggests a theoretical calculation of the association energies, which represent the primary cause of the dependence : thus far only the association energy between Cd^{++} and a positive-ion vacancy in NaCl had been computed (Reitz and Gammel 1951). Lidiard (in press) has pointed out that the theoretical interaction energies are also needed to perform a correct statistical analysis of the degree of association including the long-range Coulomb interactions.

The association energy between a positive divalent impurity ion and a positive-ion vacancy in a crystal of NaCl or KCl is given by the difference of the work necessary to create a positive-ion vacancy in the perfect lattice and the work necessary to create it in the position of next-nearest

* Gruppo di Fisica dei Solidi, Sezione di Milano dell'Istituto Nazionale di Fisica Nucleare.

neighbour of the divalent ion. The work necessary to remove an ion from a lattice is conventionally taken to be equal to the negative of the average of the potential energies in the position of the ion before and after it has been removed. Methods for performing calculations of this kind have been developed by Mott and Littleton (1938) and improved by Reitz and Gammel (1951). We have followed the latter authors in taking for the repulsive potential energy the form of Born and Mayer (1932), which considers explicitly the radii of the interacting ions, taken as equal to the Goldschmidt values.

Our results are given in the table. Their accuracy is probably of the order of 0·1 ev in the absolute values and probably better in the relative values. The association energy that we compute for Cd^{++} in NaCl

Association Energies of Divalent Impurities and Positive-Ion Vacancies (ev)

	Cd	Ca	Sr
NaCl	0·38	0·38	0·45
KCl	0·32	0·32	0·39

differs somewhat from the value reported by Reitz and Gammel (0·44 ev) mainly owing to our more accurate calculation of the energy needed to create a vacancy in the perfect lattice.

The theoretical association energies of table 1 should not be compared directly with the values obtained from analyses of experimental data, which neglect the effect of long-range interactions, since such analyses necessarily lead to low values for the association energies (Lidiard). So our value for the association energy for Cd^{++} in NaCl is definitely larger than the value obtained by Etzel and Maurer (0·24 ev) (1950)† from a simplified analysis of ionic conductivity isotherms, but it compares favourably with the value obtained by Lidiard (0·35 ev), who analysed the same data taking into account long-range interactions.

The relative values of the computed association energies seem significant. They indicate an increase of the association energy with the ionic radius of the impurity, and actually a larger radius implies a stronger opposition to the inward displacement of the surrounding negative ions, which tends to compensate the excess positive charge of the impurity ion. They are also slightly smaller in KCl than in NaCl, and this agrees with the larger inward distortion in the immediate neighbourhood of the impurity caused by the contact between positive and negative ions occurring in KCl but not in NaCl, and also with the fact that the impurity ions are smaller than K^+ but larger than Na^+.

† The value $\Delta E = 0{\cdot}24$ ev is obtained from the data of Etzel and Maurer if one uses the appropriate equation $L/F^2 = 12 \exp(\Delta E/kT)$.

A detailed discussion of our calculation and of our results in relation to available experimental data will appear soon in *Il Nuovo Cimento*.

The writers are indebted to Dr. Lidiard for stimulating correspondence on the problem.

References

Born, M., and Mayer, J. E., 1932, *Zeits. f. Phys.*, **75**, 1.
Etzel, H. W., and Maurer, R. J., 1950, *J. Chem. Phys.*, **18**, 1003.
Lidiard, A. B., 1954, *Phys. Rev.* (to appear).
Mott, N. F., and Littleton, M. J., 1938, *Trans. Faraday Soc.*, **34**, 485.
Reitz, J. R., and Gammel, J. L., 1951, *J. Chem. Phys.*, **19**, 894.

Coulomb Excitation of Levels in ^{19}F *by Alpha-Particles*

By G. A. Jones and D. H. Wilkinson
Cavendish Laboratory, Cambridge

[Received December 29, 1953]

Coulomb excitation has been discussed theoretically (Mullin and Guth 1951, Huby and Newns 1951, Ter-Martirosyan 1952, Alder and Winther 1953) and demonstrated for protons bombarding heavy nuclei (McClelland and Goodman 1953, Huus and Zupančič 1953). We have shown that the process occurs in the bombardment of a light nucleus with alpha-particles.

A thick AlF_3 target was bombarded with alpha-particles and the gamma-rays detected in a crystal of NaI(Tl) (1 cm$\times$1 cm$\times 1\frac{1}{4}$ mm); a typical spectrum is shown in fig. 1. The two large peaks represent gamma-rays of 112$\pm$1 kev and 195$\pm$1·5 kev. Levels have been located at 113$\pm$8 and 192$\pm$12 kev by Mileikowsky and Whaling (1952) using ^{21}Ne(dα)^{19}F and at 108 and 196 kev by Temmer and Heydenburg (1953) using ^{19}F($\alpha\alpha'$)^{19}F. (They report that this reaction proceeds at high alpha-particle energies through compound nucleus formation but that there is evidence of Coulomb excitation at lower energies; our own work is at far too low an energy to consider compound nucleus formation and proceeds entirely via Coulomb excitation.) The small bulge below the lower peak of fig. 1 is probably due chiefly to radiation back-scattered from material in the vicinity of the detector since its relative size depended on the proximity of the shields placed to absorb unwanted stray x-rays from the H.T. set. The relative intensity of the two strong lines of the spectrum is strongly dependent on the bombarding energy while the bulge remains in constant proportion to the total radiation; it cannot therefore be ascribed to a cascade from the 195 kev level via that at 112 kev but it could well mask a slight amount of such a cascade.

Figure 2 shows the excitation function for the higher energy radiation together with some theoretical curves for E1 and E2 excitation. The measurements were made at 90° to the alpha-particle beam; the angular

distribution at 1·10 MeV is isotropic to within 10%. Either E1 or E2 transitions give a good account of this excitation function (and also of that for the lower energy radiation).

Rough estimates have been made of the absolute yields at 1·20 MeV : they are $3{\cdot}5\times10^{-11}$ and $1{\cdot}4\times10^{-10}$ gamma-rays per alpha-particle for the low and high-energy gamma-rays respectively, corresponding to (upward) E2 transition probabilities of 3×10^{4} and 8×10^{6} sec^{-1} or to

Fig. 1

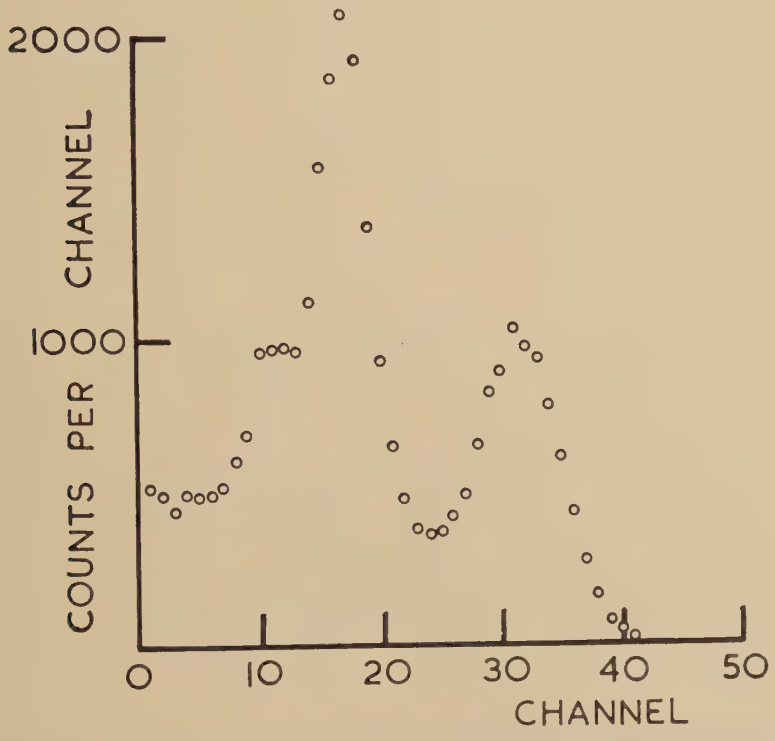

Pulse spectrum from NaI(Tl) due to gamma-rays following the bombardment of fluorine with alpha-particles of 1·10 MeV.

E1 transition probabilities of 3×10^{9} and 4×10^{11} sec^{-1}. These represent $|M|^2$ values (in Weisskopf (1951) units) of about 0·2 and 2 for E2 transitions or 0·002 and 0·04 for E1 transitions.

It seems improbable that ^{19}F shows a change of parity at such low excitation and it also seems improbable that magnetic Coulomb excitation should be sufficiently effective here. If, then, we suppose the excitation to be E2 the two excited states must be $(\frac{3}{2}+)$ or $(\frac{5}{2}+)$. If the second excited state were $(\frac{5}{2}+)$ it should decay preferentially by M1 radiation to the 112 kev state and so it appears likely to be $(\frac{3}{2}+)$. (If it were $(\frac{5}{2}+)$ we should have $|M|^2<10^{-5}$ for the M1 transition and this appears rather unlikely.) The (presumed) M1 decay of the second

excited state to the ground state competes favourably with the (presumed) M1 transition to the 112 kev state and so it appears probable that if a change of orbit is involved between the ground state and one excited state the same change does not occur for the other excited state since this situation would favour the cascade relative to the direct ground state transition from the 195 kev state, the former not requiring a change of orbit for the M1 transition. This makes it difficult to adopt the otherwise attractive assignment $(2s_{1/2})^3$ for the ground state of ^{19}F.

Fig. 2

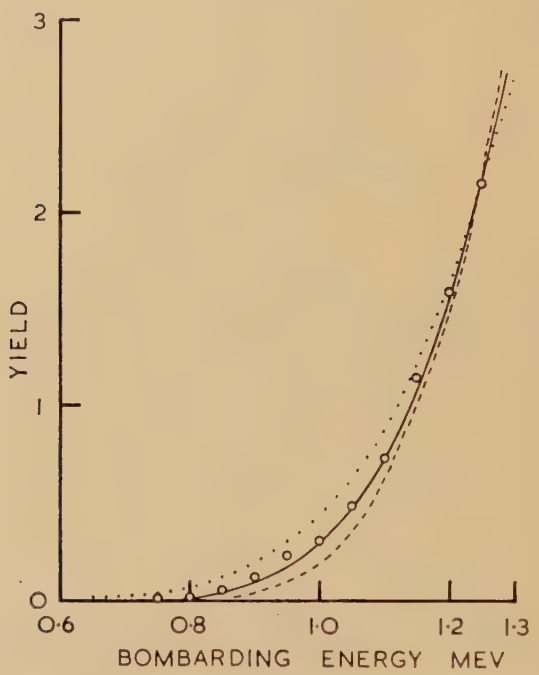

Excitation function for the 195 kev radiation. The three lines give theoretical functions for E2 excitation (Alder and Winther). The theory contains the parameter $\Delta E/E$ where ΔE is the energy lost by the particle of energy E. In the dotted curve E is the energy of the ingoing particle ; in the dashed curve E is its outgoing energy ; in the full curve E is (as seems most realistic) its mean energy. The curves are normalized at 1·25 MEV. The theoretical curve (Mullin and Guth) for E1 excitation differs inappreciably from the full curve for E2 excitation.

If the ground state were $(1d_{5/2})^2 2s_{1/2}$ as is frequently supposed it would be possible for the first excited state to be the $(\frac{5}{2}+)$ lowest state of $(1d_{5/2})^3$. The E2 excitation should then have a strength (relative to the ' single particle ' strength) of

$$\left[3U(2\,\tfrac{5}{2}\,\tfrac{1}{2}\,0,\,\tfrac{1}{2}\,\tfrac{5}{2})U(2\,2\,\tfrac{1}{2}\,\tfrac{1}{2},\,0\,\tfrac{5}{2})\frac{1}{\sqrt{3}}\frac{1}{3}\sqrt{\frac{7}{2}} \times\left(\tfrac{1}{2}+\frac{\sqrt{3}}{2}U(1\,\tfrac{1}{2}\,\tfrac{1}{2}\,1,\,\tfrac{1}{2}\,\tfrac{1}{2})C^{1\,\frac{1}{2}\,\frac{1}{2}}_{0\,\frac{1}{2}\,\frac{1}{2}}\right)\right]^2=\frac{14}{45}$$

following Lane and Radicati (1953) ; in this expression we have regarded the $(0+)$ state of $(1d_{5/2})^2$ as the principal parent of the ground state of ^{19}F. This compares with the experimental value of 0·2 Weisskopf units. The second excited state could then be perhaps a $(\frac{3}{2}+)$ coupling of $(2s_{1/2})^2 1d_{5/2}$; alternatively the $(\frac{5}{2}+)$ state of this mixed configuration may be this second excited state, its M1 transition to the 112 kev state being very powerfully forbidden by the need for two particles to change their configuration and by the double orbital change. In either event we should expect the E2 transition to be a strong one as observed. With such assignments these states would suffer considerable inter-configurational mixing and the magnetic moment of the ground state may be difficult to explain (B. H. Flowers, private communication). We may note in passing that the excitation energy of these states is much too low to associate them with the rotational levels of Bohr and Mottelson (1953).

We intend to measure the decay lifetimes directly and to make a more careful search for cascade radiation.

References

Alder, K., and Winther, A., 1953, *Phys. Rev.*, **91,** 1578.
Bohr, A., and Mottelson, B., 1953, *Dan. Mat. Fys. Medd.*, **27,** no. 16.
Huby, R., and Newns, H. C., 1951, *Proc. Phys. Soc.* A, **64,** 619.
Huus, T., and Zupančič, C., 1953, *Dan. Mat. Fys. Medd.*, **28,** no. 1.
Lane, A. M., and Radicati, L. A., 1953, *Proc. Phys. Soc.* (in press).
McClelland, C., and Goodman, C., 1953, *Phys. Rev.*, **91,** 760.
Mileikowsky, C., and Whaling, W., 1952, *Phys. Rev.*, **88,** 1254.
Mullin, C. J., and Guth, E., 1951, *Phys. Rev.*, **82,** 141.
Temmer, G. M., and Heydenburg, N. P., 1953 (unpublished).
Ter-Martirosyan, K. A., 1952, *Jour. Theor. Exp. Phys., U.S.S.R.*, **22,** 284.
Weisskopf, V. F., 1951, *Phys. Rev.*, **83,** 1073.

XXVI. *Notices of New Books and Periodicals received*

Electron Optics. By O. Klemperer. 2nd ed. (Cambridge: University Press.) Price 50*s.* net.

The second edition of Dr. Klemperer's monograph will be welcomed not only by those seeking a concise introduction to the various branches of Electron Optics, but also by those already familiar with the subject who nevertheless need an up-to-date guide to its voluminous publications. The extent to which the subject has developed since the first (1939) edition may be gauged from the fourfold increase in the numbers of pages and of references.

The first seven chapters, dealing with electron lenses and their aberrations, may be seen to have their origins in the first edition but are greatly expanded to give account of the more important developments over the intervening years. The author draws attention, for instance, to suggestions which have been advanced for eliminating spherical aberration and to current trends in the design of β-ray spectrometers.

The remaining chapters deal with topics hardly touched on in the first edition. Chapter 8 presents a useful account of the influence upon electron lenses of their intrinsic space-charge which brings out the importance of neutralization and of electrode structure. Chapter 9 sets out categories and properties of electron guns, Chapter 10 summarizes the properties of strip beams and their appropriate lenses, and Chapter 11 deals with the focusing properties of deflecting fields. The last chapter lists and describes very briefly the many applications of Electron Optics.

It is, of course, impossible to survey so wide a field in so short a space without restricting the enquiry in some respect. In this case the author has chosen to describe in some detail experimental investigations but to report theoretical developments briefly, and where possible in non-mathematical terms, if at all. This sometimes leads to confusion. For instance, it is only in the absence of theoretical guidance that the divergence of gauze lenses seems ' remarkable ' or doubt arises about the existence of spherical aberration in deflecting fields. It may also be regretted that the chapter on ray tracing did not describe a modern computational procedure and that the derivation of the erroneous formula for the focal length of thin electrostatic lenses should have been reproduced.

It is probable that this book, which is well illustrated and thoroughly indexed, will prove most useful to research workers who come into contact with electron-optical equipment for it provides brief and lucid descriptions of the various components of electron-optical apparatus together with adequate references to relevant publications. P. A. S.

Introduction to Tensors, Spinors and Relativistic Wave-Equations. By E. M. Corson, Ph.D. (Blackie & Son Ltd.) [Pp. xiv+221.] Price 55*s.*

This book dealing with a very abstract subject in a mercilessly abstract style will be wisely shunned by anyone primarily interested in the physical aspect of the problem of elementary particles. But even those of us who have drunk from the cup of abstract algebra more than perhaps is healthy for a physicist will, I am afraid, be disappointed by it.

Professor Corson has made a gallant attempt to clear the jungle of literature on the subject to which he alludes in his Preface, and he has certainly disentangled to a large extent the intricate logical relationships between the various independent developments of the theory; but the result of his endeavour somehow falls short of the synthesis which might perhaps have been achieved by

a more decided handling of the issues involved. As it is the book is too difficult to be recommended as an introduction to the subject to research students, for example, and on the other hand the physicist likely to consult it will find only the better known parts of the subject discussed at great length, whereas the more subtle and fundamental investigations are only briefly summarized with an invitation to refer to the original papers. This, however, is a rather serious shortcoming, since the papers in question make use of little known aspects of modern algebra, for which they again refer to mathematical textbooks. The *raison d'être* of a work like the one under review would just be to supply the physicist with the required mathematical background and to show more directly than can be done in original papers how it is applied to physical problems.

On the credit side, it is only fair to praise the author for the neatness of his handling of special points and for the great care that he has obviously devoted to rigour and accuracy of treatment. The publishers must be congratulated for a very high-class production. L. R.

Investigations in Physics, No. 1 : *Ferroelectricity*. By E. T. Jaynes. (Princeton : University Press ; London : Geoffrey Cumberlege, Oxford University Press.) [Pp. 142.] Price 2$.00 ; 12*s*. 6*d*.

This book is an expansion of a doctoral thesis and is concerned mainly with the theory of ferroelectricity. It opens with a brief account of the properties of Rochelle salt and KH_2PO_4 and the theories put forward to account for their behaviour. The author then discusses at greater length the properties of $BaTiO_3$ and the theories relating it, in particular to his own electronic theory. There is then a brief account of the general thermodynamic properties of ferroelectrics, and the remaining one-third of the book is devoted to methods of evaluating internal fields in crystals and finding the conditions for spontaneous polarization.

The book suffers somewhat from being a mixture of a review and an original paper. Thus the space devoted to internal fields is excessive in a general account of ferroelectricity though as it is new material it is interesting to the specialist. Nevertheless the book gives a good and readable account of the present state of the theory of ferroelectrics. A. F. D.

Principles of Transistor Circuits. Edited by Richard F. Shea. (New York : John Wiley and Sons ; London : Chapman and Hall.) Price 88*s*. net.

This volume, which has been written by members of the Electronics Laboratory of the General Electric Company, Syracuse, N.Y., provides the first systematic account of transistor circuits. It is clearly written and contains the fundamental theory needed for a full appreciation of the potentialities of the different types of transistor as circuit elements. Each chapter ends with a group of problems and a bibliography. The inclusion of problems in a monograph of this type is worthy of note at a time when interest in technical education is increasing ; the transistor and related devices will inevitably be discussed in the electronics courses of technical colleges and universities in the immediate future. The extensive bibliography provides a valuable guide to the literature of the subject. The book will need no recommendation to physicists and electronics engineers who are concerned with transistor developments. It will be widely read by directors of research in industry and service laboratories who are concerned with the assessment of the importance of the transistor in their particular fields ; this group will appreciate the balanced account of the subject which is presented. J. W. M.

The First Fifty Years, 1903–1953. The Faraday Society. (Aberdeen University Press.) [Pp. 86.] Price 10*s.* 6*d.*

In the words of the Editor : " This little publication is not a set piece ; it is more in the nature of a birthday-book in which people have been good enough to write interesting things about the Society now on the threshold of its fiftieth anniversary." But he is to be congratulated upon it as a collection of short articles from fourteen of our leading physical chemists including one of its original members, Professor F. G. Donnan. The work also contains a number of interesting portraits of Past-Presidents. These, collected in one volume, help to emphasize the prestige and influence that the Society has acquired in the first half-century of its life. A. M. T.

[*The Editors do not hold themselves responsible for the views expressed by their correspondents.*]